

Trends in Immunotherapy

2

2021 Volume 5 Issue 2.1

ISSN: 2573-5985



Special Issue

Research Progress in Immunotherapy in China



ISSN 2573-5985



02 >

9 772573 598055

Editorial Board

Editor-in-Chief

Prof. Dr. Fukumi Furukawa

Takatsuki Red Cross Hospital

Japan

Associate Editor

Prof. Hiroki Yamaue

Wakayama Medical University

Japan

Prof. Toshikazu Kondo

Wakayama Medical University

Japan

Editorial Board Member

Prof. Adam Reich

University of Rzeszow

Poland

Dr. Akihiro Aoi

Griffith University Eskitis Institute

Australia

Nada Kadhi Australia

University Medical Center Mainz

Germany

Dr. Xinzhong Wu

Ocean College, Beibu Gulf University

China

Prof. Manar Atoum

Hashemite University Dean of Scientific

Research

Jordan

Dr. Xuehui He

Laboratory Medicine - Medical Immunology,

Radboudumc

Netherlands

Dr. Wei Boon Yap

Universiti Kebangsaan Malaysia

Malaysia

Prof. Xianquan Zhan

Xiangya Hospital, Central South University

China

Dr. Andrea Casadei Gardini

Department of Oncology, IRST-IRCCS

Italy

Dr. Kwong Tsang

Precision Biologics, Inc

United States

Dr. Hideki Kawai

Department of Thoracic Surgery, Akita Red

Cross Hospital

Japan

Prof. Juraj Ivanyi

Department of Mucosal Biology, Kings

College London

United Kingdom

Volume 5 Issue 2.1 • 2021

Trends in Immunotherapy

Editor-in-Chief

Prof. Dr. Fukumi Furukawa

Takatsuki Red Cross Hospital , Japan



Trends in Immunotherapy

<https://systems.enpress-publisher.com/index.php/ti/>

Contents

Original Research Article

- 1 The effects of isolates and immune function on hematologic parameters of Blastocystis infection rats**
Ting Deng, Juan Li, Xiaohua Li, Xiaobo Li, Yiming Yan
- 8 The correlation between Serum phospholipase A2 receptor antibody and clinicopathological features in patients with membranous nephropathy**
Qipeng Huang, Gaosi Xu, Fang Wang, Fang Zeng, Weidong Fang
- 14 Studies on the proliferation inhibition effects of TUA from actinidia chinensis radix on lung cancer xenografts in nude mice and its preliminary mechanism**
Xiaohua Guo, Haibo Hu, Qi Jin, Hongliang Li, Qilai Cheng
- 24 Combining PD-1/PD-L1 inhibitor and PARP inhibitor: a new perspective on the treatment of triple negative breast cancer**
Ruilian Xie
- 30 Experimental study on the expression and diagnostic significance of I-FABP in acute intestinal ischemia**
Haikun Li, Minhua Wang, Xiansen Zhu, Xiaoqing Zhou, Bin Yang, Qinghui Yin, Xiaoping Liu, Xiangfu Zeng, Yan Hu, Xiangtai Zeng
- 36 The expression and significance of 8-Hydroxydeoxyguanosine in breast cancer patients' blood, urine and cancer tissue**
Zhiyou Liu, Jian Yi, Feng'en Liu

Review Article

- 42 Effect of 1.25(OH)₂D₃ on experimental autoimmune neuritis and its mechanism**
Di Nian, Zhouhan Li, Junjie Sun, Peng Shi
- 51 Research progress on the role of sialic acid-binding immunoglobulin-like lectin 9 in various diseases**
Ling Cao, Xiaoliang Yuan
- 58 Research progress in immunotherapy of advanced non-small cell lung**

cancer

Xiaojuan Lu, Huaqiu Shi, Qiuyang Que, Song Qiu

65 Research progress of NK cell immunodeficiency in immune escape of acute leukemia

Yuling Zhang, Zhong Yu, Hailiang Li

72 Research progress in immunological mechanisms of Cryptococcus

Ying Song, Yufang Qiu, Weiyu Liu, Xiaoliang Yuan

79 Combination of anti-angiogenic therapy Apatinib and immune therapy potentiate tumor microenvironment

Chunyi Gao, Tianhui Hu

ORIGINAL RESEARCH ARTICLE

The effects of isolates and immune function on hematologic parameters of Blastocystis infection rats

Ting Deng, Juan Li*, Xiaohua Li, Xiaobo Li, Yiming Yan*

School of Basic Medicine, Gannan Medical University, Ganzhou 341000, Jiangxi Province, China. E-mail: lily_lij@163.com (Juan Li); yym2008101@163.com (Yiming Yan)

ABSTRACT

Objective: To define a complex of changes in hematologic parameters associated with subtypes (ST) of Blastocystis sp. infections and the status of immune function in Sprague Dawley (SD) rats, and lay the foundation for Blastocystis hominis pathogenesis research. **Methods:** 5 isolates of ST1, ST3 and ST7 were used, including 1 isolate of ST1 from symptomatic patient, 2 isolates of ST3 and ST7 from symptomatic patients and asymptomatic carrier separately. Immune compromise model was set up using dexamethasone (DEX) and infection models with 5 isolates of ST1, ST3 and ST7, and then examined the hematologic changes post infection 15 days using fully automatic hematology analyzer sysmex xe-2100. **Results:** The results showed that infections of Blastocystis STs led to the increase of platelet indexes including MPV and PDW except ST3 isolated from asymptomatic carrier only with PDW increase and the higher values of PLT in ST7 isolated from asymptomatic carrier compared with the controls in the immune competence status ($P < 0.05$). However, the infections of Blastocystis ST7 isolated from symptomatic patient gave rise to higher values of WBC, LYMP, EO, MCV and RDW-SD while lower values of NEU% compared with the controls in immune compromise status ($P < 0.05$). Meanwhile, higher values of WBC and LYMP and lower NEUT% values were observed in ST1 infections compared with the controls ($P < 0.05$); lower NEUT values in ST1 infections and controls compared with ST3 and ST7 respectively were observed ($P < 0.05$); the infection of ST3 isolated from symptomatic patient resulted in higher values of MCV and RDW-SD while the asymptomatic isolate of ST3 only had higher RDW-SD ($P < 0.05$). **Conclusion:** The virulence of Blastocystis sp. isolated from symptomatic patient is higher than that of the identical subtype one isolated from asymptomatic carrier. The infection of ST7 isolated from symptomatic patients may result in the most distinct hematologic changes among STs, and then followed by ST1 symptomatic isolate. And the severity of Blastocystis sp. infection may be mediated by the immune status of host.

Keywords: Blastocystis; Immune Function; Hematologic Parameters

ARTICLE INFO

Received 16 August 2021
Accepted 28 September 2021
Available online 6 October 2021

COPYRIGHT

Copyright © 2021 Ting Deng, et al.
EnPress Publisher LLC. This work is licensed under the Creative Commons Attribution-NonCommercial 4.0 International License (CC BY-NC 4.0).
<https://creativecommons.org/licenses/by-nc/4.0/>

1. Introduction

Blastocystis is a protozoan that lives in the intestines of humans, mammals, birds, mice and reptiles. The infection rate is about 3%–5% in developed countries and about 60% in developing countries^[1]. Many intestinal symptoms and skin diseases are related to Blastocystis infection^[1–3]. The most common intestinal symptoms of Blastocystis infection are diarrhea and abdominal pain^[4], and nonspecific symptoms include nausea, vomiting and flatulence^[1,4,5]. Based on small subunit rRNA gene analysis, 13 subtypes have been found^[6]. Among them, 9 types (ST1–ST9) are found in humans^[7,8]. Recent studies have suggested that the pathogenicity of Blastocystis is related to subtypes^[9,10], but the results are still controversial^[2,11]. Some reports believe that the symptoms of ST1 infection are highly correlated with

subtypes, suggesting that ST1 has potential pathogenicity^[12]. ST3 is the most common subtype in human epidemiological investigation, having potential pathogenicity according to some studies^[5,10]. ST7 is common in Asia^[1], but rarely reported in the West^[13], and most are isolated from patients with symptoms^[5]. It has been suggested that Blastocystis is an opportunistic pathogenic protozoan, because immunosuppressed people are prone to infection and show symptoms. However, the role of this protozoan in health and disease is unknown.

It is known that many pathogens such as bacteria, viruses and fungi can cause changes in hematologic parameters^[14-16]. There are also some reports on the changes of hematologic parameters caused by parasitic infection^[17-20], but there is little study on the changes of hematologic parameters caused by Blastocystis infection. It is reported that dexamethasone can cause apoptosis of thymus, spleen and lymph node cells and significantly inhibit the immune system^[21]. In this paper, dexamethasone was used to establish an immunosuppressive animal model to explore the relationship between the changes of hematologic parameters and isolates and immune function of Blastocystis infection rats.

2. Materials and methods

2.1 Collection of isolates and capsules

Five isolates, HC07-12 (ST1), HC09-01 (ST3), HC08-03 (ST3), HC07-03 (ST7) and HC09-05 (ST7), were used in this experiment. Among them, HC07-12, HC08-03 and HC07-03 were isolated from diarrhea patients in the First Affiliated Hospital of Gannan Medical College, and the rest were isolated from asymptomatic physical examination personnel. These isolates were conserved and passaged in the laboratory. The trophozoites in the LES medium of Blastocystis hominis were inoculated into the cystic medium after preliminary centrifugation. At the peak of capsule maturation on the 6th day, the capsules in the cystic medium were separated with lymphocyte separation solution. The capsules were treated with distilled water and stored at 4 °C for standby.

2.2 Experimental animals, feed, and experimental environment

60 SPF-grade SD rats, male, with a body mass of (100 ± 10) g, were purchased from Hunan SJA Laboratory Animal Co., Ltd., (animal certificate No.: 4300016942). All animals were fed in a single cage for 1 week with mixed formula feed (provided by the Experimental Animal Center of Gannan Medical College), ate and drank freely. Change drinking water and feed every day, keep the living environment of rats ventilated and clean, observe their conditions of eating, drinking, activity and defecation, and start the experiment after confirming the health of rats.

2.3 Establishment of the dexamethasone immunosuppression model

60 SD rats were adaptively maintained for 1 week and randomly divided into two groups, namely the immunosuppression group and immunonormal group. Immunosuppressive rats were added with dexamethasone at 0.25 mg kg⁻¹ d⁻¹ in drinking water for 10 days, while the rats in the immunonormal group were routinely housed.

2.4 Infection experiments

On the 11th day after immunosuppression modeling, the immunosuppression group and immunonormal group were randomly divided into 6 groups, respectively. The infection group was orally fed with 1000 capsules of HC07-12, HC09-01, HC08-03, HC07-03 and HC09-05 respectively, and the control group was orally fed with the same amount of normal saline (0.85% NaCl). Feces of all rats were collected every other day after gavage and placed in LES medium containing 10% calf serum^[22]. Typical vacuolar or granular type found by microscopic examination was positive for infection.

2.5 Collection of blood samples and determination of hematologic parameters

On the 16th day of infection, the rats in the two groups fasted food for 24 hours and water for 12 hours. Weigh and inject 10% chloral hydrate into the standard abdominal cavity of rats according to 0.3 mL 100 g⁻¹. Fix the limbs of anesthetized rats, collect blood from their hearts and inject it into heparin sodium anticoagulant tubes for examination.

The automatic hematology analyzer sysmex xe-2100, produced by Sysmex Corporation, was used to determine hematologic parameters by the impedance method.

2.6 Statistical analysis

Express hematologic parameters as $\bar{x} \pm s$, analyze data by SPSS 14.0 two-way ANOVA, and plot with prism 5.0.

3. Results

The results of changes in hematologic parameters caused by infection of different isolates under normal immune function and immunosuppression are shown in **Figures 1–10**. **Figure 1** shows that the PDW value of Blastocystis infection rats in the immunonormal group were higher than that in the control group, which was statistically significant ($P < 0.05$). **Figure 2** shows that except HC09-01 isolated from asymptomatic carriers, the MPV value of other Blastocystis infection rats in the immunonormal group were higher than that in the control group, which is statistically significant ($P < 0.05$).

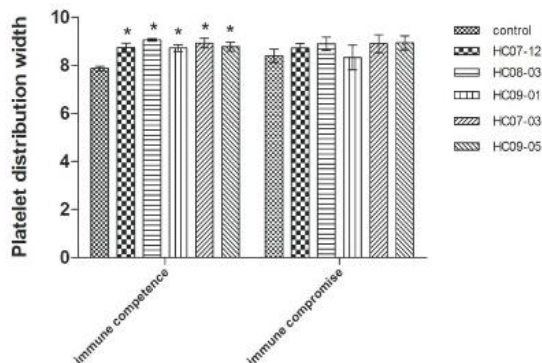


Figure 1. Effect of different isolates of Blastocystis infection on PDW of SD rats with different immune functional states. Note: * comparison with the control group, $P < 0.05$.

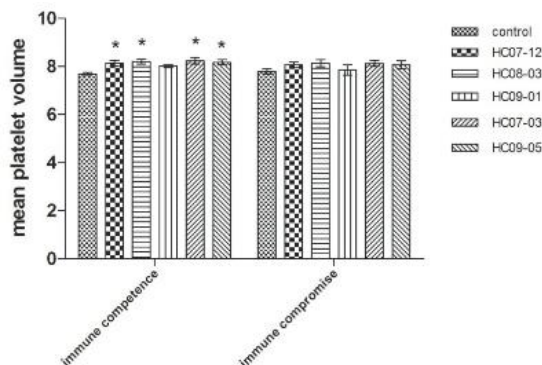


Figure 2. Effect of different isolates of Blastocystis infection on MPV of SD rats with different immune functional states. Note: * comparison with the control group, $P < 0.05$.

Figure 3 shows that ST7 HC09-05 isolated from asymptomatic carriers led to the PLT value of rats with normal immune function was higher than that of rats in the control group, which was statistically significant ($P < 0.05$).

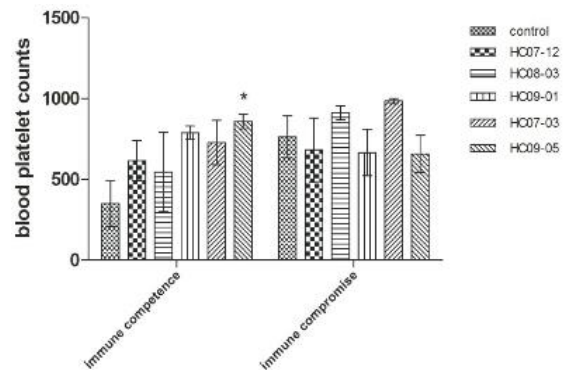


Figure 3. Effect of different isolates of Blastocystis infection on PLT of SD rats with different immune functional states. Note: * comparison with the control group, $P < 0.05$.

Figures 4 and 5 show that the WBC and LYMP values of rats in the immunosuppression group were higher than those in the control group ($P < 0.05$) due to the isolation of ST7 HC07-03 and ST1 HC07-12 from symptomatic patients.

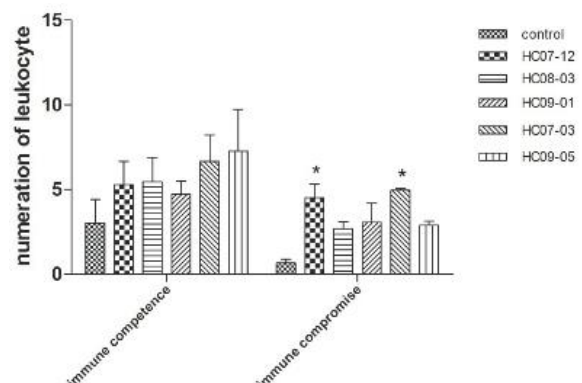


Figure 4. Effect of different isolates of Blastocystis infection on WBC of SD rats with different immune functional states. Note: * comparison with the control group, $P < 0.05$.

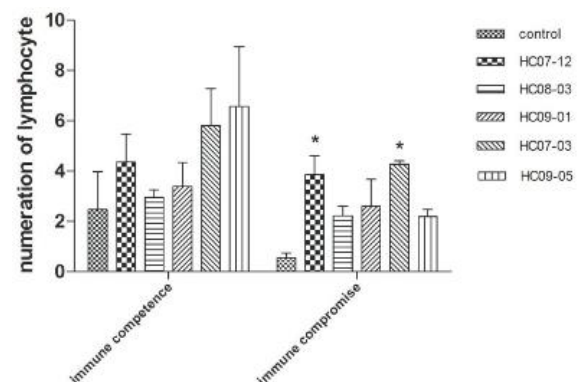


Figure 5. Effect of different isolates of Blastocystis infection on LYMP of SD rats with different immune functional states. Note: * comparison with the control group, $P < 0.05$.

Figure 6 shows that the infection of ST3 HC09-01 isolated from asymptomatic carriers resulted in the increase of NEUT value in the immunonormal group ($P < 0.05$). The infection of ST3 HC08-03 from symptomatic patients and ST3 HC09-01 and ST7 HC09-05 isolated from asymptomatic carriers resulted in the increase of NEUT value in the immunosuppression group.

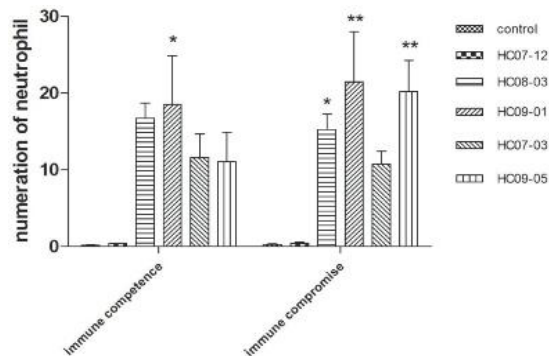


Figure 6. Effect of different isolates of Blastocystis infection on NEUT of SD rats with different immune functional states. Note: * comparison with the control group, $P < 0.05$.

Figure 7 shows that ST1 HC07-12 and ST7 HC07-03 isolated from symptomatic patients resulted in lower NEUT% of immunosuppressive rats than in the control and other subtypes ($P < 0.05$).

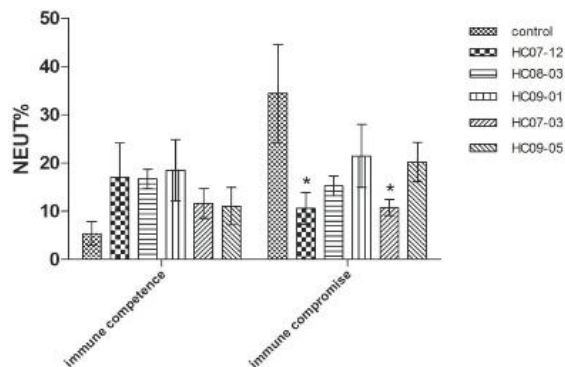


Figure 7. Effect of different isolates of Blastocystis infection on NEUT% of SD rats with different immune functional states. Note: * comparison with the control group, $P < 0.05$.

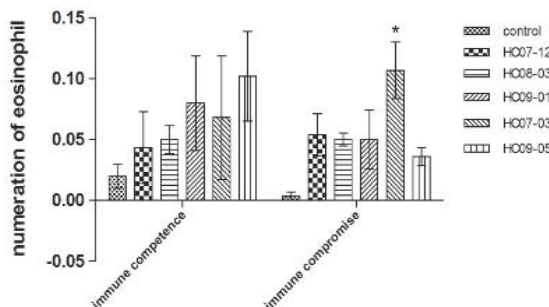


Figure 8. Effect of different isolates of Blastocystis infection on EO values of SD rats with different immune functional states. Note: * comparison with the control group, $P < 0.05$.

Figure 8 shows that ST7 HC07-03 isolated from symptomatic patients resulted in higher EO values of immunosuppressive rats compared with those of the control group ($P < 0.05$).

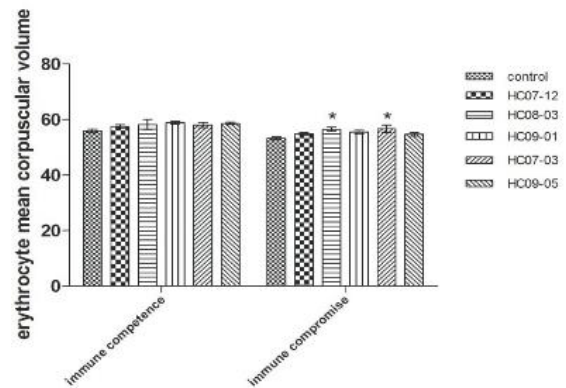


Figure 9. Effect of different isolates of Blastocystis infection on MCV values of SD rats with different immune functional states.

Note: * comparison with the control group, $P < 0.05$.

Figure 9 shows that ST7 HC07-03 and ST3 HC08-03 isolated from symptomatic patients resulted in higher MCV values of immunosuppressive rats than those of the control group ($P < 0.05$).

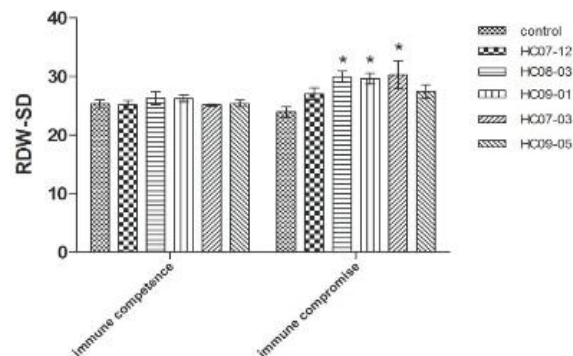


Figure 10. Effect of different isolates of Blastocystis infection on RDW-SD of SD rats with different immune functional states.

Note: * comparison with the control group, $P < 0.05$.

Figure 10 shows that the infection of ST7 HC07-03 and ST3 HC08-03 isolated from symptomatic patients and ST3 HC09-01 isolated from asymptomatic carriers was higher than that of the control group ($P < 0.05$).

4. Discussion

Blastocystis is a widely distributed intestinal parasitic protozoan of humans and many kinds of animals. Although Blastocystis infection is common, its pathogenesis is still controversial. This is because Blastocystis is not only distributed in symptomatic patients, but also in asymptomatic peo-

ple^[12,23], and Blastocystis has genetic diversity, and pathogenic strains coexist with non-pathogenic strains^[23,24]. The effects of different subtypes and different Blastocystis isolates in the same subtype on hematologic parameters in immunonormal and immunosuppressive rats were studied. Five isolates of subtypes ST1, ST3 and ST7 were used in this study. One isolate of each subtype was isolated from symptomatic patients, and ST3 and ST7 were isolated from asymptomatic carriers. In this study, it was found that under the condition of normal immune function, the infection of each isolate of Blastocystis only caused the overall or partial increase of platelet parameters PDW, MPV and PLT, suggesting that Blastocystis infection has the tendency to lead to coagulation, and its exact mechanism is not clear. Blastocystis infection releases proinflammatory factors such as IL-6, IL-8 and cysteine protease, which may have a potential mechanism to activate coagulation reaction. Blastocystis infection causes changes in the parameters of erythrocyte and leukocyte lines under immunosuppression, but it varies according to the strain. Isolation of ST3 and ST7 strains from symptomatic patients resulted in MCV and RDW-SD changes in immunosuppressive rats, suggesting that infection with strong toxic isoforms ST3 and ST7 may cause large cellular anemia, consistent with clinical reports that Blastocystis infection can cause iron deficiency anemia^[25].

The infection of ST7 isolated from symptomatic patients led to the increase of WBC, LYMP, NEUT and EO, and the decrease of NEUT%, which may be due to the increase of neutrophil number, but the increase proportion is less than that of WBC, LYMP and EO. The infection of ST1 isolated from symptomatic patients resulted in the increase of WBC and LYMP, but the decrease of NEUT and NEUT%. The infection of ST3 isolated from asymptomatic carriers increased the NEUT value of rats in the immunonormal group and immunosuppression group, while the infection of ST3 isolated from symptomatic patients only increased the NEUT value of rats in the immunosuppression group. Neutrophils are the most important movable phagocytes in mammals. As the first innate immune cell to reach the infected site, it plays an important

role in initiating innate immunity, inflammatory response and specific immune response. In this study, it was found that the number and proportion of neutrophils decreased due to the infection of ST1 with strong virulence, while the neutrophils increased due to the infection of ST3 with weak virulence. These results suggest that neutrophils may play an important role in immunity against Blastocystis infection. ST1 subtype Blastocystis may have virulence factors to kill neutrophils, but the exact mechanism needs to be further explored. This study found that the infection of ST3 isolated from asymptomatic carriers increased the number of neutrophils, but whether it could improve other natural immune functions, whether it was a normal member of intestinal microecology, and whether it had clinical application value still need to be confirmed by further research.

5. Conclusion

In conclusion, the virulence of the isolates from symptomatic patients was stronger than that of the same subtype isolated from asymptomatic carriers. The virulence of ST7 isolated from symptomatic patients was the strongest, resulting in the most extensive changes of hematologic parameters, followed by ST1, whose characteristic change was the decrease of neutrophils. The severity of Blastocystis infection also depends on the host's immune function status. Hosts with normal immune function are not pathogenic or only show a tendency to increase platelet parameters; immunosuppressive hosts can result in changing parameters of white blood cells and red blood cells.

Conflict of interest

The authors declare no potential conflicts of interest.

Acknowledgements

This research was supported by the National Natural Science Foundation of China (No. 30860254), and the Natural Science Foundation of Jiangxi Province (No. 20132BAB2050551).

References

1. Tan K. New insights on classification, identification, and clinical relevance of *Blastocystis* spp. *Clinical Microbiology Reviews* 2008; 21(4): 639–665.
2. Doğruman AF, Adisen E, Kustimur S, *et al.* The role of protozoan parasites in etiology of urticarial. *Turkiye Parazitolojii Dergisi* 2009; 33(2): 136–139.
3. Hameed DM, Hassanin OM, Zuel-Fakkar NM. Association of *Blastocystis hominis* genetic subtypes with urticarial. *Parasitology Research* 2011; 108(3): 553–560.
4. Tan K, Mirza H, Teo J, *et al.* Current views on the clinical relevance of *Blastocystis* spp. *Current Infectious Disease Reports* 2010; 12(1): 28–35.
5. Stensvold CR, Lewis HC, Hammerum AM, *et al.* *Blastocystis*: Unravelling potential risk factors and clinical significance of a common but neglected parasite. *Epidemiol Infect* 2009; 137: 1655–1663.
6. Parkar U, TraubRJ, Vitali S, *et al.* Molecular characterization of *Blastocystis* isolates from zoo animals and their animal-keepers. *Veterinary Parasitology* 2010; 169(1-2): 8–17.
7. Roberts T, Stark D, Harkness J, *et al.* Subtype distribution of *Blastocystis* isolates identified in a Sydney population and pathogenic potential of *Blastocystis*. *European Journal of Clinical Microbiology & Infectious Diseases* 2013; 32: 335–343.
8. Tan T, Sugnaseelan S, Sharma R, *et al.* Genetic diversity of caprine *Blastocystis* from Peninsular Malaysia. *Parasitology Research* 2013; 112: 85–89.
9. Domínguez-Márquez MV, Guna R, Muñoz C, *et al.* High prevalence of subtype 4 among isolates of *Blastocystis hominis* from symptomatic patients of a health district of Valencia (in Spanish). *Parasitology Research* 2009; 105: 949–955.
10. Jimenez-Gonzalez DE, Martinez-Flores WA, Reyes-Gordillo J, *et al.* *Blastocystis* infection is associated with irritable bowel syndrome in a Mexican patient population. *Parasitology Research* 2012; 110(3): 1269–1275.
11. Souppart L, Moussa H, Cian A, *et al.* Subtype analysis of *Blastocystis* isolates from symptomatic patients in Egypt. *Parasitology Research* 2010; 106(2): 505–511.
12. Yan Y, Su S, Lai R, *et al.* Genetic variability of *Blastocystis hominis* isolates in China. *Parasitology Research* 2006; 99(5): 597–601.
13. Forsell J, Granlund M, Stensvold CR, *et al.* Subtype analysis of *Blastocystis* isolates in Swedish patients. *European Journal of Clinical Microbiology & Infectious Diseases Official Publication of the Europe* 2012; 31: 1689–1696.
14. Fortun J, Sanz MA, Madero L, *et al.* Update on bacteraemia in oncology and hematology. *Enfermedades Infecciosas Y Microbiología Clínica* 2011; 29: 48–53.
15. Burciaga-Robles LO, Step DL, Krehbiel CR, *et al.* Effects of exposure to calves persistently infected with bovine viral diarrhea virus type 1b and subsequent infection with *Mannheimia haemolytica* on clinical signs and immune variables: Model for bovine respiratory disease via viral and bacterial interaction. *Journal of Animal Science* 2010; 88(6): 2166–2178.
16. Carreras E, Vazquez L, Rodriguez Tudela JL, *et al.* Update on fungemia in oncology and hematology. *Enfermedades Infecciosas Y Microbiología Clínica* 2011; 29(Suppl 4): 42–47.
17. Cheng H, Guo Y, Shin JW. Hematological effects of *Blastocystis hominis* infection in male foreign workers in Taiwan. *Parasitology Research* 2003; 90(1): 48–51.
18. Blonar CA, Curtis MA, Chan HM. Growth, nutritional composition, and hematology of Arctic charr (*Salvelinus alpinus*) exposed to toxaphene and tapeworm (*Diphyllobothrium dendriticum*) larvae. *Archives of Environmental Contamination and Toxicology* 2005; 48(3): 397–404.
19. Ruiz-Saez A, Sifontes LN, Feijoo R, *et al.* Platelet dysfunction-eosinophilia syndrome in

- parasitized Venezuelan children. *American Journal of Tropical Medicine & Hygiene* 2005; 73(2): 381–385.
20. Yasini S, Khaki Z, Rahbari S, *et al.* Hematologic and clinical aspects of experimental ovine anaplasmosis caused by *Anaplasma ovis* in Iran. *Iranian Journal of Parasitology* 2012; 7(4): 91–98.
 21. Li X, Bai S, Zhou L, *et al.* Comparison of the immunosuppressive functions induced by cyclophosphamide and dexamethasone in intestinal mucosa in mice. *Chinese Journal of Immunology* 2013; 29(1): 39–44.
 22. Malatyali E, Ozcelik S. Isolation of *Blastocystis* spp. from human hosts and *in vitro* determination of different morphological forms. *Turkiye Parazitolojii Dergisi* 2011; 35: 19–22.
 23. Nagel R, Cuttell L, Stensvold CR, *et al.* *Blastocystis* subtypes in symptomatic and asymptomatic family members and pets and response to therapy. *Internal Medicine Journal* 2012; 42(11): 1187–1195.
 24. Meloni D, Poirier P, Mantini C, *et al.* Mixed human intra- and inter-subtype infections with the parasite *Blastocystis* sp. *Parasitology International* 2012; 61(4): 719–722.
 25. El Deeb HK, Salah-Eldin H, Khodeer S. *Blastocystis hominis* as a contributing risk factor for development of iron deficiency anemia in pregnant women. *Parasitology Research* 2012; 110: 2167–2174.

ORIGINAL RESEARCH ARTICLE

The correlation between Serum phospholipase A2 receptor antibody and clinicopathological features in patients with membranous nephropathy

Qipeng Huang^{1,2*}, Gaosi Xu², Fang Wang¹, Fang Zeng¹, Weidong Fang¹

¹ Ganzhou People's Hospital, Ganzhou 341000, Jiangxi Province, China.

² The Second Affiliated Hospital of Nanchang University, Nanchang 330000, Jiangxi Province, China. E-mail: hqp77@126.com

ABSTRACT

Objective: To assess the correlation between Serum phospholipase A2 receptor antibody and clinicopathological features in patients with membranous nephropathy. **Method:** The patients being hospitalized for renal biopsy were selected in this study from January 2016 to January 2018. And normal controls were randomly selected; all the patients were divided into idiopathic membranous nephropathy and non-idiopathic membranous nephropathy groups; patients with idiopathic membranous nephropathy were divided into three groups, namely stage I, stage II and stage III; using software for statistical analysis. **Results:** A total of 357 patients were enrolled, including 155 patients with idiopathic membranous nephropathy, 183 patients with non-idiopathic membranous nephropathy, and 19 cases for normal controls. The average age of the idiopathic membranous nephropathy (IMN) group is higher than that of the membranous nephropathy group ($P = 0.01$). Different pathological stages of idiopathic membranous nephropathy general clinical characteristics analysis results showed that the age, cys c, serum creatinine (Scr) in stage III membranous nephropathy group were higher than those of the stage I and II membranous nephropathy (P values were 0.003, 0.000 and 0.000 respectively); titers of serum phospholipase A2 receptors antibody with stage II and III membranous nephropathy higher than the stage I membranous nephropathy group ($P = 0.006$); serum albumin (Alb) levels correlated inversely with serum anti-PLA2R antibody titers ($r_s = -0.234$, $P = 0.003$), serum antiphospholipase A2 receptor (PLA2R) antibody titer level in patients with idiopathic membranous nephropathy was significantly higher than that in patients with non-membranous nephropathy ($P < 0.001$). **Conclusion:** Baseline titer of serum anti-PLA2R antibody is negatively correlated with Alb in the IMN patients, and serum anti-PLA2R antibody level in patients with stage I IMN was significantly lower than stage II and III IMN patients.

Keywords: Phospholipase A2 Receptor Antibody; Idiopathic Membranous Nephropathy; Clinicopathological

ARTICLE INFO

Received 25 July 2021
Accepted 13 October 2021
Available online 17 October 2021

COPYRIGHT

Copyright © 2021 Qipeng Huang, et al.
EnPress Publisher LLC. This work is licensed under the Creative Commons Attribution-NonCommercial 4.0 International License (CC BY-NC 4.0).
<https://creativecommons.org/licenses/by-nc/4.0/>

1. Introduction

Membranous nephropathy is one of the common histopathological types in primary glomerular diseases. It is a group of diseases characterized by subepithelial immune complex deposition of glomerular basement membrane (GBM) with diffuse thickening of GBM^[1]. According to the cause, it can be divided into: (1) secondary membranous nephropathy; (2) familial membranous kidney disease; (3) idiopathic membranous nephropathy (IMN). IMN accounts for about 70% of all membranous nephropathy. Because the etiology of IMN is unclear, although it has been recognized that IMN is due to the autoantibodies against some antigens on the glomerular epithelial cell membrane, which fall off and deposit under the epithelial cells after binding with

the antigen, reactivate the complement and form a membrane attack complex C5b-9, causing a series of renal injury, its exact pathogenesis is not clear^[2]. Therefore, the diagnosis, treatment and prognosis of IMN have been controversial for a long time. With the deepening of research, Beck *et al.*^[3] found anti phospholipase A2 receptor (PLA2R) antibodies in the blood of most IMN patients through Western blotting and mass spectrometry in 2009, and inferred that a glycoprotein-m-type PLA2R with a molecular weight of 185 kD on podocytes of IMN patients is the main target antigen. However, no anti-PLA2R antibody was detected in the blood of non IMN patients, suggesting that anti-PLA2R antibody is a unique molecular biological change of IMN, which is of great significance for the diagnosis and differential diagnosis of IMN. Qin *et al.*^[4] also verified the value of detecting serum anti-PLA2R antibody in IMN patients in Chinese population. Many studies have confirmed that serum PLA2R antibody is related to the disease activity of IMN, but the relationship between serum PLA2R antibody titer and clinical biochemical indexes such as Alb and proteinuria is still controversial. There are also differences in serum PLA2R antibody titer in patients with different pathological stages. The purpose of this study is to clarify the relationship between serum PLA2R antibody and serum protein to explore the relationship between quantitative proteinuria, cystatin c (cys c), blood lipid, creatinine and other clinical and biochemical indexes, and to explore the application value of PLA2R antibody in early detection and differentiation of pathological stages of membranous nephropathy.

2. Data and methods

2.1 Research objects

Patients who underwent renal biopsy in the Department of Nephrology of Ganzhou people's Hospital from January 2016 to January 2018 were selected. Clinical indexes such as age, gender, Alb, cys c, blood cholesterol (CHO), blood creatinine (Scr) and proteinuria were collected, and randomly selected health physical examiners. The serum PLA2R antibody of healthy subjects was detect-

ed by enzyme-linked immunosorbent assay (ELISA). According to the results of pathological light microscope, immunofluorescence and electron microscope of renal biopsy, they were divided into the IMN group and the non-membranous nephropathy group. IMN patients were divided into stage I, stage II and stage III groups according to the results of the pathological stage. All patients were not given glucocorticoid before renal biopsy and immunosuppressive therapy.

2.2 Detection of serum anti-PLA2R antibody

5 mL of blood was drawn from patients before renal biopsy, and the anti-PLA2R antibody titer in blood samples was quantitatively detected by enzyme-linked immunosorbent assay (ELISA). The anti-PLA2R antibody IgG detection kit (ELISA) was produced by the Germany company EURO-IMMUN, and was operated in strict accordance with the instructions. If the serum anti-PLA2R antibody titer was greater than 14 RU mL^{-1} , it was determined as positive.

2.3 Pathological diagnosis of renal biopsy

After excluding contraindications and signing the informed consent, all patients underwent right renal inferior pole puncture under ultrasound guidance, and the renal tissues were routinely examined by HE, PAS, PASM, Masson staining, light microscope, immunofluorescence and electron microscope. The Ehrenreich Chung staging method was used for the staging of membranous nephropathy^[5].

2.4 Statistical method

SPSS 22.0 statistical software was used for analysis. The quantitative data were subject to normal distribution and expressed by mean \pm standard deviation. One-way analysis of variance (ANOVA) was used for inter group comparison, and the SNK method was used for multiple comparison. If not obeying the normal distribution, it was expressed by the median M (Min, Max). The nonparametric test of multiple independent sample data was used for the comparison between groups. When it is statistically significant, the Nemenyi method was used for multiple comparison. Qualitative data were expressed by cases (%), and comparison between

groups was tested by χ^2 . Spearman correlation coefficient was used to analyze the correlation between variables, and $P < 0.05$ was statistically significant.

3. Results

3.1 Basic data of enrolled patients

A total of 357 patients were selected, including 155 patients with IMN, 99 males and 56 females: the ratio of males to females was 1.77:1, and the average age was (50.16 ± 10.60) years. There were 183 cases of non-membranous nephropathy, including 116 males and 67 females: the ratio of males to females was 1.73:1, with an average age of (43.32 ± 16.41) years; it included 69 cases of IgA nephropathy, 26 cases of minimal change, 28 cases of focal segmental glomerulosclerosis (FSGS), 18 cases of podocyte disease (MCD or potential FSGS), 28 cases of mesangial proliferative glomerulonephritis, and 8 cases of diabetic nephropathy and 6 cases of Henoch Schonlein purpura nephritis. There were 19 healthy cases as the control group. There was no significant difference in gender ratio between IMN group and non-membranous nephropathy group ($P = 0.21$). The average age of the IMN group was higher than that of the non-membranous nephropathy group ($P = 0.01$).

3.2 Comparison of anti-PLA2R antibody (RU mL⁻¹) between IMN and non-membranous nephropathy

The serum PLA2R antibody titer in the IMN group was significantly higher than that in the non-membranous nephropathy group ($H = 235.448$, $P < 0.001$). The results are shown in **Table 1**.

Table 1. Comparison of anti-PLA2R antibody (Ru mL⁻¹) between patients with IMN and non-membranous nephropathy

Patients	M (Min, Max)	H	P
IMN	66.80 (0.60, 691.46)	235.44	<0.001
Non-membranous nephropathy	0.61 (0.60, 8.89)	8	
Control	0.615 (0.60, 2.35)		

3.3 Analysis of general clinical characteristics of IMN in different pathological stages

The age, cys c and Scr in stage III membranous nephropathy group were higher than those in stage I membranous nephropathy group and stage II membranous nephropathy group (P values were

0.003, 0.000 and 0.000, respectively); the titer of serum anti PLA2R antibody in stage II membranous nephropathy group and stage III membranous nephropathy group was higher than that in stage I membranous nephropathy group ($P = 0.006$). The results are shown in **Table 2**.

Table 2. Analysis of general clinical characteristics of IMN in different pathological stages

Clinical characteristics	Stage I	Stage II	Stage III	Test statistics	P
Number of cases	19	117	19		
Sex (M/F)	13/6	73/44	13/6	0.425	0.798
Age (years)	49.89 ± 9.75	49.26 ± 10.35	57.63 ± 6.28	5.898	0.003
Cys c (mg·L ⁻¹)	0.97 ± 0.15	1.00 ± 0.29	1.48 ± 0.58	18.208	0.000
Proteinuria (g/24 h)	5.17 ± 3.34	5.63 ± 3.25	5.39 ± 2.94	0.189	0.828
Alb (g·L ⁻¹)	26.29 ± 8.08	25.64 ± 6.32	27.41 ± 4.24	0.667	0.515
CHO (mmol·L ⁻¹)	8.18 ± 2.79	7.84 ± 2.46	7.54 ± 1.29	0.349	0.706
Scr (μmol·L ⁻¹)	75.32 ± 11.09	74.85 ± 25.63	99.67 ± 30.15	8.195	0.000
anti-PLA2R (RU·mL ⁻¹)	18.96 (0.75, 66.00)	135.90 (0.60, 691.46)	128.9 (2.88, 526.20)	10.261	0.006

3.4 Spearman correlation between anti-PLA2R antibody and clinical indexes in patients with IMN

Serum PLA2R antibody was negatively correlated with Alb ($r_s = -0.234$, $P = 0.003$) with statistical significance, and had no correlation with clinical indexes such as cys c, CHO, Scr and proteinuria ($P = 0.432$, 0.704, 0.526 and 0.078 respectively). The results are shown in **Table 3**.

Table 3. Spearman correlation analysis between anti-PLA2R antibody and clinical indexes in patients with IMN

Clinical characteristics	r_s	P
Cysc (mg L ⁻¹)	-0.064	0.432
Proteinuria (g/24 h)	-0.142	0.078
Alb (g L ⁻¹)	-0.234	0.003
CHO (mmol L ⁻¹)	-0.031	0.704
Scr (μmol·L ⁻¹)	-0.051	0.526

4. Discussions

With the development of global society, economy and environment, the incidence rate and detection rate of IMN also show a rising trend^[6], which is one of the important reasons for chronic kidney disease and progression to end-stage renal

disease. The exploration of IMN's etiology and complete exposition of its molecular biological pathogenesis has never stopped. In 1959, Heymann *et al.*^[7] established a Heymann nephropathy model similar to the pathological changes of human membranous nephropathy in rats. In 2009, Beck *et al.*^[3] found that anti-PLA2R antibody existed in the blood of most IMN patients by Western blotting and mass spectrometry and inferred that a glycoprotein M-type PLA2R with a molecular weight of 185 kD on podocytes of IMN patients is the main target antigen combined with it, but no anti-PLA2R antibody is detected in the blood of non IMN patients, which suggests that anti-PLA2R antibody is a unique molecular biological change of IMN. Through these important studies, The consensus that IMN is an organ specific autoimmune disease has become more and more clear and rich, and further research has been carried out on the detection methods and value of these target antigens and their autoantibodies, especially serum anti-PLA2R antibody and renal PLA2R have become a global research hotspot in recent years.

There are different conclusions on the correlation between serum PLA2R antibody titer and IMN disease activity at home and abroad. Most research results tend to believe that that there is negative correlation between serum PLA2R antibody and Alb. A German study^[8] shows that patients with high serum PLA2R antibody titer are often older, and the Alb level was also lower; Kei *et al.*^[9] detected the serum PLA2R antibody in 38 patients with IMN and 21 patients with secondary membranous nephropathy by enzyme-linked immunosorbent assay and indirect immunofluorescence detection at the same time. It was found that the Alb level was negatively correlated with the serum PLA2R antibody titer ($r = -0.468$, $P = 0.043$), but not with the quantification of proteinuria; Yun *et al.*^[10] observed 100 IMN patients and found that the initial Alb level of patients with positive serum PLA2R antibody was significantly lower than that of patients with negative serum PLA2R antibody ($2.5 \text{ g } \text{DL}^{-1}$ vs $3.1 \text{ g } \text{DL}^{-1}$, $P = 0.004$). The proportion of proteinuria within the scope of nephrotic syndrome in the serum antibody positive group was also significantly higher than that in the serum an-

tibody negative group (87.0% vs 48.4%, $P = 0.001$), but there was no significant difference in renal function between the two groups. Qin *et al.*^[11] found that serum PLA2R antibody was detected by enzyme-linked immunosorbent assay in a study including 572 patients diagnosed as IMN through renal biopsy. Correlation analysis showed that serum antibody titer was negatively correlated with Alb level ($r = -0.20$, $P < 0.001$), but Ramachandran *et al.*^[12] found that there was no significant correlation between PLA2R staining in renal tissue and serum PLA2R antibody titer ($r = 0.03$, $P = 0.76$), there is also no correlation between serum antibody titer and proteinuria and serum albumin. Radice *et al.*^[13] found a positive correlation between serum PLA2R antibody level and proteinuria quantification. However, Julien *et al.*^[14] did not find a correlation between serum PLA2R antibody titer and proteinuria amplitude through retrospective analysis of the clinical data of 68 patients with IMN pathologically diagnosed by renal biopsy. In terms of correlation, Zhou Guangyu *et al.*^[15] studied 15 patients with IMN and found that serum PLA2R antibody was positively correlated with proteinuria and negatively correlated with blood ALB, while Yuan Li *et al.*^[16] analyzed the antibody titer and laboratory related data of 17 patients with IMN with positive serum PLA2R antibody and found that there was no correlation between anti PLA2R antibody and proteinuria and renal function Spearman correlation analysis between anti-PLA2R antibody and clinical indexes in IMN patients in this study suggests that serum anti-PLA2R antibody and Alb was negatively correlated, and has no correlation with cys c , CHO , Scr and proteinuria, the reasons of which may be as follows. (1) Although anti-PLA2R antibody is an important serum marker of IMN, it is only a part of the molecular biology link of the specific pathogenesis of IMN patients, which reflects the immunological activity of patients to a certain extent, or it is only a initiating factor. The production of proteinuria in IMN patients is mainly related to glomerular podocytes. It is related to the destruction of basement membrane structure and functional integrity. For IMN patients with positive serum PLA2R antibody, a very complex molecular bio-

logical stimulation reaction chain is required from the synthesis and secretion of serum PLA2R antibody to the formation of proteinuria. This process also involves some other cells and molecules other than anti-PLA2R antibody. (2) The interval of the renal biopsy in different patients is in different stages of its natural course of diseases, and bias may occur when the sample size of the study is small. (3) The quantitative determination of 24-hour proteinuria is affected by many factors such as urinary volume and glomerular filtration rate. Hypoproteinemia is often more prominent in patients with serious clinical conditions. At this time, due to the low osmotic pressure of plasma colloid, the effective circulating blood volume is also reduced, with reduced blood perfusion of kidney, and the 24-hour urine volume of these patients may also be significantly reduced. So the quantitative urine protein can not well reflect their disease activity, and the Alb index is relatively affected by fewer factors, so it can more accurately reflect the severity of clinical diseases.

The analysis of the general clinical characteristics of IMN in different pathological stages showed that the age, *cys c* and serum Scr in stage III membranous nephropathy group were higher than those in stage I membranous nephropathy and stage II membranous nephropathy group (*P* values were 0.003, 0.000 and 0.000, respectively); the serum PLA2R antibody titer of stage II membranous nephropathy and stage III membranous nephropathy was higher than that of stage I membranous nephropathy (*P* = 0.006), which was basically consistent with the observation results of some previous studies^[17,18]. For patients with IMN, especially those with membranous nephropathy related to anti-PLA2R antibody, the serum PLA2R antibody titer is related to the stage of renal pathological progress. Patients with low serum antibody titer often correspond to the pathological changes of early membranous nephropathy. The serum PLA2R antibody detected in this study is IgG4. Although from the half-life and fluctuation law of IgG4, the low titer level may be at two different pinots of time of the same concentration in the early stage of antibody synthesis and the late stage of elimination. Both early membranous nephropathy and late

membranous nephropathy in the pathological progression stage of membranous nephropathy may correspond to the low titer level of serum antibody, but patients with pathological late membranous nephropathy often have clinical symptoms and signs and are detected, and have even been treated for a period of time. Therefore, for newly hospitalized IMN patients, when the serum PLA2R antibody titer is low, the renal pathology is more likely to be early membranous nephropathy. It can be inferred that the serum PLA2R antibody titer has a certain predictive value for the renal pathological development stage of newly hospitalized IMN patients, especially early membranous nephropathy. Theoretically, there are certain rules from antigen stimulation to antibody synthesis and secretion and onset time, patient body surface area or body weight, IgG half-life, kidney adsorption capacity and swelling curve characteristics of PLA2R antibody. Based on these rules, it is also possible to infer the pathological progression stage of patients with membranous nephropathy by detecting the titer level of serum PLA2R antibody. Because the sample size of this study is too small, and there are no patients with stage IV and V membranous nephropathy included in the study, more cases and patients including all pathological stages are needed as the research objects, and the establishment of a biological and mathematical model based on the half-life and inflation law of PLA2R antibody in blood and the relationship between quantitative and qualitative change of immune complex in the process of kidney deposition gives the possibility to further explore the exact relationship between the quantitative change of serum PLA2R antibody and the progression stage of nephrosis in patients with IMN.

Therefore, the conclusion of this study is that the baseline titer of serum PLA2R antibody in patients with IMN is negatively correlated with serum albumin, and may be related to the pathological progression stage of membranous nephropathy. The titer of serum PLA2R antibody in patients with stage I IMN is significantly lower than that in patients with stage II and III IMN. Limited to conditions, this study is a single center with a small sample size research, its limitations are inevitable. We

expect a larger sample size and multicenter research to provide more powerful evidence.

Conflict of interest

The authors declare no potential conflicts of interest.

References

1. Wang H. Nephrology (in Chinese). 3rd ed. Beijing: People's Medical Publishing House; 2008. p. 1032–1042.
2. Lai W, Yeh T, Chen P, *et al.* Membranous nephropathy: A review on the pathogenesis, diagnosis, and treatment. *Journal of the Formosan Medical Association* 2015; 114(2): 102–111.
3. Beck LH, Bonegio RG, Lambeau G, *et al.* M-type phospholipase A2 receptor as target antigen in idiopathic membranous nephropathy. *The New England Journal of Medicine* 2009; 361(1): 11–21.
4. Qin W, Beck LH, Zeng C, *et al.* Anti-phospholipase A2 Receptor antibody in membranous nephropathy. *Journal of the American Society of Nephrology* 2011; 22(6): 1137–1143.
5. Ehrenreich T, Chung J. Pathology of membranous nephropathy. *Patho Annu* 1968; 3: 145–186.
6. Couser WG. Primary membranous nephropathy. *Clinical Journal of the American Society of Nephrology Cjasn* 2017; 12(6): 983.
7. Heymann W, Hackel DB, Harwood S, *et al.* Production of nephrotic syndrome in rats by Freund's adjuvants and rat kidney suspensions. *Experimental Biology & Medicine* 1959; 100: 660–664.
8. Hoxha E, Harendza S, Pinnschmidt H, *et al.* M-type phospholipase A2 receptor autoantibodies and renal function in patients with primary membranous nephropathy. *Clinical Journal of the American Society of Nephrology Cjasn* 2014; 9(11): 1883–1890.
9. Kei H, Masayuki I, Shohei T, *et al.* Anti-phospholipase A2 receptor (PLA2R) antibody and glomerular PLA2R expression in Japanese patients with membranous nephropathy. *Plos One* 2016; 11(6): e0158154.
10. Yun J, Yang S, Dong K, *et al.* Autoantibodies against phospholipase A2 receptor in Korean patients with membranous nephropathy. *Plos One* 2013; 8(4): e62151.
11. Qin H, Zhang M, Le W, *et al.* Combined assessment of phospholipase A2 receptor autoantibodies and glomerular deposits in membranous nephropathy. *Journal of the American Society of Nephrology* 2016; 27(10): 3195–3203.
12. Ramachandran R, Kumar V, Kumar A, *et al.* PLA2R antibodies, glomerular PLA2R deposits and variations in PLA2R1 and HLA-DQA1 genes in primary membranous nephropathy in South Asians. *Nephrology, Dialysis, Transplantation: Official Publication of the European Dialysis and Transplantation Association-European Renal Association* 2016; 31(9): 1486–1493.
13. Radice A, Trezzi B, Maggiore U, *et al.* Clinical usefulness of autoantibodies to M-type phospholipase A2 receptor (PLA2R) for monitoring disease activity in idiopathic membranous nephropathy (IMN). *Autoimmunity Reviews* 2016; 15(2): 146–154.
14. Jullien P, Barbara SP, Maillard N, *et al.* Anti-phospholipase A2 receptor antibody levels at diagnosis predicts spontaneous remission of idiopathic membranous nephropathy. *Clinical Kidney Journal* 2017; 10(2): 209–214.
15. Zhou G, Jin L, Yu J, *et al.* Correlation between serum anti PLA2R antibody and disease condition in adult patients with membranous nephropathy (in Chinese). *Chinese Journal of Nephrology* 2012; 28(2): 111–114.
16. Yuan L, Shi L, Xu Y, *et al.* Clinical significance of anti-M type phospholipase A2 receptor antibody in treatment of idiopathic membranous nephropathy. *Chinese Journal of Clinical Laboratory Science* 2015; 33 (8): 581–585.
17. Ping Z, Fu D Z, Su X, *et al.* Increasing frequency of idiopathic membranous nephropathy in primary glomerular disease: A 10-year renal biopsy study from a single Chinese nephrology centre. *Nephrology* 2015; 20 (8): 560–566.
18. Cattran DC. Idiopathic membranous glomerulonephritis. *Kidney International* 2001; 59(5): 1983–1994.

ORIGINAL RESEARCH ARTICLE

Studies on the proliferation inhibition effects of TUA from *Actinidia chinensis Radix* on lung cancer xenografts in nude mice and its preliminary mechanism

Xiaohua Guo, Haibo Hu, Qi Jin, Hongliang Li, Qilai Cheng*

School of Pharmacy, Gannan Medical University, Ganzhou 341000, Jiangxi Province, China. E-mail: cql_57@126.com

ABSTRACT

Objective: To investigate inhibitory effect of TUA (2β , 3β , 23-trihydroxy-urs-12-en-28-oic acid) isolated from *Actinidia chinensis Radix* on the lung cancer xenografts in nude mice and explore its preliminary mechanism. **Methods:** NCI-H460 cells were implanted into nude mice and the transplantation tumor block from nude mice of more than 2 generations was inoculated to the right armpits of BALB/c mice with dissecting needle to establish a lung cancer xenograft model. When the transplanted volume was about 50 mm^3 , the mice were randomly divided into 6 groups: (1) model group; (2) 10 mg kg^{-1} cisplatin group; (3) 10 mg kg^{-1} PDTC group; (4) TUA high dose group (30 mg kg^{-1}); (5) TUA middle dose group (12 mg kg^{-1}); (6) TUA low dose group (6 mg kg^{-1}). Administration approach was intratumoral injection. The effects of each group on the weight of transplanted tumor animals, the volume and weight of tumor were continuously observed for 14 days. Tumor volume growth curve was drawn and tumor inhibitory rate and index were calculated; HE staining was used to observe nude mice tumor tissue pathological changes. The effects of TUA on NF- κ B signaling pathway related proteins were detected by immunohistochemistry and Western blot. **Results:** *In vivo* experiments showed that the transplanted tumors in nude mice became smaller compared with the models. With the increase of TUA dose, the tumor tissue became smaller and smaller, especially in high TUA dose (30 mg kg^{-1}). It had the similar size with the NF- κ B inhibitor PDTC (10 mg kg^{-1}) group. HE dyeing observation results confirmed the degree of tumor necrosis and fission in TUA treated tumor tissues obviously decreased. Immunohistochemical results showed that comparing the TUA treatment group with the model group, p65 expression in tumor tissues was reduced, and expression of I κ B α increased. Western blot results also showed that the NF- κ B related p65 protein expression levels decreased, at the same time I κ B α protein expression level increased; the apoptosis related proteins Survivin protein expression was depressed, Caspase-3 protein expression was promoted. **Conclusion:** TUA significantly inhibits the growth of lung transplantation tumor and its mechanism. It may be related to the decreasing the expression of p65, Survivin and increasing the expression of I κ B α , Caspase-3 in tumor tissues.

Keywords: 2, 3β , 23-Trihydroxy-urs-12-en-28-oic Acid; Lung Cancer; Xenograft; Apoptosis-Related Proteins

ARTICLE INFO

Received 29 August 2021
Accepted 24 October 2021
Available online 29 October 2021

COPYRIGHT

Copyright © 2021 Xiaohua Guo, et al.
EnPress Publisher LLC. This work is licensed under the Creative Commons Attribution-NonCommercial 4.0 International License (CC BY-NC 4.0).
<https://creativecommons.org/licenses/by-nc/4.0/>

1. Introduction

At present, lung cancer is still the main cause of mortality of cancer patients all over the world, among which patients with non-small cell lung cancer (NSCLC) account for almost 85%–90%^[1]. The main reasons for the high mortality of lung cancer are the difficulty of early diagnosis, easier metastasis to surrounding tissues and organs, and lower and lower sensitivity to chemotherapeutic drugs^[2]. Although the double platinum chemotherapy regimen containing cisplatin and carboplatin has been used for many years in the treatment of more than 50% of NSCLC patients, the 5-year survival rate is only 15.7%–17.5%, and most patients eventually deteriorate and die in the next decade. Alth-

ough many countries in the world have been trying to apply some new strategies for the prevention and treatment of lung cancer, the 5-year survival rate will not exceed 18%^[3]. Therefore, in order to improve the survival rate of lung cancer patients, the most urgent task is to develop new clinical drugs, especially some natural products derived from animals and plants, which have extensive biological activities and almost no adverse reactions.

Over the past century, natural products have provided a large number of drug sources for the treatment of human diseases^[4]. In recent years, *in vivo* and *in vitro* studies have shown that a considerable number of terpenoids isolated and identified from plants have significant antitumor activities against different kinds of tumor cell lines. Some of them have been successfully applied to the prevention of clinical human tumor diseases, especially some pentacyclic triterpenoids compounds such as oleanolic acid, glycyrrhetic acid and carbenoxolone^[5]. Therefore, the research and development of new pentacyclic triterpenoids and their derivatives with stronger antitumor activity have attracted more and more interest of researchers with life science related professional backgrounds such as medicine, biochemistry and molecular biology.

TUA (2 β , 3 β , 23-trihydroxy-urs-12-en-28-oic acid) is one of the main active components of Ursane type triterpenoids extracted, isolated and identified from *Actinidia chinensis* Radix, a traditional Chinese medicine. *Actinidia chinensis* Radix, also known as Chinese actinidia root, is a folk Chinese herbal medicine widely used in Jiangxi, Guangxi and Sichuan. It has always been said that it can treat “unknown swelling poison” among the people. It has been used in many areas to prevent and treat tumors and has achieved good curative effects, including gastric cancer, esophageal cancer, liver cancer, and lung cancer^[6]. A large number of studies have shown that Ursane type triterpenoids and their derivatives with the similar structure to TUA have a wide range of pharmacological activities, such as antioxidant effect, anti-immune effect, neuroprotective effect, and anti-tumor effect^[7].

Previous studies of our research group showed that TUA could inhibit the proliferation of lung cancer cell NCI-H460 to induce tumor cell apopto-

sis *in vitro*^[8]. In this experiment, the lung cancer cell NCI-H460 cell line was used to prepare the nude mouse transplantation tumor model and TUA was taken as the research object to observe the effect of TUA application on the NCI-H460 xenografts *in vivo* and explore the mechanism of action, which can provide a theoretical basis for the further elaboration of the potential chemoprevention use of cancer.

2. Materials

2.1 Drugs (reagent)

TUA was isolated from the root of *Actinidia chinensis* Radix (*Actinidiaceae*) in this laboratory. The *Actinidia chinensis* Radix was separated by solvent extraction and various column chromatography. The obtained compounds were identified by physical and chemical analysis and spectral technology, and finally the Ursane triterpenoids were obtained. The purity of TUA was examined by Agilent 1100 HPLC, DAD detector and the area normalization method. The content was more than 97%. In this experiment, TUA was dissolved with dimethyl sulfoxide (DMSO). The final concentration of solvent DMSO shall not exceed 0.1%. The drugs used in the experiment were generally stored in -4°C refrigerator for no more than 4 days. The concentration of drugs was adjusted by RPMI-1640 medium; using it right after it was ready. Roswell Park Memorial Institute 1640 medium (RPMI1640, GIBCO Company, USA); SDS (Bio-Rad company, Batch No.: 210008353); DAB color development kit (Zhongshan Jinqiao, Batch No.: K133319D); various antibodies: (1) GAPDH high-quality internal reference labeled with internal reference antibody HRP (Shanghai Kangcheng Biology, Article No.: KC-5G5); (2) primary antibody name: Caspase-3 (novusibo, Article No.: NB500-210), corresponding secondary antibody: Rabbit Anti-Mouse IgG (H + L)-HRP; primary antibody name: Survivin (Cell signaling, Article No.: 2802), corresponding secondary antibody: Rabbit Anti-Mouse IgG (H + L)-HRP; primary antibody name: p65, I κ B α (abcam, Article No.: 16502), corresponding secondary antibody: Goat Anti-Rabbit IgG (H + L), Mouse/Human ads-HRP; (3) secondary antibody

name: Goat Anti-rabbit IgG (H + L), Mouse/Human ads-HRP (southern biotech, Article No.: 4050-05); secondary antibody name: Rabbit Anti-Mouse IgG (H + L)-HRP (southern biotech, Article No.: 6170-05); DMSO and all other biochemical reagents were purchased from Sigma-Aldrich (St. Louis, MO, USA).

2.2 Key instruments

Inverted optical microscope (CKX41, OLYMPUS); cell constant temperature incubator (HERACELL150i, Thermo scientific); desktop high-speed frozen centrifuge (H1650R, Shanghai Luxiangyi); microplate reader (SPECTRA max Plus 384, Molecular Devices, Inc); electrophoresis system (Mini-Proten Tetra System, Bio-RAD Corporation); gel imager: (ChemiDoc XRS + System, Bio-RAD Corporation).

2.3 Cell system and experimental animals

The human lung cancer cell line NCI-H460 was purchased from the Shanghai Cell Bank, Chinese Academy of Sciences. 70 SPF-level BALB/c nude mice, 18–22 g, 6–8 weeks old, female, were purchased from Shanghai Slac Laboratory Animal Co., Ltd. with license No.: SCXK (Shanghai) 2012–0002.

3. Experimental methods

3.1 Cell culture and treatment

NCI-H460 cells were placed in RPMI 1640 medium (which mainly contained 10% fetal bovine serum (FBS), 100U mL⁻¹ penicillin, 2 mmol L⁻¹ L-glutamine, and 100 mg L⁻¹ streptomycin, *etc.*) and routinely cultured in a confined incubator with 95% saturated humidity and 5% CO₂, at 37 °C. Cell growth was observed daily, with a single passage cycle of 3 days. All subsequent experiments used normally cultured NCI-H460 cells in the log growth phase. Meanwhile, the final concentration of dimethyl sulfoxide (DMSO) of the dissolved samples (test drug and control products) was ≤0.1%.

3.2 Preparation of the transplanted tumor animal model

Collect NCI-H460 cells in logarithmic growth stage, wash them with serum-free and anti-

otic-free RPMI-1640 culture medium for 3 times, count the cells by flow cytometry, adjust the cell density, conduct animal experiments in the ultra-clean stage, briefly disinfect them with alcohol cotton. Then blow and mix the cell suspension with 1 mL sterile syringe, and inoculate 0.1 mL subcutaneously on the right side of nude mice for 5×10^5 cells/animal to prepare tumorigenic animals. After 2 weeks, the subcutaneous tumor tissue was taken, soaked in precooled PBS. The tumor capsule and internal tissue were removed, the active tissue was cut into small squares of about 1 cm³, and the anatomical needle was inserted into the subcutaneous part of the right limb of nude mice.

3.3 Tumor suppressor experiments

Three days after inoculation, the growth of nude mice was observed every day. The action, response to external stimuli, diet, fecal color and weight (W) of nude mice were observed, as well as the tumor growth. After the third day of transplantation, when the transplanted volume was about 50 mm³, the mice were randomly divided into 6 groups. Intraperitoneal administration was started and the tumor diameter was measured. The specific grouping is as follows: (1) the model group: given normal saline after tumor inoculation; (2) the positive control group 1: given cisplatin after tumor inoculation, with a dose of 10 mg kg⁻¹; (3) the positive control group 2: given NF-κB inhibitor pyrrolidine dithiocarbamate (PDTC), with a dose of 10 mg kg⁻¹; (4) the TUA high dose group: with a dose of 30 mg kg⁻¹; (5) the TUA medium dose group: with a dose of 12 mg kg⁻¹; (6) the TUA low dose group: with a dose of 6 mg kg⁻¹. The longest diameter (a) and the shortest diameter (b) of the tumor were measured with a vernier caliper, and the tumor volume (V) was calculated. $V \text{ (cm}^3\text{)} = 1/6\pi ab^2 = 0.5236ab^2$. Draw tumor volume growth curve. At the end of the experiment, the nude mice were killed by cervical dislocation. The subcutaneous tumor blocks were taken, weighed and photographed, soaked in 4% paraformaldehyde for fixation, and half of the tumor samples from each group were frozen in liquid nitrogen (–80 °C) for subsequent pathological sections, such as HE staining, immunohistochemistry and Western blotting. A. growth index: the longest

diameter (a) and shortest diameter (b) were measured for 4 to 5 times per week, and the calculated volume: $V = 1/6\pi ab^2 = 0.5236ab^2$; then draw the tumor volume growth curve. B. tumor index: tumor index (mg/g) = tumor weight (mg)/mouse weight (g). C. tumor suppressor rate (%) = $[(1 - T/C)] \times 100\%$. In the formula, T means the average tumor weight of the test drug group; C means the average tumor weight of the control group (the model group, tumor bearing animals without being given drugs).

3.4 Using HE staining to observe the histopathological changes of tumors in nude mice

3.4.1 Making slices

The tumor tissue was fixed in 4% formaldehyde solution for 5 days. Remove the tissue from the fixed solution and trim it to an appropriate shape and thickness. The tissue blocks were dehydrated by 80%, 90%, 95%, 100% ethanol I, 100% ethanol II and 100% ethanol III, given transparent treatment carried with xylene I for 45 min, and xylene II for 15 min, and soaked in wax for 5 h. According to the principle that the material is taken from the bottom, the tissue is embedded with paraffin, and the wax block is placed at $-20\text{ }^{\circ}\text{C}$ for refrigeration after cooling and solidification. Make slices (with $4\text{ }\mu\text{m}$ thickness) and put the slices into $65\text{ }^{\circ}\text{C}$ incubator for 6–12 h; box and store at room temperature.

3.4.2 HE staining

Xylene I for 15 min, xylene II for 15 min, absolute ethanol I for 5 min, absolute ethanol II for 5 min, 95% ethanol for 5 min, 80% ethanol for 5 min, tap water immersion for 1 min. Immerse the slices in Hematoxylin dyeing solution, dye at room temperature for 5 min, and wash with tap water for 1 min. Immerse the slices in 1% hydrochloric acid alcohol solution for a few seconds and in tap water until the tissue returns to blue. Immerse the slices in Eosin staining solution for 3–5 min, and wash off the floating color on the slide with tap water. 80% ethanol for 0.5 min, 95% ethanol I for 0.5 min, 95% ethanol II for 0.5 min, absolute ethanol I for 0.5 min, absolute ethanol II for 0.5 min, xylene I transparent for 3 min, xylene II transparent for 3 min. After taken out, they were sealed with neutral gum, ob-

served with microscopic and photographed; staining results were analyzed.

3.5 Using immunohistochemistry (IHC) to detect the expression of p65 and I κ B α in tumor tissues

3.5.1 Making slices

Tissue slices were placed in a $65\text{ }^{\circ}\text{C}$ incubator for 6–12 h.

3.5.2 IHC to detect the expression of p65 and I κ B α in tumor tissues

Using Xylene to dewax. Gradient alcohol rehydration: xylene I for 20 min—xylene II for 20 min—100% ethanol for 5 min—100% ethanol II for 5 min—95% ethanol for 5 min—80% ethanol for 5 min—PBS washing for 3×3 min. Block and inactivate endogenous peroxidase: incubate with 3% H_2O_2 at $37\text{ }^{\circ}\text{C}$ for 10 min, and rinse with PBS for 3×3 min. Antigen repair: microwave repair in 0.01 M citric acid buffer (pH 6.0), natural cooling to room temperature, PBS washing for 3×3 min, drop the primary antibody and incubate it in the refrigerator at $4\text{ }^{\circ}\text{C}$ to overnight (use PBS buffer to replace the primary antibody as negative control), then turn to room temperature equilibrium for 30 minutes, and rinse with PBS for 3×5 min. Then add secondary antibody, incubate at $37\text{ }^{\circ}\text{C}$ for 15 min, and rinse with PBS for 3×5 min. DAB reaction staining, observe the reaction progress under the microscope, and rinse with tap water; hematoxylin re-staining, drying, and sealing.

3.5.3 Data statistics

Under the microscope, three different visual fields were randomly selected for each immunohistochemical section ($\times 200$) to observe and interpret the positive expression intensity and positive rate. The staining results were analyzed by semi-quantitative analysis: scored by staining intensity combined with the percentage of positive cells.

3.6 Western blot to test the expression of p65, I κ B α , Caspase-3

Take an appropriate amount of tumor tissues preserved in liquid nitrogen, add 1 mL of cell lysate containing 1% protease inhibitor, homogenize it in a homogenizer, extract the total protein of cells,

quantify it with BCA. Equal amount of total protein (40 μg) was taken for semi-dry transmembrane with a 10% SDA-PAGE, Bio-Rad transmembrane ometer, and 5% skimmed milk was used to seal. Adding the primary antibody and incubating at 4 $^{\circ}\text{C}$ for the night, and washing the membrane. Adding the secondary antibody and incubating at room temperature for 1 h, and washing the membrane. Using ECL to show colors, and analyzing the image by Gel-pro Analyzer software. The protein content was expressed by the ratio of the primary antibody/GAPDH. The dilution ratio of the primary antibody p65, I κ B α was 1:2,000, while the dilution ratio of the corresponding secondary antibody Goat Anti-Rabbit IgG (H + L), Mouse/Human ads-HRP was 1:20,000; the dilution ratio of the primary antibody Caspase-3 was 1:500, the dilution ratio of the primary antibody Survivin was 1:1,000, while that of the corresponding secondary antibody Rabbit Anti-Mouse IgG (H + L)-HRP was 1:1,000. GAPDH labeled by HRP was taken as an internal reference with a dilution ratio of 1:10,000.

3.7 Statistical analysis

The experiments were repeated at least 3 times. The data were statistically analyzed by SPSS 17.0 software. The measurement data were expressed with $\bar{x} \pm s$, and the counting data were expressed in rate. The comparison between measurement data groups was tested by independent sample t , and analysis of variance was used for multi group comparison. $P < 0.05$ means the difference was statistically significant.

4. Results

4.1 Tumor suppressor experiments

Animal tumorigenesis and growth: 59 of 60 nude mice in this experiment had tumorigenesis, with the tumorigenesis rate of 98.30%. After inoculating the tumor block for 3 days, tumor like nodules with a diameter of about 3–4 mm could be seen, and the texture was soft. After that, the neoplastic nodules became harder and the volume increased significantly. The change of subcutaneous transplanted tumor in nude mice after administration is shown in **Figure 1**, the growth curve after administration for 2 weeks (day 1–day 14) is shown in

Figure 2, and the tumor weight inhibition rate and tumor index are shown in **Table 1**. It can be seen from **Figure 1** that after administration, the tumor tissue in nude mice became smaller; with the increasing dose of TUA, the tumor tissue became smaller and smaller, especially at the high dose of TUA (30 mg kg^{-1}), and the tumor tissue size was similar to that of NF- κ B inhibitor PDTC (10 mg kg^{-1}). Similar results can be obtained from the growth curve in **Figure 2**. The tumor tissue volume in the model group gradually increased (from 59.16 mm^3 to 1177.81 mm^3), and the tumor volume in the administration group increased slowly, which was more obvious at the high dose of TUA (30 mg kg^{-1}) (from 59.16 mm^3 to 429.11 mm^3), further indicating that TUA has a certain inhibitory effect on the growth of tumor tissues. Similar conclusions can be drawn from the tumor weight inhibition rate and tumor index in **Table 1**. Comparing high and medium dose of TUA with model groups, the differences were statistically significant ($P < 0.05$ or $P < 0.01$). The treatment effects of cisplatin and the NF- κ B inhibitor PDTC, the drugs commonly used clinically for lung cancer, were also statistically significant when compared with model groups ($P < 0.01$) (**Table 2**).

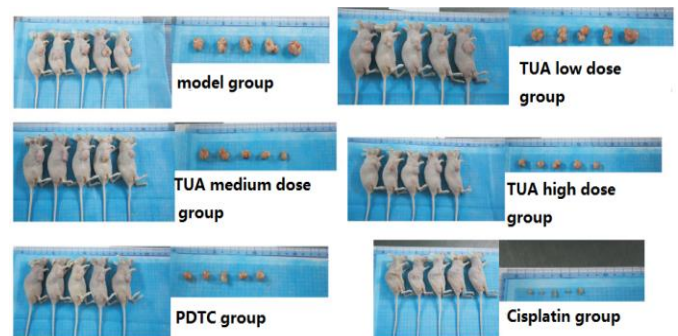


Figure 1. Effect of TUA on the tumor growth in nude mice.

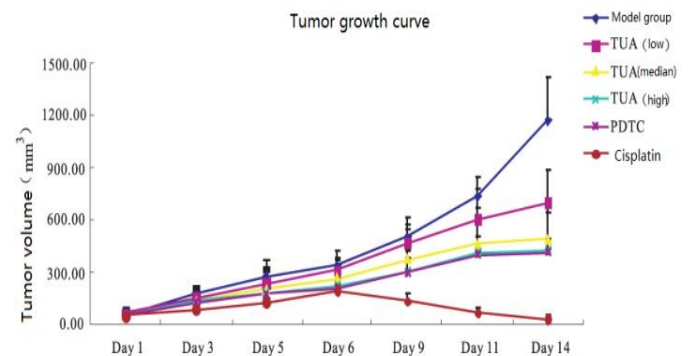


Figure 2. The inhibition effect of TUA on the tumor growth in nude mice (Growth curve).

Table 1. Tumor growth inhibitory rate and tumor markers/ $\bar{x} \pm s$, n = 5

Groups	Tumor inhibitory rate /%	P	Tumor index	P
Model group	0.00 ± 0.00		2.40 ± 12.36	
TUA (high)	85.81 ± 16.33**	0.007	26.52 ± 5.48**	0.006
TUA (median)	58.53 ± 10.54*	0.021	32.07 ± 10.77*	0.042
TUA (low)	45.07 ± 9.95*	0.025	40.62 ± 9.58*	0.018
PDTC	84.23 ± 13.24**	0.003	27.06 ± 6.85**	0.007
Cisplatin	90.31 ± 16.84**	0.008	20.88 ± 5.02**	0.008

Table 2. Analysis of variance results (ANOVA)

Source of difference	Quadratic sum	Free degree	Variance	Value F	Value P
Between groups	39.45	4	9.86	18.60	0.00
Within group	12.19	23	0.53		
Total difference	51.64	27			

4.2 HE staining

Transplanted tumor tissues by He staining presented blue nucleus, pink cytoplasm and bright red blood cells, which are shown in **Figure 3**. As can be seen from the figure, a large number of tumor necrosis areas and nuclear division phenomenon were visible in the tissue slices of the model group. In the TUA group, similar to the PDTC and cisplatin groups, the degree of tumor necrosis and nuclear division image were significantly reduced, and more collagen fibers can be seen. It is further proved that TUA has some inhibitory effect on the proliferation of transplanted tumors from the perspective of the pathology.

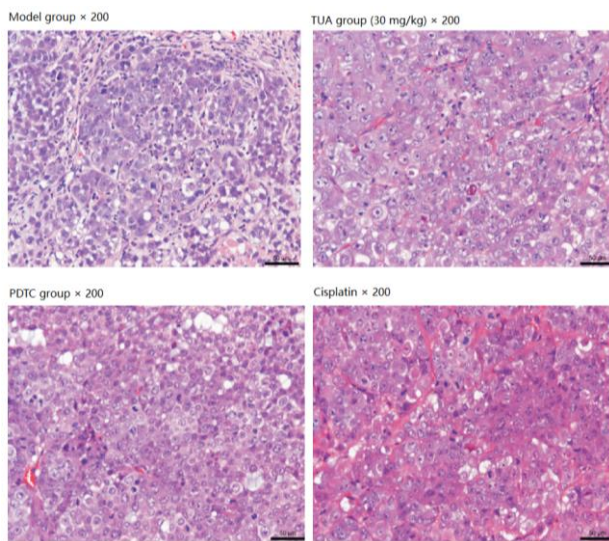
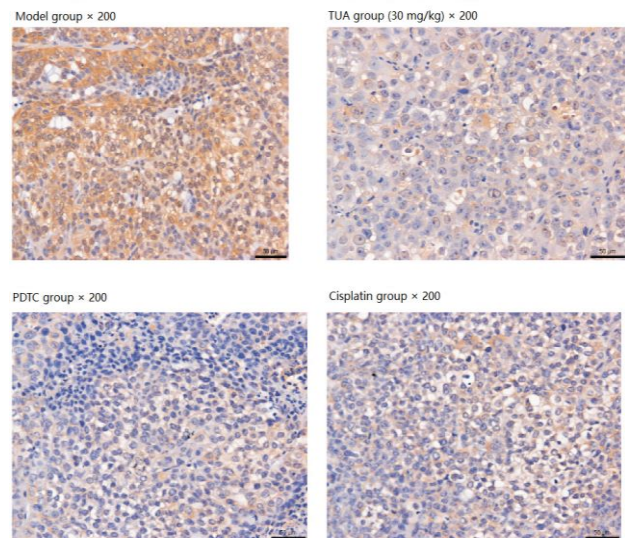


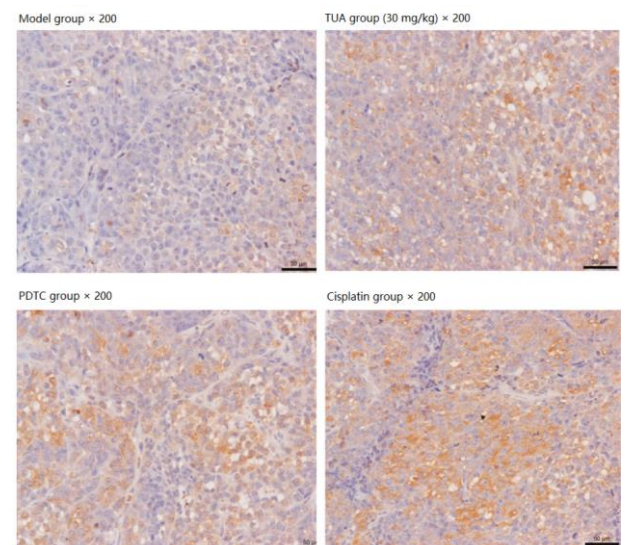
Figure 3. Histopathological changes of tumor after TUA treatment (HE staining).

4.3 Immunohistochemistry

The immunohistochemical method was used to detect the expression of NF- κ B (p65), I κ B α in transplanted tumor tissues. Immunostaining results are shown in **Figure 4**. It can be seen from the figure that p65 immune positive was mainly located in the nucleus and cytoplasm, while I κ B α immunopositivity was mainly localized in the cytoplasm of cells, both of which were brownish yellow. Compared with the model group, the expression of p65 in tumor tissues decreased in the TUA treatment group (**Figure 4A**), while the expression of I κ B α increased (**Figure 4B**), and the positive control drugs PDTC and cisplatin also showed similar effects.



A. p65 immunohistochemistry results.



B. I κ B α immunohistochemistry results.

Figure 4. Effect of TUA on expressions of p65, I κ B α in tumor.

4.4 Western blot results

The changes of apoptosis-related protein ex-

pression in transplanted tumor tissues were analyzed by Western blot, and the results of each treatment group are shown in **Figure 5**. It is known from the figure that the expression level of p65 protein associated with NF- κ B decreased, along with the increase of the expression of I κ B α protein. Survivin protein expression associated with apoptosis was inhibited and Caspase-3 protein expression was increased. The TUA high-dose group (30 mg kg⁻¹) was comparable to the positive control drugs PDTC and cisplatin.

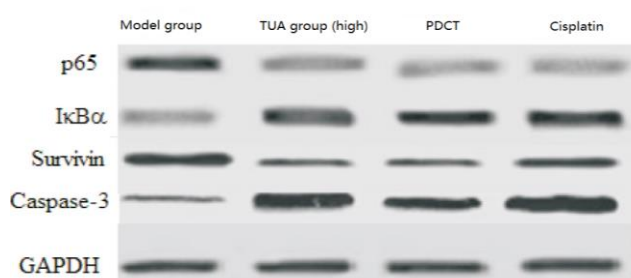


Figure 5. Influence of TUA on expressions of apoptosis-related proteins in tumor.

5. Discussion

As we all know, the urgent problem encountered in the treatment of lung cancer is the wide range of adverse reactions and drug resistance of antitumor drugs used in chemotherapy. It is urgent to adopt new treatment strategies for the diagnosis and treatment of lung cancer. For example, extracting and separating natural products from driven plants with strong anti-lung cancer effect and small toxic and side effects has always been an effective way. In recent years, many studies have demonstrated that TUA isolated from Chinese herbal medicine have extensive antitumor activity. In order to develop more effective anticancer drugs, plant extracts or monomer compounds rich in TUA have attracted more and more interest of researchers. For example, the antitumor effects of ursolic acid, asiatic acid, ilein and a series of its derivatives isolated from Chinese herbal medicine have been confirmed, and some compounds have been applied in clinical trials. However, the antitumor effect of TUA in *Actinidia chinensis* Radix has not been reported, especially the anti-lung cancer effect of TUA. Therefore, it is necessary to systematically investigate its pharmacological activity. In this study, the results confirmed that TUA had potential inhibitory effect

on lung cancer growth *in vivo* (transplanted tumor), and had less toxic and side effects on normal tissues. The experiment also confirmed that its mechanism of inhibiting tumor growth may be related to tumor cell apoptosis through inhibiting NF- κ B signaling pathway.

NF- κ B is an important transcription factor involved in tumorigenesis associated with inflammatory diseases^[9]. NF- κ B is generally highly expressed in human lung tumor tissues or tumor cells. High expression of NF- κ B is associated with many aspects of tumorigenesis, such as tumor cell growth, anti-apoptotic effect, metastasis, tumor angiogenesis and resistance to chemotherapeutic drugs^[10]. The activation of NF- κ B is related to tumor cell apoptosis, tumorigenesis and development, so it can inhibit IKK β /NF- κ B signaling pathway to achieve the purpose of treating related tumors^[11]. A large number of studies have confirmed that when NF- κ B is inhibited, the proliferation of tumor cells is inhibited. At the same time, the cell cycle is also blocked, and the apoptosis is increased gradually^[12]. NF- κ B combines with DNA target to form homologous or heterodimer and regulates the transcription of downstream genes, resulting in tumor cell proliferation and diffusion^[13]. In conclusion, NF- κ B plays an important role in the development of innovative antitumor drugs. NF- κ B is likely to be a new therapeutic target.

During the research on the prevention and treatment of lung cancer (NSCLCCs), whether *in vivo* or *in vitro*, there are many natural products, such as curcumin^[14], vinorelbine^[15], Feroniellin A^[16], and Minnelide^[17]. It has been demonstrated that inhibiting tumor tissue growth and inducing tumor cell apoptosis can be achieved by inhibiting NF- κ B pathway. The Tsao's research group showed that Protocatechuic acid (PCA) enables the dose-dependent downregulation of the expression of the NF- κ B p50 and NF- κ B p65 protein in the lung cancer cell line A549, H3255, and Calu-6^[18]. Another study also proved that Bee venom (BV) can regulate NF- κ B activity to inhibit the further proliferation of lung cancer A549 and NCI-H460 cell lines^[19]. The results of Western blot showed that the expression of p65 protein in transplanted tumors was inhibited after TUA treatment. At the same

time, I κ B α protein expression increased. It indicated that the apoptosis of NSCLCCs mediated by TUA is related to the inhibition of NF- κ B activity, which is consistent with the above results.

In the development of tumors, cells apoptosis generally plays the role of reversing regulation (which can prevent the rapid proliferation and differentiation of tumor cells). This process is co-regulated by a number of apoptosis promoters and repressors of apoptosis. The ability to stimulate and restore apoptosis of tumor cells is an effective tumor control pathway. Activated NF- κ B can inhibit tumor cell apoptosis in a variety of ways, mainly by inducing the expression of anti-apoptotic proteins such as tumor apoptosis protein inhibitory family (IAPs), Bcl-2 family and TRAF family, or inhibiting the expression of apoptosis promoting proteins such as Caspase family. Therefore, inhibition of NF- κ B signaling pathway will contribute to the expression of genes involved in tumorigenesis and development, which in turn will accelerate the apoptosis of tumor cells. Survivin, an important member of the IAPs family—tumor apoptosis suppressor proteins, is expressed only in embryonic tissues in non-pathological states but not in adult terminal differentiated tissues. However, in pathological cases, Survivin is expressed in the vast majority of tumor tissues. It is currently believed that the mechanism that Survivin promotes tumor development is probably related to its promoting tumor cell proliferation, inhibiting tumor cell apoptosis, and promoting tumor metastasis and invasion^[20]. In recent years, many studies have shown that Survivin upregulates its expression in lung and gastric cancer tissues^[21]. The results of this study showed that NCI-H460 cells had decreased Survivin expression in tumor cells after TUA treatment, and that Survivin expression in it was diminished with increasing TUA's concentration. It is speculated that it is due to the regulatory function of gene expression being inhibited, which cannot help tumor cells avoid apoptosis, at the same time blocking the abnormal proliferation of tumor cells and accelerating the further apoptosis of tumor cells. Caspase-3 is an important effector molecule in apoptosis signal transduction pathway, leading to apoptosis^[22]. The results also confirmed that the expression level

of Caspase-3 in NCI-H460 cells increased after TUA treatment.

The xenograft tumor model of lung cancer NCI-H460 cells in nude mice was prepared to observe the effect of TUA on transplanted tumor in nude mice, so as to provide experimental basis for further study of the anti-lung cancer effect and mechanism of TUA. The results of tumor inhibition experiment and HE staining showed that after treatment with different concentrations of drugs, TUA had a certain inhibitory effect on the transplanted tumor of NCI-H460 nude mice. Compared with the model group, the difference was significant ($P < 0.01$), and the tumor inhibition effect was similar to that of cisplatin and NF- κ B inhibitor PDTC. In order to explore the mechanism of the anti-tumor effect of TUA on NCI-H460 nude mice, in this experiment, immunohistochemistry and Western blot technology were used to detect the expression of the transplanted tumor and the apoptosis-related protein p65, I κ B α , Survivin, Caspase-3 in each experimental group. The results also confirmed that the levels of p65 protein expression were decreased. At the same time, the level of protein I κ B α expression was increased. Survivin protein expression of proteins associated with apoptosis was inhibited and Caspase-3 protein was upregulated.

In conclusion, this experiment confirmed that TUA has potential inhibitory effect on human lung cancer cell line NCI-H460 by transplanting tumor *in vivo*, and its possible anti-tumor mechanism is mainly to inhibit the NF- κ B signaling pathway and the expression of related genes regulated by it, so as to promote tumor cell apoptosis. The results of this study can provide a theoretical basis for the further development of TUA as a clinical anti-lung cancer drug.

Conflict of interest

The authors declare no potential conflicts of interest.

Acknowledgements

Fund project: National Natural Science Foundation of China (81360627); Science and Technology Research Project of Jiangxi Provincial Department of Education (GJJ14694).

References

1. Burris HA. Shortcomings of current therapies for non-small-cell lung cancer: Unmet medical needs. *Oncogene* 2009; 28(Suppl 1): 4–13.
2. Benlloch S, Alenda C, Galbis-Caravajal JM, *et al.* Expression of molecular markers in mediastinal nodes from resected stage I non-small-cell lung cancer (NSCLC): Prognostic impact and potential role as markers of occult micrometastases. *Annals of Oncology* 2009; 20(1): 91–97.
3. Song J, Sohn EJ, Kim B, *et al.* Inhibition of protein kinase C α/β II and activation of c-Jun NH2-terminal kinase mediate glycyrrhetic acid induced apoptosis in non-small cell lung cancer NCI-H460 cells. *Bioorganic & Medicinal Chemistry Letters* 2014; 24(4): 1188–1191.
4. Mishra BB, Tiwari VK. Natural products: An evolving role in future drug discovery. *European Journal of Medicinal Chemistry* 2011; 46(10): 4769–4807.
5. Li J, Huang R, Yao G, *et al.* Synthesis and biological evaluation of novel aniline-derived asiatic acid derivatives as potential anticancer agents. *European Journal of Medicinal Chemistry* 2014; 86(4): 175–188.
6. Zuo L, Wang Z, Fan Z, *et al.* Evaluation of antioxidant and antiproliferative properties of three Actinidia (*Actinidia kolomikta*, *Actinidia arguta*, *Actinidia chinensis*) extracts *in vitro*. *International Journal of Molecular Sciences* 2011; 13(5): 5506–5518.
7. Zhang X, Wu J, Dou Y, *et al.* Asiatic acid protects primary neurons against C2 -ceramide-induced apoptosis. *European Journal of Pharmacology* 2012; 679(1-3): 51–59.
8. Cheng Q, Li H, Huang Z, *et al.* 2 β , 3 β , 23-trihydroxy-urs-12-ene-28-olic acid (TUA) isolated from *Actinidia chinensis* Radix inhibits NCI-H460 cell proliferation by decreasing NF- κ B expression. *Chemico Biological Interactions* 2015; 240: 1–11.
9. Lee H, Herrmann A, Deng J, *et al.* Persistently activated Stat3 maintains constitutive NF-kappaB activity in tumors. *Cancer Cell* 2009; 15(4): 283–293.
10. Hu F, Qiao T, Xie X, *et al.* Knockdown of the inflammatory factor pentraxin-3 suppresses growth and invasion of lung adenocarcinoma through the AKT and NF-kappaB pathways. *Journal of Biological Regulators & Homeostatic Agents* 2014; 28(4): 649–657.
11. Luo J, Kamata H, Karin M. IKK/NF-kappaB signaling: Balancing life and death—A new approach to cancer therapy. *Journal of Clinical Investigation* 2005; 115(10): 2625–2632.
12. Bharti AC, Aggarwal BB. Chemopreventive agents induce suppression of nuclear factor-kappaB leading to chemosensitization. *Annals of the New York Academy of Sciences* 2002; 973(1): 392–395.
13. Rayet B, Gálinas C. Aberrant rel/nfkb genes and activity in human cancer. *Oncogene* 1999; 18(49): 6938–6947.
14. Mehta HJ, Patel V, Sadikot RT. Curcumin and lung cancer—A review. *Targeted Oncology* 2014; 9(4): 295–310.
15. Qi C, Gao S, Li H, *et al.* The effect and mechanism of vinorelbine on cisplatin resistance of human lung cancer cell line A549 /DDP. *Chinese Journal of Lung Cancer* 2014; 17(2): 148–154.
16. Kaewpiboon C, Surapinit S, Malilas W, *et al.* Feroniellin A-induced autophagy causes apoptosis in multidrug-resistant human A549 lung cancer cells. *International Journal of Oncology* 2014; 44(4): 1233–1242.
17. Rousalova I, Banerjee S, Sangwan V, *et al.* Minnelide: A novel therapeutic that promotes apoptosis in non-small cell lung carcinoma *in vivo*. *Plos One* 2013; 8(10): e77411.
18. Tsao SM, Hsia TC, Yin MC. Protocatechuic acid inhibits lung cancer cells by modulating FAK, MAPK, and NF- κ B pathways. *Nutrition & Cancer* 2014; 66(8): 1331–1441.
19. Choi KE, Hwang CJ, Park MH, *et al.* Cancer cell growth inhibitory effect of bee venom via increase of death receptor 3 expression and inactivation of NF-kappa B in NSCLC cells. *Toxins* 2014; 6(8): 2210–2228.
20. Bai X, Wu Y, Wang T, *et al.* Expression of Survivin and Caspase-3 in cholangiocarcinoma and relationship with HBV infection. *Journal of Harbin*

Medical University 2014; 48(1): 25–28.

21. Zhang S, Liu X, Du J, *et al.* Survivin-siRNA inhibits proliferation of lung cancer A549 cells and enhances their chemosensitivity to cisplatin. *Chinese Journal of Cancer Biotherapy* 2009; 16(6): 583–

587.

22. Lv L, An X, Li H, *et al.* Effect of miR-155 knock-down on the reversal of doxorubicin resistance in human lung cancer A549/dox cells. *Oncology Letters* 2016; 11(2): 1161–1166.

ORIGINAL RESEARCH ARTICLE

Combining PD-1/PD-L1 inhibitor and PARP inhibitor: a new perspective on the treatment of triple negative breast cancer

Ruilian Xie

Department of Oncology, The First Affiliated Hospital of Gannan Medical University, Ganzhou 341000, Jiangxi Province, China. E-mail: xieruilian163@163.com

ABSTRACT

Compared with other types of breast cancer, triple negative breast cancer has a poor survival prognosis due to its high aggressiveness and lack of effective therapeutic targets. Immune checkpoint (PD-1/PD-L1 and CTL-4) inhibitors have emerged as a breakthrough therapy in the treatment in various metastatic cancers. PARP inhibitors promote DNA damage in tumor cells, not only promoting immune initiation through a series of molecular mechanisms, but also leading to adaptive upregulation of programmed death ligand 1 (PD-L1) expression. Therefore, the combination of the two inhibitors can improve the efficacy of tumor treatment. We reviewed the research progress of their combined use in triple negative breast cancer, and put forward relevant ideas for further development, hoping to find the best treatment mode of the combined use of the two.

Keywords: Immunotherapy; PARP Inhibitors; Combined Therapies; Triple Negative Breast Cancer

ARTICLE INFO

Received 3 September 2021
Accepted 25 October 2021
Available online 1 November 2021

COPYRIGHT

Copyright © 2021 Ruilian Xie.
EnPress Publisher LLC. This work is licensed under the Creative Commons Attribution-NonCommercial 4.0 International License (CC BY-NC 4.0).
<https://creativecommons.org/licenses/by-nc/4.0/>

1. Introduction

Triple negative breast cancer (TNBC) is that estrogen receptor (ER) progesterone receptor (PR), and human epidermal growth factor receptor 2 (HER-2) are all breast cancers with negative expression. It accounts for about 15% of all breast cancer, and it is characterized by high aggression, easy metastatic recurrence, and poor prognosis. At present, according to the gene expression and biological characteristics of breast cancer, it is divided into four categories: ER +/Luminal group, normal breast group, HER2 + group, basal-like group. About 85% of basal-like group breast cancers belong to TNBC, and some of them express at least one of ER, PR and Her-2. However, there are some differences in gene expression profile and immunophenotype between TNBC and basal-like group breast cancers, so they cannot be completely identical. TNBC lacks endocrine therapy and corresponding treatment for HER2 target, so the treatment methods are limited. Although TNBC is relatively sensitive to chemotherapy, it is prone to recurrence and metastasis in the short term. Therefore, breast cancer researchers have been actively exploring new therapeutic approaches for TNBC, such as anti-tumor angiogenesis, EGFR inhibitors, multitarget drugs, PARP inhibitors and comprehensive utilization of various methods. According to the current preliminary research results, it is shown that the combination of immune detection point PD-1/PD-L1 inhibitor and PARPis can improve the therapeutic effect of TNBC. This paper reviews the role of PD-1/PD-L1 and PARP, the basic re-

search of their combination and the related research contents in TNBC.

Triple negative breast cancer (TNBC) is that estrogen receptor (ER) progesterone receptor (PR), and human epidermal growth factor receptor 2 (HER-2) are all breast cancers with negative expression. It accounts for about 15% of all breast cancer, and it is characterized by high aggression, easy metastatic recurrence, and poor prognosis. At present, according to the gene expression and biological characteristics of breast cancer, it is divided into four categories: ER +/Luminal group, normal breast group, HER2 + group, basal-like group. About 85% of basal-like group breast cancers belong to TNBC, and some of them express at least one of ER, PR and Her-2. However, there are some differences in gene expression profile and immunophenotype between TNBC and basal-like group breast cancers, so they cannot be completely identical. TNBC lacks endocrine therapy and corresponding treatment for HER2 target, so the treatment methods are limited. Although TNBC is relatively sensitive to chemotherapy, it is prone to recurrence and metastasis in the short term. Therefore, breast cancer researchers have been actively exploring new therapeutic approaches for TNBC, such as anti-tumor angiogenesis, EGFR inhibitors, multitarget drugs, PARP inhibitors and comprehensive utilization of various methods. According to the current preliminary research results, it is shown that the combination of immune detection point PD-1/PD-L1 inhibitor and PARP is can improve the therapeutic effect of TNBC. This paper reviews the role of PD-1/PD-L1 and PARP, the basic research of their combination and the related research contents in TNBC.

2. Programmed death protein-1/programmed death ligand-1(PD-1/PD-L1)

Tumor cells can use immune checkpoints to escape the attack of immune cells. At present, studies have confirmed that the immune checkpoint is cytotoxic T lymphocyte-associated antigen-4 (CTLA-4), programmed cell death protein-1 (PD-1) and programmed death ligand-1 (PD-L1). By designing

and synthesizing these immune checkpoint inhibitors, the activity of immune checkpoint can be inhibited and reactivate the immune response effect of T cells on tumor, so as to achieve the anti-tumor effect. However, the roles of the two immune checkpoints are different: CTLA-4 mainly plays a role in the activation stage of T cells induced by antigen-presenting cells in lymph nodes, while PD-1 plays a role in the effector stage of T cells at tumor sites. Therefore, the antitumor activity of PD-1/PD-L1 antibody may be better than CTLA-4 antibody.

PD-1, a member of the immunoglobulin B7 family, was first identified in apoptotic T cell lymphomas, a transmembrane protein on the T cell surface and an important inhibitory receptor. It was named the programmed death receptor-1 (PD-1) for its promotion to programmed cell death. PD-1 is mainly expressed in activated T/B lymphocytes, NK cells, monocytes, mesenchymal stem cells (BMSCs) and dendritic cells (DCs)^[1], which plays an important role in immune cell differentiation and apoptosis and is an important immunosuppressive molecule for maintaining autoimmune tolerance^[2].

Currently, PD-1 has identified two ligands: PD-L1 and PD-L2. They all belong to the B7 family and are similar^[3]. The affinity between PD-L2 and PD-1 is about 3 times higher than PD-L1, but PD-L1 is the most dominant ligand of PD-1, which is highly expressed in multiple tumor tissues and is closely related to the pathological type, pathological stage, survival prognosis, etc^[4].

The immunosuppressive effect of PD-1/PD-L1 signaling pathway plays an important role in maintaining body health and internal environment stability. Its immunosuppressive activity has a great impact on the occurrence and development of malignant tumors. The combination of PD-1 and PD-L1 can inhibit the proliferation of CD4⁺ T lymphocytes and CD8⁺ T lymphocytes, so it weakens the tumor killing effect of T lymphocytes, leads to immune escape of tumor cells, and promotes the rapid growth of tumors^[5]. Therefore, blocking the combination of PD-1 and PD-L1 can restore the immune killing effect of T lymphocytes in tumor patients and enhance the efficacy of killing tumors, and finally block the development process of ma-

lignant tumors. Many studies have confirmed that tumor immunotherapy by blocking PD-1 and PD-L1 is very effective in the treatment of a variety of malignant tumors.

3. Poly ADP-ribose polymerase (PARP)

PARP is a kind of poly ADP ribose polymerase, which plays an important role in DNA damage repair and cell apoptosis. It is activated by identifying DNA fragments with structural damage, participates in base excision repair (BER), and is used to repair single-strand breaks (SSBs) closely related ribozymes^[6]. So far, more than 18 members of PARP family have been found, of which PARP-1 and PARP-2 are the earliest and most mature members and PARP-1 is involved in the PARP activities of most enzymes^[6,7]. PARP-1 includes three domains: (1) N-terminal DNA binding domain (DBD), which is composed of two zinc finger structures and a nuclear localization signal region. Zn I and Zn II recognize damaged DNA, and Zn III participates in the connection between domains and activates proteins; (2) intermediate autoregulation domain (AD), which is rich in glutamate residues and a BRCA1 carboxyl terminal, as well as Caspase-3 digestion function; (3) The C-terminal catalytic domain is the main binding region of adenine dinucleotide. PARP catalyzes the decomposition of nicotinamide adenine dinucleotide (NAD⁺) into nicotinamide and ADP ribose through its own glycosylation, and then takes ADP ribose as substrate to “PAR” the receptor protein and PARP1 itself to form PARP-ADP ribose branched chain^[8].

By activating NF- κ B, PARP-1 upregulates of pro-inflammatory cytokines such as tumor necrosis factor α (TNF α) and IL-6, and their inhibitors down regulate these cytokines and reduce the occurrence of local inflammation^[9]. The balance of pro-inflammatory and anti-inflammatory responses was maintained by PARP-1 and its inhibition^[10]. In monocytes, PARP-1 controls the development of dendritic cell (DC). PARP inhibitors suppress CD86, CD8, IL-12, and IL-10 expression^[11]. CD86 expression can be restored by exogenous IL-12. As a result, depending on the expression of cytokines, PARPis may have a role in the maturation and

function of DC^[10,11]. Activated T nuclear factor (NFAT), which is required for T cell activity, is regulated by PARP-1. Therefore, increased trans-activation is caused by PARPis that NFAT depends on and the delay of NFAT nuclear export^[12]. PARPis can shield CD8⁺ T lymphocytes from oxygen radicals produced by phagocytes, and it can also protect CD8⁺ lymphocytes from apoptosis caused by oxygen radicals^[13]. Therefore, PARPis may be used in conjunction with immunotherapy ionizing radiation treatment of tumors with significantly invasive CTL.

BRCA1/2 is a tumor suppressor gene. The loss of BRCA1 and BRCA2 expression causes homologous recombination repair damage, followed by genomic instability, and increases frequency of DNA mutations. Its genetic mutant phenotype induces the risk of breast and ovarian cancer, and improves sensitivity to DNA damage drugs. BRCA1/2 mutant cells are defective in DNA damage repair. Cells cannot repair duplex damaged DNA by homologous recombination when cellular PARP activity is inhibited, and repair the damaged DNA by another error-prone repair pathway, resulting in chromosomal group instability, cell cycle inhibition and apoptosis.

The close relationship between PARP and the development of multiple malignant tumors, which, as a new target of tumor treatment, has become a hot target in recent years.

4. A combination of PD-1/PD-L1 inhibitors and PARP inhibitors to treat TNBC

PARPis and immune checkpoint inhibitors cooperate with and enhance the tumor antigen-specific activation of the CD8⁺ T lymphocyte-mediated antitumor immune response. PARPis promotes tumor-infiltrating lymphocytes (TILs) by upregulating chemokines and induces a CTL-mediated immune response. PARPis induces the upregulation of PDL-1, suppresses CTL, and promotes the escape of immune tumors. Anti-CTLA-4 immunotherapy stimulates T cells and works in tandem with PARP inhibitors to trigger an anti-tumor immune response. Anti-PDL-1/PD-1 immunother-

apy restores the PARPis-induced increase of PDL-1-mediated CTL inhibition. Therefore, anti-PDL-1/Pd-1 antibodies can work together with PARPis to stimulate an anti-tumor immune response^[14].

Lymphocytes inoculated in a mouse model identified in the BR5FVB1-Akt cell line “BRCA-1 deficient ovarian cancer”, PARPis elicited a local immune response^[15]. Intraperitoneal cytotoxic CD8⁺ T cells and NK cells increased, producing greater IFN γ and α . Furthermore, the proportion of MDSCs (bone marrow-derived suppressor cells) dropped. MDSCs aid tumor growth, particularly by inhibiting T cells^[16]. Therefore, PARPis boosts antitumor immunity by boosting TIL (like NK cells and CTL) and lowering MDSC levels. The overexpression of CCL2 and CCL5 in this model can explain the rise in TILs^[16], because CCL2 can deliver TIL in ovarian disease patients^[17]. PARPis’ capacity to influence the makeup and function of TILs is being used in conjunction with immunotherapy to maximize response. Several mouse models reported the advantages of PARPis and immunotherapy^[15,18,19]. The emergence of immunotherapy and PARPis in the treatment of some cancers has prompted research on their combination. The majority of malignancies discovered by these combinations are tumors that lack DNA repair activity, such as BRCA defective tumor cells. PARPis^[20] and immune checkpoint inhibitors like anti-PD-1 work effectively on these cancers^[21]. Immune checkpoint inhibiting agents might be used to increase TAA expression in tumors that have been mutated, promoting a particular immune response^[22]. High mutation load is related to improving survival rate where anti-PD-1 therapy was used to treat melanoma patients, even as tumors from responding sufferers are rich because of mutations in DNA restore function, which include BRCA-2^[23]. These findings reinforce the rationale for combining immunodetection point inhibitors with PARP inhibitors in malignancies with DNA repair defects.

Recently, Jiao *et al.* have observed the combination of PARPis (olaparib) and anti-PD-1/PD-L1 in the treatment of TNBC by *in vivo* and *in vitro* experiments. The expression of PARP protein is opposite to that of PD-L1 in human breast cancer. In the syngeneic mouse model inoculated with

TNBC cell system, PARPis up-regulated PD-L1 expression on the surface of EMT6 tumor cells. This was accomplished via generating a reduction in TILs and facilitating the deactivation of the GSK3 β mechanism, so PARPis plays an immunosuppressive role by reducing the level of TILs. Anti-PD-L1 reversed the inhibitory effect on TILs, and combined with PARPis, enhanced expression of TILs with antitumor responses over PARPi and anti-PD-L1 alone. These data further support the study of PARPis combined with anti-PD-L1/PD-1 immunotherapy^[19]. *In vivo*, inhibition of PARP has been demonstrated to trigger PD-L1 upregulation, which may be the result of the described interferon expression. However, *in vitro* and xenotransplantation are also viable options^[24]. The latter result implies that PD-L1 regulation downstream of PARP is parallel to the internal mechanism of cells, but independent of external signals. The adaptable and inherent overexpression of PD-L1 may stamp down PARP inhibitor-mediated downstream immune response and may be overcome by binding of PARP inhibitors to PD-1/PD-L1 inhibitors.

Because the response rate of TNBC against PDL-1 or anti-PD-1 treatment is still unsatisfactory, only 10%–20% of TNBC patients respond partially. Glycosylation PD-L1 is the operative part of PD-L1 which is of necessity to the interaction between PD-L1 and PD-1. TNBC cells had much greater levels of glycosylated PD-L1 than non-TNBC cells. Bin *et al.* discovered that 2-deoxyglucose (2-DG) may be utilized as an analog of glucose to diminish PD-L1 glycosylation during the selecting of glucose to prevent PD-L1 glycosylation. Because PARP inhibition increases PD-L1 expression, 2-DG lowers glycosylated PD-L1 expression mediated by PARP inhibition. PARP inhibition in combination with 2-DG provides a powerful anticancer effect^[25]. Therefore, the results provide a strong theoretical basis for the combination of PD-1/PDL-1 inhibitors and PARPis in the treatment of TNBC.

Till now, only three PARP inhibitor/anti-PD-1/L1 combos have been studied: olaparib/durvalumab^[26,27], niraparib/pd-1 inhibitor^[28,29], and BGB-A 317/BGB-290^[30]. The premier combination of the two was well-tolerated, and its toxicity was consistent with that of the related drugs observed in

single drug environment. The latter, on the other hand, had a higher risk of hepatotoxicity, showing the tolerance of the combining of PARPis and PD-1/PD-L1 inhibition agents may vary depending on the drug used and/or the exact environment. Niraparib/pbrobroli-zumab combined treatment for advanced three negative breast cancer (100 cases) also showed initial activity. The ORR was 28% and 60% in patients with BRCA 1/2 mutations, again consistent with PARP inhibitor monotherapy^[31]. These preliminary breast and ovarian findings back up the theory for further exploration of joint application. Because compared with PARPis with single treatment, combined application may bring benefits to a wider population without DDR defects, or have longterm benefits for all patients; the latter is likely because the benefits of ICB are mainly considered to improve survival^[32].

5. Conclusion

At present, the preliminary research shows that the composition between PD-1, PD-L1 inhibitor and PARP inhibitor has better clinical efficacy in the treatment of TNBC, and provides the basic research basis for the combination, which allows us to see a little breakthrough in the treatment of TNBC, brings a glimmer of confidence to clinical workers and a glimmer of dawn to patients, but there are still several key questions to be further answered: (1) Compared with monotherapy, what are the advantages of comprehensive treatment? Are potential disadvantages beneficial to long-term survival? (2) What is the best dose or time arrangement for combination therapy? (3) Is it possible to improve the curative effect by combining other treatment methods, such as chemotherapy, radiotherapy, anti-vascular growth, ATR inhibitors, etc? Can the patient tolerate it? How to optimize the treatment plan? These need our vast number of breast cancer researchers to actively explore and research, to find effective treatment for TNBC patients, so that patients can achieve long-term survival purposes.

Conflict of interest

No conflict of interest was reported by the au-

thor.

References

1. Böger C, Behrens HM, Mathiak M, *et al.* PD-L1 is an independent prognostic predictor in gastric cancer of Western patients. *Oncotarget* 2016; 7(17): 24269–24283.
2. Larkin J, Hodi FS, Wolchok JD. Combined nivolumab and ipilimumab or monotherapy in untreated melanoma. *New England Journal of Medicine* 2015; 373(13): 1270–1271.
3. Zak KM, Kitel R, Przetocka S, *et al.* Structure of the complex of human programmed death1 PD-1 and its ligand PD-L1. *Structure* 2015; 23(12): 2341–2348.
4. Boussiotis VA. Molecular and biochemical aspects of the PD-1 checkpoint pathway. *New England Journal of Medicine* 2016; 375(18): 1767–1778.
5. Zheng Z, Bu Z, Liu X, *et al.* Level of circulating PD-L1 expression in patients with advanced gastric cancer and its clinical implications. *Chinese Journal of Cancer Research* 2014; 26(1): 104–111.
6. Anwar M, Aslam HM, Anwar S. PARP inhibitors. *Hereditary Cancer in Clinical Practice* 2015; 13(1).
7. Vyas S, Chang P. New PARP targets for cancer therapy. *Nature Reviews Cancer* 2014; 14: 502–509.
8. Wang Y, Liu W, Ning Y, *et al.* Progress in the research of PARP inhibitors and their mechanisms of action. *Chinese Journal of New Drugs* 2018; 27(3): 306–313.
9. Haddad M, Rhinn H, Bloquel C, *et al.* Anti-inflammatory effects of PJ34, a poly (ADP-ribose) polymerase inhibitor, in transient focal cerebral ischemia in mice. *British Journal of Pharmacology* 2006; 149(1): 23–30.
10. Laudisi F, Sambucci M, Pioli C. Poly (ADP-ribose) polymerase-1 (PARP-1) as immune regulator. *Endocrine Metabolic & Immune Disorders Drug Targets* 2011; 11(4): 326–333.
11. Aldinucci A, Gerlini G, Fossati S, *et al.* A key role for poly (ADP-ribose) polymerase-1 activity during human dendritic cell maturation. *Journal of Immunology* 2007; 179(1): 305–312.
12. Valdor R, Schreiber V, Saenz L, *et al.* Regulation of NFAT by poly (ADP-ribose) polymerase activity in T cells. *Molecular Immunology* 2008; 45(7): 1863–1871.
13. Davalli P, Marverti G, Lauriola A, *et al.* Targeting oxidatively induced DNA damage response in cancer: Opportunities for novel cancer therapies. *Oxidative Medicine and Cellular Longevity* 2018; 21(3): 1–21.
14. Césaire M, Tharit J, Candéias SM, *et al.* Combining PARP inhibition, radiation and immunotherapy: A possible strategy to improve the treatment of cancer. *International Journal of Molecular Sciences* 2018; 19(12): 3793.
15. Huang J, Wang L, Cong Z, *et al.* The PARP1 inhibitor BMN673 exhibits immunoregulatory effects in

- a Brca1(-/-) murine model of ovarian cancer. *Biochemical and Biophysical Research Communications* 2015; 463(4): 551–556.
16. Ostrand-Rosenberg S, Sinha P. Myeloid-derived suppressor cells: Linking inflammation and cancer. *Journal of Immunology* 2009; 182(8): 4499–4506.
 17. Lanca T, Costa MF, Goncalves-Sousa N, *et al.* Protective role of the inflammatory CCR2/CCL2 chemokine pathway through recruitment of type 1 cytotoxic $\gamma\delta$ T lymphocytes to tumor beds. *Journal of Immunology* 2013; 190(12): 6673–6680.
 18. Higuchi T, Flies DB, Marjon NA, *et al.* CTLA-4 blockade synergizes therapeutically with PARP Inhibition in BRCA1-deficient ovarian cancer. *Cancer Immunology Research* 2015; 3(11): 1257–1268.
 19. Jiao S, Xia W, Yamaguchi H, *et al.* PARP inhibitor upregulates PD-L1 expression and enhances cancer associated immunosuppression. *Chinese Journal of Cancer Research* 2017; 23(14): 3711–3720.
 20. Scott CL, Swisher EM, Kaufmann SH. Poly (ADP-Ribose) polymerase inhibitors: Recent advances and future development. *Journal of Clinical Oncology* 2015; 33(12): 1397–1406.
 21. Le DT, Durham JN, Smith KN, *et al.* Mismatch repair deficiency predicts response of solid tumors to PD-1 blockade. *Science* 2017; 357(6349): 409–413.
 22. Nebot-Bral L, Brandao D, Verlingue L, *et al.* Hypermutated tumours in the era of immunotherapy: The paradigm of personalised medicine. *European Journal of Cancer* 2017; 84: 290–303.
 23. Hugo W, Zaretsky JM, Sun L, *et al.* Genomic and transcriptomic features of response to anti-PD-1 therapy in metastatic melanoma. *Cell* 2016; 165(1): 35–44.
 24. Garcia-Diaz A, Shin DS, Moreno BH, *et al.* Interferon receptor signaling pathways regulating PD-L1 and PD-L2 expression. *Cell Reports* 2017; 19(6): 1189–1201.
 25. Shao B, Li C, Lim S, *et al.* Deglycosylation of PD-L1 by 2-deoxyglucose reverses PARP inhibitor-induced immunosuppression in ple-negative breast cancer. *American Journal of Cancer Research* 2018; 8(9): 1837–1846.
 26. Karzai F, Madan RA, Owens H, *et al.* A phase 2 study of olaparib and durvalumab in metastatic castrate-resistant prostate cancer (mCRPC) in an unselected population. *Journal of Clinical Oncology* 2018; 36: 163.
 27. Drew Y, Park YH, Hong SH, *et al.* An open-label, phase II basket study of olaparib and durvalumab (MEDIOLA): Results in germline BRCA-mutated (gBRCAm) platinum-sensitive relapsed (PSR) ovarian cancer (OC). *Gynecologic Oncology* 2018; 149: 246–247.
 28. Vinayak S, Tolaney SM, Schwartzberg LS, *et al.* TOPACIO/Keynote-162: Niraparib + pembrolizumab in patients (pts) with metastatic triple-negative breast cancer (TNBC), a phase 2 trial. *Journal of Clinical Oncology* 2018; 36: 1011.
 29. Konstantinopoulos PA, Waggoner SE, Vidal GA, *et al.* TOPACIO/Keynote-162 (NCT02657889): A phase 1/2 study of niraparib + pembrolizumab in patients (pts) with advanced triple-negative breast cancer or recurrent ovarian cancer (ROC)—Results from ROC cohort. *Journal of Clinical Oncology* 2018; 36: 106.
 30. Friedlander M, Meniawy T, Markman B, *et al.* A phase 1b study of the anti-PD-1 monoclonal antibody BGB-A317 (A317) in combination with the PARP inhibitor BGB-290 (290) in advanced solid tumors. *Journal of Clinical Oncology* 2017; 35(15): 3013.
 31. Robson M, Im SA, Senkus E, *et al.* Olaparib for metastatic breast cancer in patients with a germline BRCA mutation. *New England Journal of Medicine* 2017; 377(6): 523–533.
 32. Kaufman H, Schwartz LH, William WN, *et al.* Evaluation of clinical endpoints as surrogates for overall survival in patients treated with immunotherapies. *Journal of Clinical Oncology* 2017; 35: e14557.

ORIGINAL RESEARCH ARTICLE

Experimental study on the expression and diagnostic significance of I-FABP in acute intestinal ischemia

Haikun Li¹, Minhua Wang¹, Xiansen Zhu², Xiaoqing Zhou³, Bin Yang³, Qinghui Yin³, Xiaoping Liu⁴, Xiangfu Zeng⁴, Yan Hu⁵, Xiangtai Zeng^{3*}

¹ Gannan Medical University, Ganzhou 341000, Jiangxi Province, China.

² Department of Pathology, Gannan Medical University, Ganzhou 341000, Jiangxi Province, China.

³ Department of General Surgery, The Second Affiliated Hospital of Gannan Medical University, Xinfeng 341600, Jiangxi Province, China. E-mail: zxtjxgz888@sohu.com

⁴ Department of Gastro-intestinal Surgery, The First Affiliated Hospital of Gannan Medical University, Jiangxi Province, China.

⁵ Ganzhou Institute of Animal Husbandry Science, Ganzhou 341000, Jiangxi Province, China.

ABSTRACT

Objective: To detect the expression and distribution of I-FABP in intestinal tissue and the changes of serum concentrations at different time of acute intestinal ischemia, and explore the significance and mechanism of I-FABP in early diagnosis of acute ischemic bowel disease. **Methods:** The selected 96 healthy adult SD rats were randomly divided into the experimental group and control group; 48 in each group. Each group was randomly subdivided into 6 groups with 8 rats in each group. The superior mesenteric artery was ligated in the experimental group and the peritoneal switch operation was performed in the control group. The venous blood samples were extracted from each group rats' right ventricle at 0.5 h, 1 h, 2 h, 4 h, 8 h, 12 h after the operation and the concentration of I-FABP was tested respectively. Then the rats were killed, and the diseased intestinal tubes were cut out for paraffin sections. The I-FABP in intestinal tissue was stained by routine HE staining and direct immunofluorescence staining. **Results:** The I-FABP was mainly expressed in the epithelial villi of intestinal mucosa, and there was a small amount of expression in the intestinal submucosa and even the muscularis. Within 1 hour of intestinal ischemia, the number of I-FABP positive granules in the intestine and intestinal cavity increased gradually, and then gradually decreased after 1 hour. The difference has statistically significant between the experimental group and the control group ($P < 0.05$). The serum I-FABP: In the experimental group, the serum I-FABP concentration began to increase at 0.5 h, and reached a peak at 1 h (290.24 ± 156.69) $\mu\text{g}\cdot\text{L}^{-1}$, then gradually decreased. Compared with the control group, the difference was statistically significant ($P < 0.05$). **Conclusion:** I-FABP usually mainly exists in the epithelial cells of intestinal mucosa. When acute intestinal ischemia occurs, the epithelial cells of intestinal mucosa permeability changes; I-FABP expression rapidly releases to intestinal tissue and intestinal cavity, and is absorbed into the blood. Therefore, I-FABP has certain clinical significance in early diagnosis and treatment of acute intestinal ischemia.

Keywords: Intestinal Fatty Acid Binding Protein; Acute Intestinal Ischemia; Immunofluorescence; Diagnosis

ARTICLE INFO

Received 2 September 2021
Accepted 27 October 2021
Available online 3 November 2021

COPYRIGHT

Copyright © 2021 Haikun Li, *et al.*
EnPress Publisher LLC. This work is licensed under the Creative Commons Attribution-NonCommercial 4.0 International License (CC BY-NC 4.0).
<https://creativecommons.org/licenses/by-nc/4.0/>

1. Introduction

Acute intestinal ischemia (AII) is a kind of acute, critical and severe diseases of the digestive system. The early symptoms and signs are nonspecific, so it is difficult to judge the ischemic state of the intestinal tract in time, and it is very easy to develop into irreversible intestinal necrosis in a short time^[1,2]. Therefore, the early diagnosis of AII is particularly important. It has been found that the early intestinal fatty

acid binding protein (I-FABP) in AII patients is higher than that in normal people^[3,4]. Blood I-FABP is significantly increased in patients with narrow intestinal obstruction compared with simple intestinal obstruction, so the detection of I-FABP content in blood can be used as an auxiliary means for the diagnosis of AII. However, some studies believe that the concentration of I-FABP in blood is positively correlated with the degree of intestinal ischemia in the early stage of AII^[5]. With the extension of ischemia time, the concentration of I-FABP in blood gradually decreases. In this study, the concentration of serum I-FABP in different periods of intestinal ischemia in rat acute mesenteric ischemia models was detected and combined with the I-FABP immunofluorescence labeling of intestinal tissue in the process of intestinal ischemia to understand the serological changes of I-FABP in the development of AII and its significance. The expression of intestinal ischemia further proves the significance of I-FABP as a laboratory serum biochemical index in the early diagnosis of AII, providing effective help for clinical diagnosis and treatment of acute small intestinal obstruction.

2. Materials and methods

2.1 Materials and instruments

Materials and instruments include experimental rats that were purchased from the animal room of Gannan Medical University, PE labeled rabbit anti-intestinal fatty acid binding protein antibody (Shanghai Anyan), centrifuge (LC-4012), microplate reader (SK202, Shenzhen, Sinothinker Company), biochemical analyzer (BECKMAN COULTER, AU680), electron microscope (OLYMPUS, CX31), and fluorescence microscopy (OLYMPUS, CX31).

2.2 Grouping of experimental animals and establishment of intestinal ischemia models

96 healthy SD rats (half male and half female) were randomly divided into two groups (the experimental group and control group), with 48 rats in each group. The two groups were randomly subdivided into 6 groups (I, II, III, IV, V, VI), with 8 rats in each group. The intestinal ischemia model was established by ligating the superior mesenteric ar-

tery in the experimental group, and the peritoneal switch operation was performed in the control group.

2.3 Blood samples being collected and assayed

3 mL of venous blood samples were extracted from each group rats' right ventricle with sterile syringes at 0.5 h, 1 h, 2 h, 4 h, 8 h, 12 h after the operation. The supernatant was taken after centrifugation at 3000 r min⁻¹ for 10 min at 4 °C, and serum I-FABP concentration was measured by ELISA.

2.4 Staining intestinal tissue by HE staining and staining I-FABP by immunofluorescence staining

Experimental animals in each group were killed immediately after blood collection, the diseased intestinal tubes were cut, then fixed, embedded, sectioned, HE stained, and intestinal pathological changes were observed by 400-fold microscopy. Sections were prepared in the same method, dewaxed, and antigen repaired; and I-FABP in intestinal tissue was stained by direct immunofluorescence staining of PE-labeled rabbit anti-I-FABP antibody. At the same time, a blank control group was also set and I-FABP expression in intestinal tissue at different periods of time of intestinal ischemia under a 100 x fluorescence microscope. The acquired images were analyzed by the Image-pro plus 6.0 software and the number of positive particles was calculated.

2.5 Statistical method

Statistics data were processed and analyzed by using the SPSS 22.0 statistical software. The measuring data of each group were shown as $\bar{x} \pm s$. One-way ANOVA was used for comparisons between groups, and SNK-q test for pairwise comparisons between groups, $P < 0.05$ was statistically significant.

3. Results

3.1 Measurement of serum I-FABP concentration in each group

The changes of serum I-FABP concentration in

each group are shown in **Table 1**. It began to rise at 0.5 h and reached the peak at 1 h ($P < 0.05$). Then, with the lasting of ischemia, the I-FABP concentration gradually decreased.

Table 1. Changes of serum I-FABP concentration in each group / $\mu\text{g}\cdot\text{L}^{-1}$, $\bar{x} \pm s$

Time	Experimental group	Control group	F	P
Superior mesenteric artery ligation for 0.5 h (I)	182.63 \pm 64.56*	52.54 \pm 29.36		
Superior mesenteric artery ligation for 1 h (II)	290.24 \pm 156.69* [@]	50.10 \pm 37.48		
Superior mesenteric artery ligation for 2h (III)	251.91 \pm 109.62* [#]	41.83 \pm 20.77	27.6	< 0.001
Superior mesenteric artery ligation for 4 h (IV)	228.09 \pm 99.29* [※]	33.53 \pm 7.06	83	
Superior mesenteric artery ligation for 8 h (V)	191.29 \pm 85.64* [‡]	35.74 \pm 12.14		
Superior mesenteric artery ligation for 12 h (VI)	176.19 \pm 86.02*	51.48 \pm 30.63		

Note: * Comparison of each experimental group and control group, $P < 0.05$; @ comparison of II and I, $P < 0.05$; # comparison of III and II, $P < 0.05$; ※ comparison of IV and III, $P < 0.05$; ‡ comparison of V and VI, $P < 0.05$.

3.2 Analysis of immunofluorescence staining images and statistical analysis

The number of I-FABP positive particles in each experimental group and control group is shown in **Table 2**. Compared with the control group, the number of I-FABP positive particles in each experimental group was significantly higher than that in the control group within 2 hours of intestinal ischemia. After 2 hours, the number of I-FABP positive particles gradually decreased and significantly lower than that in the control group, the difference was statistically significant ($P < 0.05$).

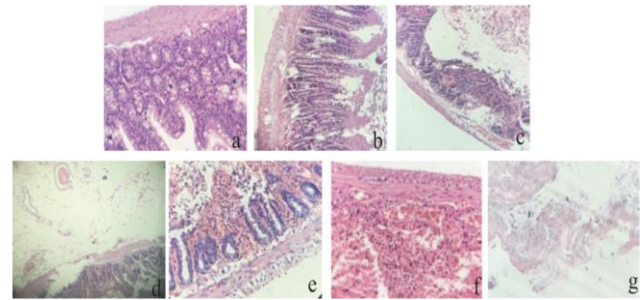
Table 2. Expression of I-FABP in ischemic intestinal tissue/ $\bar{x} \pm s$

Time	Experimental group	Control group	F	P
Superior mesenteric artery ligation for 0.5 h (I)	451 \pm 34*	323 \pm 36		
Superior mesenteric artery ligation for 1 h (II)	705 \pm 71* [@]	328 \pm 40		
Superior mesenteric artery ligation for 2h (III)	441 \pm 35* [#]	329 \pm 23	103.669	< 0.001
Superior mesenteric artery ligation for 4 h (IV)	273 \pm 37* [※]	323 \pm 23		
Superior mesenteric artery ligation for 8 h (V)	224 \pm 31* [‡]	341 \pm 32		
Superior mesenteric artery ligation for 12 h (VI)	161 \pm 15* ^{&}	375 \pm 23		

Note: * Comparison of each experimental group and control group $P < 0.05$; @ comparison of II and I, $P < 0.05$; # comparison of III and II, $P < 0.05$; ※ comparison of IV and III, $P < 0.05$; ‡ comparison of V and IV, $P < 0.05$; & comparison of VI and V, $P < 0.05$.

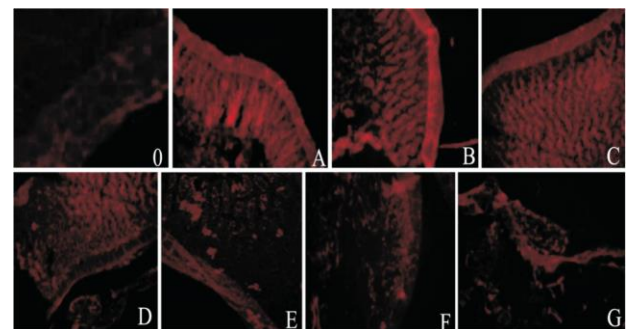
3.3 Intestinal histopathology

HE staining of rat intestine at various periods of time of ischemia is shown in **Figure 1**.



a: In the control group, the villi of small intestine were arranged orderly without obvious necrosis and abscission. **b:** After intestinal ischemia for 0.5 h, the villi of small intestine began to fall off. **c:** After intestinal ischemia for 1 h, there was partial and obvious necrosis of the villus of the small intestine. **d:** After intestinal ischemia for 2 h, most of the small intestinal villi were necrotic and exfoliated, and the normal villi structure was rare. **e:** After intestinal ischemia for 4 h, small intestinal villus was almost necrotic, the normal villus structure was rare, and there was no obvious necrosis of the muscular layer. **f:** After intestinal ischemia for 8 h, small intestinal villus and gland were necrotic, the blood vessels of mesentery were dilated and congested, with obvious bleeding, and the muscular layer was necrotic. **g:** After intestinal ischemia for 12 h, intestinal tissue cells dissolved.

Figure 1. HE staining of rat intestine at each time point ($\times 400$).



0: Blank group: no positive staining was found. **A:** In the control group, more positive particles were found in the intestinal tissue. I-FABP was mainly expressed in the intestinal mucosal epithelial villi, and a small amount was also expressed in the intestinal submucosa and even the muscular layer. **B:** After intestinal ischemia for 0.5 h, the morphology of intestinal wall was normal. I-FABP positive particles increased in intestinal mucosal glands and intestinal wall muscular layers, especially granular fluorescence was obvious in intestinal wall. **C:** After intestinal ischemia for 1 h, the morphology of intestinal wall was basically normal. I-FABP positive granular fluorescence was found in intestinal mucosal glands and intestinal wall muscular layers, with the most uniform distribution. **D:** After intestinal ischemia for 2 h, I-FABP positive particles were less than those of C. **E:** After intestinal ischemia for 4 h, the positive particles of I-FABP were less than those of D. **F:** After 8 h of intestinal ischemia, I-FABP positive particles were scattered in intestinal tissue and lumen, and the number was lower than that of E. **G:** After intestinal ischemia for 12 h, intestinal tissue cells dissolved. A small amount of I-FABP positive particles were scattered among necrotic tissue, and the number was significantly lower than that of F.

Figure 2. Expression of intestinal tissue in each group ($\times 400$).

3.4 Observation of the immunofluorescence staining images for I-FABP

As observed under a 100 x fluorescence microscope, PE produced an emission fluorescence wavelength of 450 nm with positive I-FABP staining in orange. See **Figure 2**.

4. Discussion

AII is divided into two main categories according to the etiology^[6]. The first category is ischemia caused by intravascular factors, such as mesenteric arteriovenous embolism and thrombosis, also known as acute mesenteric ischemic syndrome (AMIS). The second type is the disorder of intestinal blood supply caused by some factors other than blood vessels, such as volvulus, intussusception and incarcerated inguinal hernia, that is, strangulated mechanical small bowel obstruction (SMSBO). Although there are many and different causes of AII, the ischemic changes of the intestinal canal itself are basically the same, that is, a process from ischemia to necrosis. In the early stage of ischemia, the histopathology of intestinal tissue mainly showed the damage of intestinal wall glandular duct, the abscission of intestinal mucosal epithelial cells, edema, inflammatory cell infiltration and so on^[7]. After stopping the blood supply for several minutes, the intestinal mucosa will suffer ischemic injury. With the extension of ischemic time, the epithelial cells of intestinal mucosa will fall off obviously, the normal villus structure is rare, and myometrial necrosis will occur, resulting in cell lysis and changes in the tissue structure of intestinal canal.

I-FABP is a water-soluble protein that is relatively stable to heat. Its molecular weight is small, about 12–15 KD^[8]. It is abundant in the intestine and mainly exists at the top of intestinal mucosal epithelial villi^[9]. Its main function is to regulate fatty acid metabolism. Intestinal bile acid salts and trypsin emulsify and decompose food derived lipids into medium and short chain fatty acids and long chain fatty acids. The former is absorbed by intestinal epithelial cells in a diffusion manner. Long chain fatty acids (C16–20) combining with I-FABP are targeted and transported to intracellular mito-

chondria, endoplasmic reticulum and other places to participate in lipid synthesis and decomposition in the body^[10–12]. The main metabolic pathway of I-FABP is glomerular filtration and it is removed from the body by the kidney. Its half-life period is 11 min. Therefore, I-FABP can also be detected through urine^[13]. Under normal circumstances, the concentration of I-FABP in peripheral blood is very low and can hardly be detected. Because the blood flow at the intestinal villi is a countercurrent exchange mechanism, it is most difficult to tolerate ischemia, hypoxia and other injuries. In the early stage of intestinal ischemia, the oxygen partial pressure at the top of intestinal villi is significantly reduced, resulting in ischemic necrosis of cells at the top of intestinal villi, and the I-FABP in it can pass through the cell membrane earlier, capillaries, lymphatic capillaries and portal veins to enter the blood circulation, as well as the intestinal cavity and abdominal cavity^[14].

It was found that the concentration of serum I-FABP increased significantly at 0.5 h of intestinal ischemia, reached the peak at 1 h of intestinal ischemia, and then decreased gradually with the extension of ischemia time. It is mainly due to the continuous destruction of intestinal mucosal epithelial villi and the release of a large amount of I-FABP to peripheral blood in the early stage of intestinal ischemia (<1 h). 1 h after intestinal ischemia, the epithelial villi of intestinal mucosa have been largely destroyed, and the I-FABP released to peripheral blood gradually decreases. At the same time, due to the short half-life period of I-FABP and its metabolism through the kidney, it is continuously consumed, so that the concentration of I-FABP in peripheral blood continuously decreases with the extension of ischemia time. At the same time, immunofluorescence showed that after PE labeling with I-FABP antibody, I-FABP was mainly expressed in intestinal mucosal epithelial villi, and a small amount was also expressed in intestinal submucosa and even the muscular layer. Within 1 h of intestinal ischemia, the expression of I-FABP positive particles in intestinal tissue gradually increased. Considering that in acute intestinal ischemia, intestinal tissue mainly mobilizes and uses fatty acids for energy supply, the transport and metabolism of fatty

acids need to be combined with FABP, so as to indirectly activate FABP in tissue. At the same time, the fatty acids entering the cell are transported to the nucleus after binding with FABP, and then bind with the fatty acid activation receptor in the nucleus to activate the downstream nuclear factor signal transduction pathway, so as to regulate the synthesis and expression of intracellular FABP at the transcriptional level and make the synthesis and expression of intracellular FABP further increase^[15,16]. When ischemia reached 1 h, the number of I-FABP positive particles in intestinal tissue was the largest, which further verified that the damaged intestinal mucosal tissue released the most I-FABP. After 1 h, with the extension of intestinal ischemia time, the number of I-FABP positive particles in intestinal tissue gradually decreased, the normal villi gradually decreased or even disappeared, the intestinal mucosal epithelial villi had been largely destroyed, and the mucosal epithelial cells necrotized and dissolved.

In conclusion, I-FABP mainly exists in intestinal mucosal epithelial cells at ordinary times. In the early stage of acute ischemia, I-FABP is rapidly expressed, released into intestinal wall tissue and intestinal cavity, and absorbed into blood. When the serum I-FABP concentration reaches the peak, the intestinal mucosal epithelial villi have been seriously damaged. At this time, the ischemic damage may have reached the submucosa. Clinicians should consider surgical treatment. This suggests that I-FABP can not only be used for the early diagnosis of intestinal ischemia, but also play a guiding role in the treatment of intestinal ischemia. Therefore, I-FABP has certain clinical significance in the early diagnosis and treatment of acute intestinal ischemia.

Conflict of interest

The authors declare no potential conflicts of interest.

Acknowledgements

Fund project: Science and technology project of Jiangxi Provincial Department of Education (No.: GJJ08402).

References

1. Karaca Y, Gündüz A, Türkmen S, *et al.* Diagnostic value of procalcitonin levels in acute mesenteric ischemia. *Balkan Medical Journal* 2015; 32(3): 291–295.
2. Van den Heijkant TC, Aerts BAC, Tejjink JA, *et al.* Challenges in diagnosing mesenteric ischemia. *World Journal of Gastroenterology* 2013; 19(9): 1338–1341.
3. Zheng L, Feng Z, Wei F. The value of I-FABP measurement in the diagnosis of intestinal ischemic in patients with acute intestinal obstruction. *International Journal of Laboratory Medicine* 2014; 35(4): 410–411.
4. Hirotada K, Hiroshi A, Hitoshi T, *et al.* Usefulness of intestinal fatty acid-binding protein in predicting strangulated small bowel obstruction. *Plos One* 2014; 9(6): e99915.
5. Shi H, Wu B. Correlation of serum intestinal fatty acid binding protein and D-lactate with ischemic time and intestinal injury in acute mesenteric ischemia rats. *Chinese journal of Multiple Organ Diseases in the Elderly* 2013; 12(7): 526–529.
6. Zeng X, Xu Z, Ling X. Early diagnosis of acute ischemic bowel disease progress (in Chinese). *Progress of Modern General Surgery in China* 2007; 10(5): 438–441.
7. March DS, Marchbank T, Playford RJ, *et al.* Intestinal fatty acid-binding protein and gut permeability responses to exercise. *European Journal of Applied Physiology* 2017; 117(5): 931–941.
8. Güzel M, Sözüer EM, Salt O, *et al.* The value of the serum I-FABP level for diagnosing acute mesenteric. *Surgery Today* 2014; 44(11): 2072–2076.
9. Van der Voort PHJ, Westra B, Wester JPJ, *et al.* Can serum L-lactate, D-lactate, creatine kinase and I-FABP be used as diagnostic markers in critically ill patients suspected for bowel ischemia. *BMC Anesthesiology* 2014; 14: 111–121.
10. Angela M, Gajda, Storch J. Enterocyte fatty acid-binding proteins (FABPs): Different functions of liver and intestinal FABPs in the intestine. *Prostaglandins, Leukotrienes and Essential Fatty Acids* 2015; 93: 9–16.
11. Acosta S, Nilsson T. Current status on plasma bi-

- omarkers for acute mesenteric ischemia. *Thromb Thrombolysis* 2012; 33: 355–361.
12. Loor JJ, Yudell BE, Nakamura TM. Regulation of energy metabolism by long-chain fatty acids. *Progress in Lipid Research* 2014; 53: 124–144.
 13. Salim SY, Young PY, Churchill TA, *et al.* Urine intestinal fatty acid-binding protein predicts acute mesenteric ischemia in patients. *Journal of Surgical Research* 2017; 209: 258–265.
 14. Powell A, Armstrong P. Plasma biomarkers for early diagnosis of acute intestinal ischemia. *Seminars in Vascular Surgery* 2014; 27(3-4): 170–175.
 15. Venkatachalam AB, Sawler DL, Wright JM. Tissue-specific transcriptional modulation of fatty acid-binding protein genes, *fabp2*, *fabp3* and *fabp6*, by fatty acids and the peroxisome proliferator, clofibrate, in zebrafish (*Danio rerio*). *Gene* 2013; 520(1): 14–21.
 16. Venkatachalam AB, Lall SP, Denovan-Wright EM, *et al.* Tissue-specific differential induction of duplicated fatty acid-binding protein genes by the peroxisome proliferator, clofibrate, in zebrafish (*Danio rerio*). *BMC Evolutionary Biology* 2012; 12: 112–126.

ORIGINAL RESEARCH ARTICLE

The expression and significance of 8-hydroxydeoxyguanosine in breast cancer patients' blood, urine and cancer tissue

Zhiyong Liu, Jian Yi*, Feng'en Liu

The First Affiliated Hospital of Gannan Medical University, Ganzhou 341000, Jiangxi Province, China. E-mail: yi.j@sohu.com

ABSTRACT

Objective: To explore the expression and clinic significance of 8-OHdG in breast cancer. **Methods:** Pre-operative serum 8-OHdG levels were detected with an enzyme-linked immunosorbent assay in a well-defined series of 173 breast cancer patients. 8-OHdG expression in cancer cells from 150 of these patients was examined by immunohistochemistry. The HPLC-ECD method is used to determine 8-OHdG concentration in urine. **Results:** The serum 8-OHdG levels and immunohistochemical 8-OHdG expression were in concordance with each other ($P < 0.05$, $r = 0.163$). Breast cancer patients with negative 8-OHdG immunostaining show lower survival rate according to the multivariate analysis ($P < 0.01$). This observation was even more remarkable in ductal carcinomas (n = 140) patients ($P < 0.001$). A low serum 8-OHdG level was associated statistically significantly with lymphatic vessel invasion and a positive lymph node status. Comparison of 8-OHdG concentration in urine of breast cancer patients and healthy women was statistical significance ($P < 0.01$). **Conclusion:** Low serum 8-OHdG levels and a low immunohistochemical 8-OHdG expression were associated with an aggressive breast cancer phenotype. In addition, negative 8-OHdG immunostaining was an independent prognostic factor for breast cancer-specific death in breast carcinoma patients. Using 8-OHdG concentration in urine to predict DNA damage resulting from breast cancer can provide good biological indicators for detecting harm in early breast cancer.

Keywords: 8-OHdG; Enzyme-linked Immunosorbent Assay; Immunohistochemistry; Reactive Oxygen Species

ARTICLE INFO

Received 14 September 2021
Accepted 26 October 2021
Available online 4 November 2021

COPYRIGHT

Copyright © 2021 Zhiyong Liu, et al.
EnPress Publisher LLC. This work is licensed under the Creative Commons Attribution-NonCommercial 4.0 International License (CC BY-NC 4.0).
<https://creativecommons.org/licenses/by-nc/4.0/>

1. Introduction

ROS (reactive oxygen species) is a metabolite of normal cells, which can act on pyrimidine, purine and chromatin proteins, resulting in gene base modification and gene mutation. These reactions interact with oncogenes and may lead to cancer formation^[1].

Because the life of ROS is very short, for example, the life of the most harmful -OH is estimated to be less than 1 ns, it is difficult to detect ROS directly. Therefore, the most effective method to detect ROS is to use antibodies to neutralize the "footprint" of oxidative damage^[2]. 8-hydroxydeoxyguanosine (8-OHdG) is a specific marker of 2-deoxyguanosine damage caused by ROS attacking DNA. The molecular weight of 8-OHdG is 283.2. It is formed after the hydroxyl radical (-OH) in oxygen-containing radical (ROS) attacks the DNA base guanine and is removed from the DNA chain after enzyme repair. It is water-soluble and can be excreted from the body through urine^[3]. 8-OHdG is one of the biomarkers of oxidative stress. It can be detected by immunohistochemistry, enzyme-linked immunosorbent assay and HPLC-ECD^[4]. In this study, we analyzed the level of 8-OHdG in

serum and urine, 8-OHdG expression in tissue, and combined with clinicopathological parameters to evaluate the feasibility of 8-OHdG as a predictor and prognostic factor of breast cancer.

2. Materials and methods

2.1 Data collection

A total of 173 breast cancer patients admitted to the First Affiliated Hospital of Gannan Medical University from 1982 to 2011 were selected. All cases were histologically confirmed as breast cancer, and the staging criteria were based on the tumor staging established by WHO. None of them received any treatment before blood collection. All the patients were female, including 140 cases of ductal carcinoma, 25 cases of lobular carcinoma and 8 cases of other types of breast cancer. The average follow-up time of this study was 40.5 months. Serum samples were stored in polystyrene tubes at -80°C . Pathological wax blocks of 150 patients were randomly selected from the 173 patients for immunohistochemical examination. Urine of 60 normal women of the same age group who had not suffered from gynecological diseases or received treatment in the past were collected as the control group, and the concentration of 8-OHdG in urine was analyzed. This study was approved by the medical ethics committee of the First Affiliated Hospital of Gannan Medical University.

2.2 Using ELISA to detect the expression level of 8-OHdG in blood of breast cancer patients

The level of 8-OHdG in serum was determined by ELISA (ELISA kit was purchased from Shanghai Esha Biotechnology Co., Ltd., as well as all the following reagents). Anti 8-OHdG monoclonal antibody was used. Blood samples were pre-treated with a microporous filter. 200 μL serum was added to each test tube, centrifuged at 140 rpm for 30 min; the supernatant was taken, added with primary antibody. Another test tube was added with samples, plate vibrated, and incubated at 4°C for the night. Each tube was rinsed with 250 μL rinse solution for 3 times, followed by secondary antibody, plate vibration, and incubation at room temperature for 1 h. Then, each test tube was added

with 100 μL reaction stopper, and plate vibrated, and the absorbents were measured at 450 nm on the panel display. The standard curve was used to calculate the amount of 8-OHdG in the samples.

2.3 Using immunohistochemistry to detect 8-OHdG expression in breast cancer tissue samples

Paraffin blocks were conventionally sliced, de-waxed with xylene, dehydrated with alcohol of different gradients, and heated with 10 mm citric acid in a microwave oven for 10 min. The slices were cooled at room temperature, soaked in 3% hydrogen peroxide in methanol for 15 min, and incubated overnight at 4°C . The incubation solution was 1:125 primary antibody (8-OHdG), colorant was 1:400 biological secondary antibody and avidin-biotin-peroxidase complex. Aminobtetraethyl lead was used as color-changing material, while xylitol was used for the staining count.

The intensity of 8-OHdG in cells was divided into four groups: – negative (nuclear staining $<5\%$), + weak (nuclear staining $5\%–20\%$), ++ medium (nuclear staining $21\%–80\%$), +++ strong (nuclear staining $>80\%$). For statistical analysis, staining results were divided into negative (–) and positive (+, ++, +++).

2.4 Examination of the concentration of 8-OHdG in urine by HPLC-ECD

Urine samples from breast cancer patients were collected by catheterization before surgery, and those from normal women were collected by natural urination. Urine samples were stored in a refrigerator at -80°C . Adjust pH value of urine to 4.5 by HCl solution. 5 mL urine was put into a 15 mL centrifuge tube, centrifuged at 1,500 rpm for 5 min, and 2 mL supernatant was taken and added to the first extraction tube. Add 10 mL MeOH into the extraction tube; add 5 mL distilled water; add 10 mL buffer A; add 3 mL buffer A for washing, and add 3 mL 5% MeOH into buffer A for washing, and collect it in a 15 mL centrifuge tube. Add the collected solution to the second extraction tube. Add 1.5 mL 20% MeOH into buffer A for washing, and collect it in a 15 mL centrifuge tube. Remove MeOH in a vacuum concentrator and condense it for 1.5 h. Use buffer A for quantification to 1 mL.

Inject 100 μ L of it into HPLC-ECD for analysis.

2.5 Statistical analysis

Software spss 15.0 was used for statistical analysis. Spearman's test, Mann-Whitney U-test and Pearson χ^2 were used to calculate the results of ELISA, immunohistochemistry and HPLC-ECD, respectively. The survival rate was analyzed by the survival curve. External factor analysis was performed by lox regression analysis, $P < 0.05$ means the difference is statistically significant.

3. Results

3.1 Expression of 8-OHdG in breast cancer tissue samples

8-OHdG immunohistochemical staining was located in the nucleus (**Figure 1**). Among all patients, 147 patients had positive 8-OHdG immunohistochemistry; among the patients with intraductal carcinoma, there were 120 patients with positive 8-OHdG immunohistochemical expression. The distribution of immunohistochemical staining is shown in **Table 1**. According to Spearman's test, the expression of 8-OHdG in serum was positively correlated with that in tissue ($P < 0.05$, $r = 0.163$).

Table 1. 8-OHdG immunohistochemical results

Group	n	8-OHdG expression							
		-		+		++		+++	
		n	%	n	%	n	%	n	%
All the patients	173	26	15.0	26	15.0	73	42.1	48	27.7
Ductal carcinoma patients	140	20	14.2	27	19.2	59	42.1	34	24.2

Table 2. Statistical relationship between 8-OHdG and biological characteristics of breast cancer

Clinical information	8-OHdG value	P value	Clinical information	8-OHdG value	P value	Clinical information	8-OHdG value	P value
T staging			Lymphatic metastasis			Progesterone receptor		
1	0.18 \pm 0.13	0.09	Positive	0.12 \pm 0.09	< 0.05	Positive	0.16 \pm 0.12	0.35
2~4	0.15 \pm 0.11		Negative	0.17 \pm 0.13		Negative	0.19 \pm 0.13	
N staging			Vascular metastasis			Ki-67		
0	0.18 \pm 0.12	< 0.05	Positive	0.10 \pm 0.04	0.18	0~2	0.16 \pm 0.12	0.41
1~2	0.15 \pm 0.13		Negative	0.17 \pm 0.13		3	0.19 \pm 0.14	
Grading			Estrogen receptor			Her-2		
1~2	0.17 \pm 0.12	0.37	Positive	0.16 \pm 0.12	0.24	Positive	0.15 \pm 0.09	0.14
3	0.17 \pm 0.13		Negative	0.19 \pm 0.14		Negative	0.17 \pm 0.13	

3.3 Relationship between 8-OHdG and clinicopathological parameters in breast cancer tissue

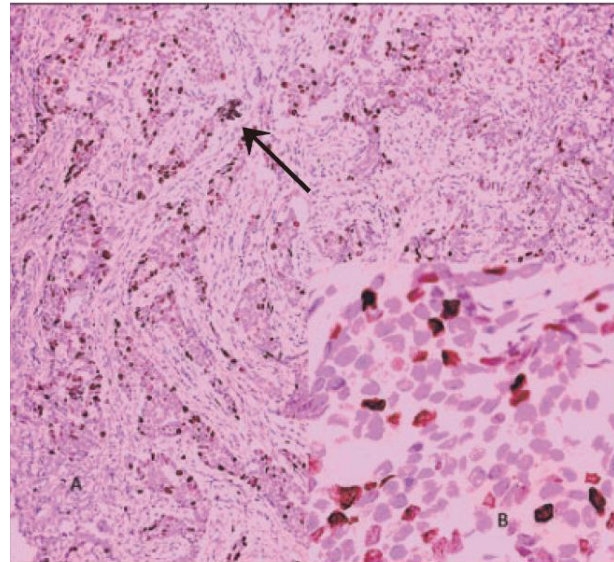


Figure 1. Strong positive 8-OHdG expression in breast cancer. Note: A: $\times 10$; B: $\times 40$; arrows indicate positive cells.

3.2 Relationship between the expression of 8-OHdG in blood and the biological characteristics of breast cancer patients

Among patients with breast cancer, the level of serum 8-OHdG in patients with lymphatic metastasis and lymph node metastasis is relatively low. When comparing the biological characteristics of tumor in all patients, there was statistical significance between the two characteristics of lymphatic metastasis and the number of lymph node metastasis and the level of serum 8-OHdG ($P < 0.05$) (**Table 2**).

Compared with patients with positive 8-OHdG immunohistochemical expression, those with negative expression had a higher risk of death. Survival

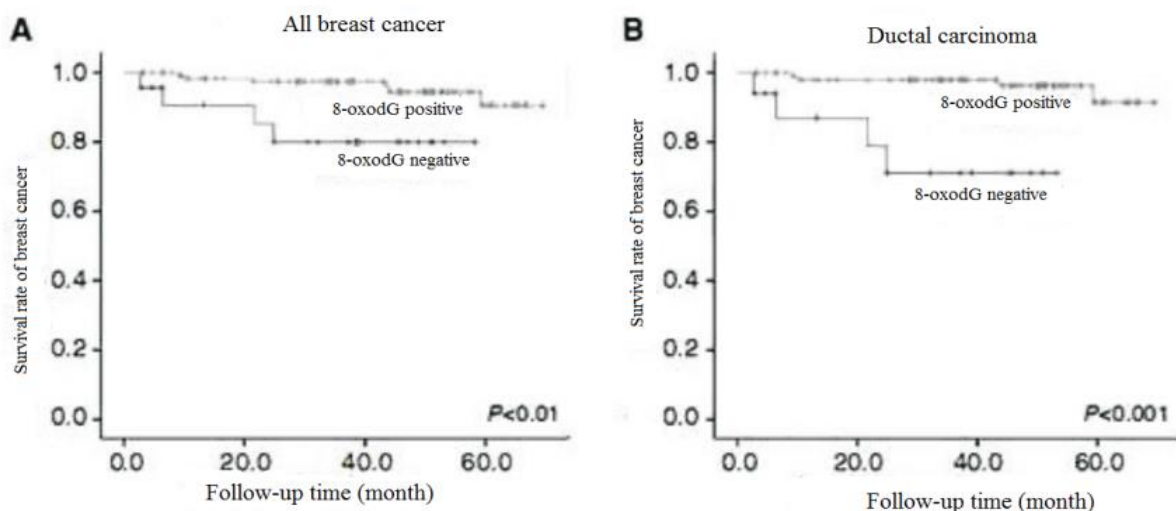
rate data are shown in **Table 3**. In survival factor analysis, negative 8-OHdG is an independent prognostic factor in patients with low survival rate. The results of survival curve analysis showed that there

was a significant difference in disease-free survival time between positive and negative 8-OHdG positive (see **Figure 2**).

Table 3. Relationship between 8-OHdG and biological characteristics of breast cancer

Clinical information	n	Average survival time/month	P value	Clinical information	n	Average survival time/month	P value
T staging				Progesterone receptor			
1	110	68.7	<0.01	Positive	116	67.5	<0.05
2~4	63	63.5		Negative	57	64.3	
N staging				Ki-67			
0	97	70.4	<0.01	0~2	127	69.6	<0.001
1~2	76	62.6		3	46	56.7	
Tissue grading				Her-2			
1~2	110	70.0	<0.01	Positive	22	60.8	0.21
3	63	62.1		Negative	151	67.6	
Lymphatic metastasis				Histological type			
Positive	16	55.6	0.16	Ductal	140	66.4	0.33
Negative	151	67.9		Others	33	67.7	
Vascular metastasis				8-OHdG expression			
Positive	9	58.2	0.09	Positive	127	66.9	<0.01
Negative	158	67.6		Negative	23	49.5	
Estrogen receptor				8-OHdG expression in ductal carcinoma			
Positive	140	69.0	<0.01	Positive	106	67.4	<0.001
Negative	33	55.9		Negative	17	42.1	

Note: only 167 patients with lymphatic and vascular metastasis were collected, and the other 6 patients in the early stage had no relevant information.



A: all breast cancer ($P < 0.01$); B: ductal carcinoma ($P < 0.001$)

Figure 2. Survival curve analysis.

3.4 Concentration of 8-OHdG in urine of breast cancer patients and healthy women

The 8-OHdG concentration in urine and the

correction by creatinine and body weight of breast cancer patients and healthy women were compared (**Table 4**). The concentration of 8-OHdG in the two

groups was statistically significant ($P < 0.01$). The mean 8-OHdG concentration in urine of breast cancer patients was (81.81 ± 74.4) nmol, which was higher than that of healthy women (33.14 ± 18.1) nmol ($P < 0.01$). Corrected by creatinine in urine, the mean 8-OHdG concentration in urine of breast cancer patients was (16.39 ± 17.3) $\mu\text{mol}\cdot\text{mol}^{-1}$, still higher than that of healthy women (4.70 ± 7.1) $\mu\text{mol}\cdot\text{mol}^{-1}$ ($P < 0.01$). After corrected by body weight, the mean value of 8-OHdG/kg in urine of breast cancer patients was (676.82 ± 608.0) $\text{pmol}\cdot\text{kg}^{-1}$, which was also higher than that of healthy women (286.37 ± 160.7) $\text{pmol}\cdot\text{kg}^{-1}$ ($P < 0.01$).

Table 4. Comparison of 8-OHdG concentration in urine between breast cancer patients and the control group/ $\bar{x} \pm s$

Group	8-OHdG /nmol	8-OHdG/Creatinine $\mu\text{mol}\cdot\text{mol}^{-1}$	8-OHdG / $\text{pmol}\cdot\text{kg}^{-1}$
Breast cancer n = 173	81.81 ± 74.4 (15.45–354.27)	16.39 \pm 17.3 (1.64–90.01)	676.82 \pm 608.0 (131.09–3163.11)
Control group n = 60	33.14 \pm 18.1 (16.86–101.81)	4.70 \pm 7.1 (0.94–53.22)	286.37 \pm 160.7 (127.62–808.53)
P value	<0.01	<0.01	<0.01

4. Discussion

ROS is a by-product of normal cell metabolism and may also be produced by stimulation of foreign substances. 8-OHdG is the product formed after ROS attacks DNA. The formation of 8-OHdG is easy to cause errors in DNA replication, resulting in gene mutation, and then cancer; at the same time, it will be removed from the DNA strand after repaired by repair enzyme *in vivo*^[5].

Studies have pointed out that when cells are attacked by carcinogens, they may produce some oxygen-containing free radicals, which may cause oxidative damage to nucleic acids; when these products are attacked by oxygen-containing radicals, they cause more than dozens of products of nucleic acids oxidative damage, of which 8-OHdG is the most representative; and because 8-OHdG will cause the error of deoxyribose insertion during DNA replication, G \rightarrow T conversion occurs^[6]. It is found that 8-OHdG can be used as a biological index related to mutation formation or cancer formation^[7]. Through this study, it is found that

8-OHdG negative staining in breast cancer tissue may be an independent prognostic factor for breast cancer patients with poor prognosis. The low level of 8-OHdG expression in serum and tissue may be a strong feature of breast cancer invasion. This study found that there was a positive correlation between oxidative stress and serum 8-OHdG level in breast cancer cells.

In this study, the low expression of 8-OHdG in breast cancer tissue and the low level of 8-OHdG in preoperative serum were significantly correlated with the prognosis of breast cancer. This correlation is more obvious in ductal carcinoma. Ductal carcinoma is an important histological subtype of breast cancer with different prognosis. Therefore, more accurate prognostic factors need to be identified. According to our experimental results, negative 8-OHdG expression and low serum 8-OHdG levels in tumor tissue are independent prognostic factors of low survival rate in breast cancer patients.

The low level of serum 8-OHdG is a sign of weak DNA repair after oxidative damage, or the improvement of antioxidant defense function relative to ROS. The main repair enzyme of 8-OHdG is DNA glycosylase 1, whose function is very important to prevent base pair G \rightarrow T mutation^[8]. ROS can damage DNA glycosylase 1 and cannot cleave damaged guanine, resulting in the decrease of 8-OHdG level in extracellular fluid^[9]. The improvement of antioxidant defense in tumor tissue provides advantages for cancer cell growth by avoiding apoptosis and ROS induced necrosis. Excessive antioxidant enzymes will prevent the interaction between ROS and DNA, thus reducing the formation of 8-OHdG in tissue^[10]. Translation factor Nrf 2 is an up-regulator of multifunctional antioxidant enzymes, which can remove ROS from cells. On the other hand, Nrf 2 upregulation is very common in drug-resistant cancer cells. It can provide cancer cell growth advantage in the tumor treatment stage^[11]. Although 8-OHdG is relatively less studied in breast cancer patients, Nrf 2 up-regulated, and antioxidant enzyme inducers and resistance may explain the poor prognosis of patients with low 8-OHdG in the initial stage of 8-OHdG.

By comparing the concentration of 8-OHdG in

the urine of breast cancer patients and healthy women, the former was 81.81 nmol, which was significantly higher than that of the latter, 33.14 nmol, with statistical difference ($P < 0.001$). The same results were obtained after adjustment by creatinine and body weight. There has been no studies on the correlation between 8-OHdG in the urine of breast cancer patients and healthy women. From the results of this study, it has been found that there was a statistically significant correlation between the concentration of 8-OHdG in urine and breast cancer patients. Therefore, the concentration of 8-OHdG in urine can be used to predict the DNA damage caused by breast cancer and provide good biological indicators for the early damage of breast cancer.

We believe that the expression of immunohistochemical 8-OHdG expression in breast cancer patients is related to the level of 8-OHdG in plasma. The decrease of 8-OHdG in plasma and breast cancer cells indicates the increase of invasiveness, especially in ductal cancer. Negative immunohistochemical 8-OHdG expression is an independent predictor in breast cancer patients. These results provide a standard for judging the prognosis of breast cancer, and provide an important preliminary study for further better treatment of tumors.

Conflict of interest

The authors declare no potential conflicts of interest.

Acknowledgements

Project: Project of Ganzhou Health Bureau in 2014.

References

1. Cho H, Ahn KC, Choi JY, *et al.* Luteolin acts as a radio-sensitizer in non-small cell lung cancer cells by enhancing apoptotic cell death through activation of a p38/ROS/caspase cascade. *International Journal of Oncology* 2015; 46(3): 1149–1158.
2. Seino M, Okada M, Shibuya K, *et al.* Differential contribution of ROS to resveratrol-induced cell death and loss of self-renewal capacity of ovarian cancer stem cells. *Anticancer Research* 2015; 35(1): 85–96.
3. Yang H, Mao G, Zhang H, *et al.* Association between dyslipidemia and 8-OHdG/Cr among a population exposed to chronic arsenic. *Chinese Journal of Epidemiology* 2014; 35(7): 802–805.
4. Gürler H, Bilgici B, Akar AK, *et al.* Increased DNA oxidation (8-OHdG) and protein oxidation (AOPP) by low level electromagnetic field (2.45 GHz) in rat brain and protective effect of garlic. *International Journal of Radiation Biology* 2014; 90(10): 892–896.
5. Kotani K, Yamada T. Association between urinary 8-OHdG and pulse wave velocity in hypertensive patients with type 2 diabetes mellitus. *Singapore Medical Journal* 2014; 55(4): 202–208.
6. Tanaka M, Takano H, Fujitani Y, *et al.* Effects of exposure to nanoparticle-rich diesel exhaust on 8-OHdG synthesis in the mouse asthmatic lung. *Experimental and Therapeutic Medicine* 2013; 6(3): 703–706.
7. Tang Y, Li X, Tang Z, *et al.* Observation on urinary 8-OHdG level of patients with primary hepatocellular carcinoma. *Chinese Journal of Laboratory Diagnosis* 2013; 17(10): 1804–1806.
8. Kumar A, Pant MC, Singh HS, *et al.* Assessment of the redox profile and oxidative DNA damage (8-OHdG) in squamous cell carcinoma of head and neck. *Journal of Cancer Research and Therapeutics* 2012; 8(2): 254–259.
9. Saito K, Aoki H, Fujiwara N, *et al.* Association of urinary 8-OHdG with lifestyle and body composition in elderly natural disaster victims living in emergency temporary housing. *Environmental Health and Preventive Medicine* 2013; 18(1): 72–77.
10. Siva Prasad B, Vidyullatha P, Vani GT, *et al.* Association of gene polymorphism in detoxification enzymes and urinary 8-OHdG levels in traffic policemen exposed to vehicular exhaust. *Inhalation Toxicology* 2013; 25(1): 1–8.
11. Huang YW, Jian L, Zhang MB, *et al.* An investigation of oxidative DNA damage in pharmacy technicians exposed to antineoplastic drugs in two Chinese hospitals using the urinary 8-OHdG assay. *Biomedical and Environmental Sciences* 2012; 25(1): 109–116.

ORIGINAL RESEARCH ARTICLE

Effect of 1.25(OH)₂D₃ on experimental autoimmune neuritis and its mechanism

Di Nian¹, Zhuohan Li¹, Junjie Sun¹, Peng Shi^{2*}

¹ Department of Medical Examination, Bengbu Medical College, Bengbu 233000, Anhui Province, China.

² Department of Neurology, The First Affiliated Hospital of Bengbu Medical College, Bengbu 233000, Anhui Province, Chin. E-mail: 1439768337@qq.com

ABSTRACT

Objective: To study the potential therapeutic effects of active vitamin D₃ (1.25(OH)₂D₃) in the experimental autoimmune neuritis (EAN). **Methods:** The EAN model was established by actively immunizing Lewis rats with synthetic PO₁₈₀₋₁₉₉ peptide and Freund's complete adjuvant. 1.25(OH)₂D₃ treatment was given, weight change of rats and clinical score were analyzed. HE staining was used to detect the inflammatory cell infiltration of sciatic nerves and demyelination of sciatic nerves was observed by transmission electron microscope (TEM) at the same time. The expressions of inflammatory cytokines IL-17, IL-10, TGF-β, IFN-γ were detected by ELISA, and the expressions of Th17, Treg were examined by RT-PCR. **Results:** 1.25(OH)₂D₃ ameliorated body weight loss and myelin lesions. It decreased expressions of inflammatory cytokines IL-17, IFN-γ and RORrt while those of IL-10, TGF-β and FoxP3 were increased. **Conclusions:** 1.25(OH)₂D₃ can improve the clinical pathological changes of EAN rats, and the mechanism may be related to the changes of inflammatory cytokines. 1.25(OH)₂D₃ is expected to become a new strategy for the clinical treatment of GBS/EAN.

Keywords: Experimental Autoimmune Neuritis; 1.25(OH)₂D₃; Inflammation Cytokines; T-lymphocytes

ARTICLE INFO

Received 20 September 2021
Accepted 3 November 2021
Available online 13 November 2021

COPYRIGHT

Copyright © 2021 Di Nian, et al.
EnPress Publisher LLC. This work is licensed under the Creative Commons Attribution-NonCommercial 4.0 International License (CC BY-NC 4.0).
<https://creativecommons.org/licenses/by-nc/4.0/>

1. Introduction

Guillain-Barré syndrome (GBS), also known as acute inflammatory demyelinating polyneuropathy, is an autoimmune disease characterized by demyelination of peripheral nerves and nerve roots and infiltration of small vascular inflammatory cells. Due to the unknown etiology, symptomatic supportive therapy and specific immunotherapy, such as plasma exchange and intravenous immunoglobulin, are mainly used, but the effects of the two treatments are not satisfactory. At present, there is no measure to block the progress of the disease. EAN is a classic animal model of GBS. It has the pathological characteristics of peripheral nerve demyelination and inflammatory cell infiltration. Its clinical manifestations and neurophysiological changes are very similar to human GBS. It is widely used in the basic research of the pathogenesis and treatment of GBS. 1.25(OH)₂D₃ is the active form of vitamin D. After binding with vitamin D receptor (VDR), it forms a dimer with retinoid X receptor (RXR) and binds to vitamin D response elements (VDRE) on the DNA sequence of downstream genes, so as to control the transcription of downstream genes. It has long been believed that vitamin D mainly plays a role in calcium and phosphorus metabolism and bone metabolism. However, VDR is expressed in almost all human

tissue types, including immune cells^[1]. Recent studies have shown that vitamin D plays a role in innate and specific immunity by regulating the activation of T lymphocytes, B lymphocytes and macrophages. Epidemiological studies show that vitamin D deficiency is associated with a variety of autoimmune diseases^[2-5]. Spanier *et al.*^[6] found that supplementation of vitamin D₃ can reduce the incidence rate and severity of experimental autoimmune encephalomyelitis (EAE). However, Meehan *et al.*^[7] proposed that it's hypercalcemia caused by 1.25(OH)₂D₃ which can improve EAE, rather than the therapeutic effect of 1.25(OH)₂D₃ itself. However, the effect of vitamin D on EAN is not clear. Therefore, this study established an EAN rat model, observed the behavioral manifestations, pathological changes and inflammatory cytokines of EAN rats after 1.25(OH)₂D₃ treatment, and comprehensively evaluated the effect of 1.25(OH)₂D₃ on EAN and its mechanism.

2. Materials and methods

2.1 Materials

2.1.1 Experimental animals

Healthy male Lewis rats, 6–8 w, weighing 160–180 g, were purchased from Beijing Charles River Laboratory Animal Technology Co., Ltd.

2.2.2 Main reagents

Peripheral nerve myelin antigen PO₁₈₀₋₁₉₉ was purchased from GL Biochem (Shanghai) Ltd.; Freund's incomplete adjuvant and active vitamin D₃ were purchased from Sigma company of the United States; mycobacterium tuberculosis H37Ra was purchased from Difco company; Trizol was purchased from Invitrogen; ELISA kits for IL-17, IL-10, TGF-β, and IFN-γ were purchased from ABclonal.

2.2 Methods

2.2.1 Establishment of the EAN model and treatment with 1.25(OH)₂D₃

25 Lewis rats were randomly divided into the normal control group (Control), model group (EAN), low-dose vitamin D group (VDI), medium-dose vitamin D group (VDM) and high-dose

vitamin D group (VDh), with 5 rats in each group. 250 μg PO₁₈₀₋₁₉₉ was emulsified in the same amount of complete Freund's adjuvant (containing 10 mg·mL⁻¹ mycobacterium tuberculosis H37Ra) as the sensitizers. The rats in the model group and vitamin D treatment groups were injected with sensitizers at multiple points on the soles of both feet of the hind limbs for a total of 100 μL/rat. From the 5th day after immunization, VDI, VDM, and VDh groups were given 0.25 μg·kg⁻¹, 1 μg·kg⁻¹, 4 μg·kg⁻¹ 1.25(OH)₂D₃ by gavage administration once a day for 7 days. The control and EAN groups were given 0.2 mL peanut oil by gavage administration every day for 7 days.

2.2.2 Clinical score of nervous system signs

From the 0 day of immunization, two experimenters weighed, observed and scored the rats at the same time every day. The scoring criteria are as follows: 0 point: normal; 1 point: the tension of rat tail muscle decreases and the tail tip turns up; 2 points: caudal paralysis, and loss of righting reflex; 3 points: loss of righting reflex; 4 points: gait disorder and abnormal posture; 5 points: hemiplegia of hind limbs; 6 points: moderate paralysis of hind limbs; 7 points: severe paralysis of hind limbs; 8 points: quadriplegia; 9 points: on the verge of death; 10 points: death.

2.2.3 Evaluation of action potential of sciatic nerves

The action potential conduction velocity and latency of rat sciatic nerves were measured by a biological signal recorder. The methods are as follows: at the peak of onset, lay the rats in a prone position on a constant temperature operating table under 10% chloral hydrate anesthesia, shave the hair of the left leg, cut off the skin of the left hip after routine disinfection, cut off the blunt separation along the fascia, free and expose the sciatic nerves, and put them in the stimulating electrode recording electrode, set the nerve stimulation indexes as: 1 Hz, 5 mA, 0.1 ms, and evoke compound muscle action potential (CAMP). The CAMP amplitude, latency and motor nerve conduction velocity (MNCV) were detected and recorded by a four-channel biological signal collector. The nerve

conduction of each rat was recorded 3 times. During the measurement, the nerve stem was kept moist with tabletop liquid.

2.2.4 Morphological evaluation of sciatic nerves

On the 15th day after immunization, the sciatic nerves were immediately separated under 10% chloral hydrate anesthesia, fixed in 4% paraformaldehyde, dehydrated with gradient alcohol, transparentized by xylene, and then embedded in paraffin, and sectioned. The infiltration of lymphocytes and macrophages between sciatic nerve bundles and around small vessels was observed under HE staining light microscope.

2.2.5 Ultra-structural observation of sciatic nerves

On the 15th day after immunization, the sciatic nerves were immediately isolated under 10% chloral hydrate anesthesia, and fixed in 0.2 mol·L⁻¹ glutaraldehyde. The demyelination of sciatic nerve axons was observed by a transmission electron microscope after routine dehydration, embedding, ultrathin section and staining.

2.2.6 Detection of IL-17, IL-10, TGF- β and IFN- γ levels by ELISA

On the 15th day after immunization, blood was collected from the retroorbital venous plexus, centrifuged at 3,000 rpm for 5 min, and the supernatant was retained. Add 100 μ L standard substances or samples to be tested into the detection hole of the enzyme plate according to the requirements of the manual and incubate at 37 °C for 2 h. Add 100 μ L antibodies to each hole after plate washing and incubate at 37 °C for 1 h. After plate washing, add 100 μ L enzyme binding substrate respectively and incubate at 37 °C for 30 min. Discard the liquid in the hole and add 100 μ L TMB after plate washing. Add 100 μ L termination solution after 15 min. Set the wavelength at 450 nm, zero the blank hole, and immediately detect the OD value with an enzyme labeling instrument. The concentration of IL-17, IL-10 TGF- β and IFN- γ in serum was calculated according to the standard curve.

2.2.7 Detection of IL-17, IFN- γ , RORrt,

FoxP3 mRNA levels by RT-PCR

On the 15th day after immunization, the rats were anesthetized with 10% chloral hydrate and routinely disinfected, and the spleen was taken out in a sterile environment. Grind the spleen with Trizol in liquid nitrogen, and extract total RNA. The RNA concentration was measured by ultraviolet spectrophotometer and then reverse transcribed into cDNA for RT-PCR to detect the level change of IL-17, IFN- γ , RORrt, FoxP3 mRNA. The primer design was as follows: FoxP3 F: 5' CCT ACC CAC TGC TGG CAA ACG 3', R: 5' ACT TCT CTC TGG AGG AGG CAC TG 3'; RORrt F: 5' AGG TAT GAC CGA TGC TCT TA 3', R: 5' TAT TTT CGG ATA AGT CTA GG 3'; IL-17 F: 5' TGG ACT CTG AGC CGC ATT GA 3', R: 5' GAC GCA TGG CGG ACA ATA GA 3'; IFN- γ F: 5' AAA GAC AAC CAG GCC ATC AG 3', R: 5' CTT TTC CGC TTC CTT AGG CT 3'; GAPDH F: 5' TCG TGG AGT CTA CTG GCG TCT T 3', R: 5' CAT TGC TGA CAA TCT TGA GGG AG 3.

2.3 Statistical methods

SPSS 16.0 statistical software was used to analyze the data. The measurement data were expressed as $\bar{x} \pm s$. The measurement data between groups were compared by analysis of variance. The pairwise comparison between multiple samples was carried out by Mann-Whitney test. The difference $P < 0.05$ is statistically significant.

3. Results

3.1 Weight change and clinical score of rats

The rats in the EAN group began to appear symptoms on the 5th day after immunization, which reached the peak on the 15th day. The clinical scores of the VDI group (6.6 ± 0.23), the VDM group (5.2 ± 0.28) and the VDh group (6.2 ± 0.33) were lower than those of the EAN group (7.1 ± 0.35). The effect in the VDM group was more obvious, but there was no significant difference between groups ($P > 0.05$). The weight gain rate of rats in the EAN group decreased from the onset of clinical symptoms, and the weight decreased rapidly at the peak of onset on the 13th–15th day. However, the weight gain rate of rats in the 1.25(OH)₂D₃ intervention

group decreased from the onset of clinical symptoms, but there was no significant weight loss. The weight loss of the VDI, VDM and VDh groups was lower than that of the EAN group, but there was no significant difference compared with the EAN group ($P > 0.05$). See **Figure 1**.

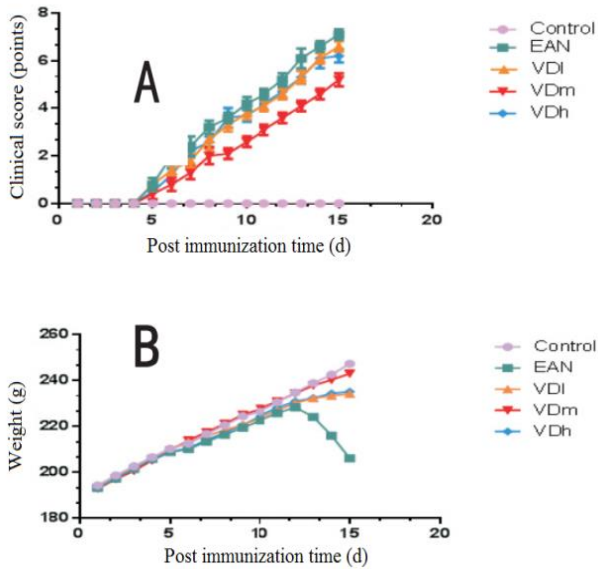


Figure 1. Effects of $1.25(\text{OH})_2\text{D}_3$ treatment on clinical scores (A) and weight (B) of EAN rats.

3.2 Neurophysiological changes in EAN rats

The sciatic nerve conduction velocity in the EAN group was $(57.7 \pm 0.78) \text{ m}\cdot\text{s}^{-1}$, which was significantly lower than that in the control group $(133.3 \pm 0.28) \text{ m}\cdot\text{s}^{-1}$ ($P < 0.05$); the conduction velocity of sciatic nerves in the VDI group, VDM group and VDh group were $(66.7 \pm 0.45) \text{ m}\cdot\text{s}^{-1}$, $(71.8 \pm 0.56) \text{ m}\cdot\text{s}^{-1}$ and $(66.4 \pm 1.15) \text{ m}\cdot\text{s}^{-1}$ respectively, which were significantly improved compared with the EAN group, especially in the VDM group ($P < 0.05$). The amplitude of action potential of sciatic nerves in the EAN group was $(7.49 \pm 0.13) \text{ m}\cdot\text{s}^{-1}$, which was lower than that in the control group $(17.8 \pm 0.44) \text{ m}\cdot\text{s}^{-1}$ ($P < 0.05$); the action potential amplitudes of sciatic nerves in the VDI group, VDM group and VDh group were $(13.3 \pm 0.36) \text{ m}\cdot\text{s}^{-1}$, $(14.8 \pm 0.31) \text{ m}\cdot\text{s}^{-1}$ and $(13.6 \pm 0.47) \text{ m}\cdot\text{s}^{-1}$, respectively, which were significantly higher than those in the EAN group. In conclusion, $1.25(\text{OH})_2\text{D}_3$ treatment reduced peripheral nerve injury in EAN rats, and the VDM group had the best effect. See **Figure 2**.

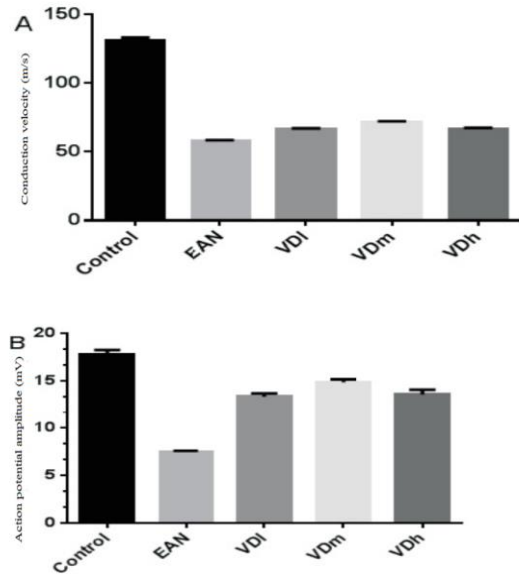


Figure 2. Effects of $1.25(\text{OH})_2\text{D}_3$ treatment on sciatic nerve conduction velocity (A) and action potential amplitude (B) in EAN rats.

3.3 Sciatic nerve inflammatory cell infiltration and demyelination in EAN rats

At the peak of the disease, the sciatic nerves were examined by HE staining and a transmission electron microscope.

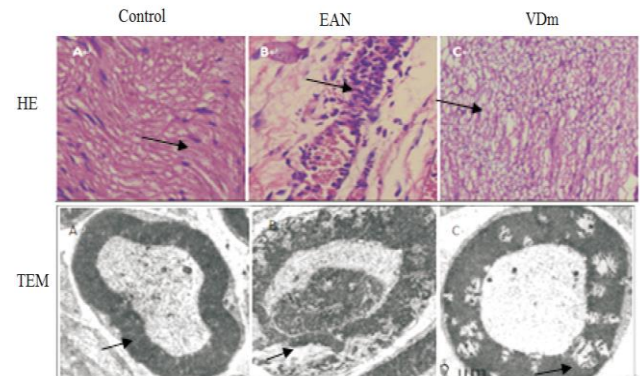


Figure 3. Inflammatory cell infiltration and demyelination of sciatic nerves were detected by HE staining and a transmission electron microscope.

The results of HE staining showed that compared with the control group, a large number of inflammatory cells infiltrated around the small vessels of sciatic nerves in the EAN group, while the inflammatory cell infiltrated around the vessels in the VDM group was significantly reduced (**Figure 3** HE - A, B, C). The results of the transmission electron microscope showed that the axonal structure of myelinated nerve fibers in the control group was normal, and the myelin lamina was regularly arranged around the center of the circle. In the EAN group, there were swelling of myelin lamina, non-

eycomb changes and peeling of myelin inner layer and axon. After treatment with $1.25(\text{OH})_2\text{D}_3$, the changes of myelin swelling and cavity formation in the VDM group were less than those in the EAN group (Figure 3 TEM - A, B, C).

3.4 Detection of IL-17, IL-10, TGF- β and IFN- γ in rats' serum by ELISA

Existing theories believe that inflammatory cytokines are one of the factors aggravating the disease of EAN. Therefore, we used ELISA to detect IL-17, IL-10, TGF- β and IFN- γ level in peripheral blood of rats in each group. The results showed that compared with the control group, the serum inflammatory cytokines IL-17 and IFN- γ in the EAN group increased obviously. The levels of IL-10 and TGF- β decreased significantly. The difference ($P < 0.05$) is of statistical significant. Compared with the EAN group, serum IL-17 and IFN- γ in the VDI, VDM and VDh groups after $1.25(\text{OH})_2\text{D}_3$ treatment decreased significantly. The levels of IL-10 and TGF- β increased significantly ($P < 0.05$). There were significant differences in the pairwise comparison between the VDI group vs the VDM group and the VDM group vs the VDh group

($P < 0.05$), but there was no significant difference between the VDI group vs the VDh group ($P > 0.05$). See Figure 4.

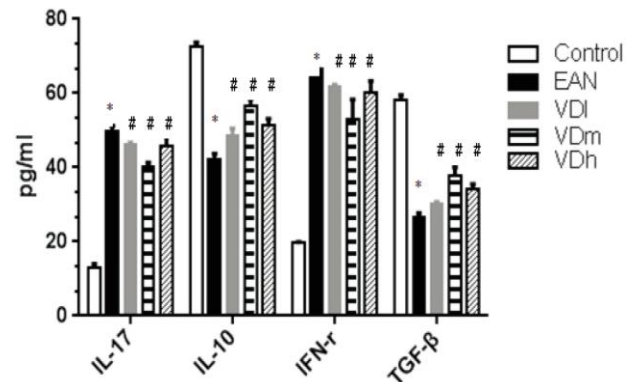


Figure 4. The level of inflammatory cytokines in peripheral blood ($\bar{x} \pm s$).

Note: * compared with the control group, $P < 0.05$; # compared with the EAN group, $P < 0.05$.

3.5 Detecting of the expression level of inflammatory cytokine mRNA in rat spleen by RT-PCR

At the peak of onset, the inflammatory cytokine mRNA in the spleen of rats in each group was detected by RT-PCR.

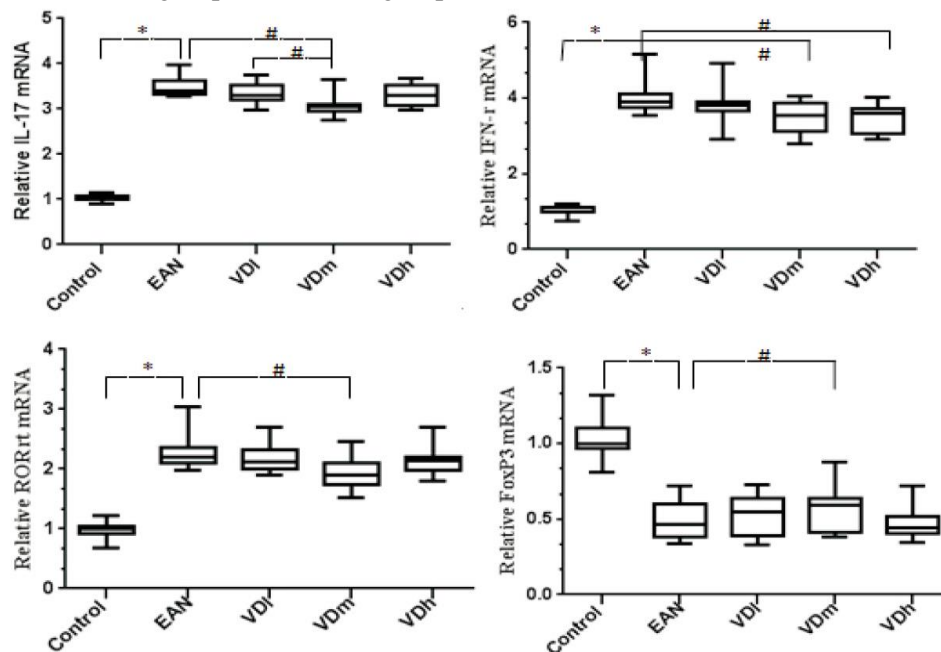


Figure 5. Expression levels of inflammatory cytokines and T lymphocyte mRNA in spleens ($2^{-\Delta\Delta CT}$, $\bar{x} \pm s$).

Note: * compared with the control group, $P < 0.05$; # compared with the EAN group, $P < 0.05$.

The results showed that compared with the control group, the expression level of IL-17 and IFN- γ , RORrt mRNA in the EAN group increased significantly and the level of FoxP3 mRNA de-

creased significantly. The difference was of statistical significance ($P < 0.05$). Compared with EAN group, the expression level of IL-17 and IFN- γ , RORrt mRNA in VDM decreased significantly, and

the level of FoxP3 mRNA increased significantly ($P < 0.05$). Compared with the EAN group, the VDh group showed obvious decrease only in the IFN- γ level. The level of IL-17 in the VDM group was significantly lower than that in the VDI group ($P < 0.05$). The above experimental results showed that the expression level of inflammation related cytokines decreased after 1.25(OH) $_2$ D $_3$ intervention treatment, and the therapeutic effect of medium-dose 1.25(OH) $_2$ D $_3$ was significantly better than that of the low- and high-dose groups. See **Figure 5**.

4. Discussion

At present, it is considered that GBS is an autoimmune disease mediated by T cells. The main clinical symptoms are limb weakness and symmetrical delayed paralysis of limbs. The main pathological features are demyelination of peripheral nerves and nerve root and infiltration of small vasculitis cells. EAN is a classic animal model of GBS, very similar to GBS in pathological changes, clinical manifestations and neuroelectrophysiological changes, and is widely used in the study of the pathogenesis and treatment of GBS^[8]. Many studies have shown that the destruction of immune homeostasis is the basis of GBS. Th17, Treg cells and their effectors constitute a complex network of downstream genes regulated by VDR and systemic lupus erythematosus and multiple sclerosis, which are involved in the occurrence, development and prognosis of GBS. Under physiological homeostasis, Th1/Th2 and Th17/Treg cells are in dynamic balance^[9,10]. The characteristic cytokine IL-17 secreted by Th17 cells participates in the occurrence of autoimmune diseases by inducing the inflammatory cascade of target organs. Treg cells with high expression of transcription factor FoxP3 inhibit Th cell function, secrete inhibitory inflammatory cytokines, inhibit autoimmune response and maintain immune homeostasis through direct contact. When the body is stimulated by pathogens, Th1 and Th17 cells are activated to produce inflammatory response against pathogens. If the regulation of this process is unbalanced, it may lead to autoimmune diseases. In the early stage of EAN, IFN- γ and IL-17 levels in peripheral blood increase signifi-

cantly; after the disease enters the recovery period, IFN- γ and IL-17 levels decrease gradually^[11]. The content of IL-17A in lymphocytes of EAE rat model increases significantly^[12], Th1 cells in peripheral blood of patients with GBS increases significantly, and Treg cells decreases significantly. Our previous study found that the expression of Th1/Th2 and Th17/Treg in peripheral blood of GBS patients is unbalanced. Gastrointestinal perfusion of bifido-bacterium infantis in ENA rats can improve the Th17/Treg imbalance and autoimmune inflammatory response^[13,14].

Vitamin D has no biological activity. It is transformed into the active form of 1.25(OH) $_2$ D $_3$ and plays a role in combination with VDR. VDR widely exists in immune cells and the central nervous system, such as hypothalamus, hippocampus and cortical neurons. Recent studies have shown that vitamin D plays a role in innate and specific immunity by regulating T lymphocytes; at the same time, studies have shown that vitamin D can not only affect the proliferation and maturation of T cells, but also reduce the expression of IL-17, promote the proliferation of Treg cells and enhance their immune tolerance^[15,16]. Kevin *et al.*^[17], Tedeschi *et al.*^[18] and Volt *et al.*^[19] detected that the downstream genes regulated by VDR are related to systemic lupus erythematosus and multiple sclerosis. Studies of Hau *et al.*^[20], and Jeffery *et al.*^[21] showed that the therapeutic effect of 1.25(OH) $_2$ D $_3$ in rheumatoid arthritis and psoriasis was related to IL-17A.

In this study, 0.25 $\mu\text{g}\cdot\text{kg}^{-1}$, 1 $\mu\text{g}\cdot\text{kg}^{-1}$, 4 $\mu\text{g}\cdot\text{kg}^{-1}$ 1.25(OH) $_2$ D $_3$ were used to intragastric treatment of EAN rats. The results showed that compared with the P0 peptid-induced EAN model group, 1.25(OH) $_2$ D $_3$ reduced the clinical symptoms, clinical scores and weight loss in EAN rats. The sciatic nerve conduction velocity was significantly improved. From the perspective of morphology, the method effectively reduced the sciatic neuritis cell infiltration and myelin sheath loss, among which the 1 $\mu\text{g}\cdot\text{kg}^{-1}$ VDM group had the best effect. Research of Mohammadi *et al.*^[22] showed that vitamin D reduces infiltration and demyelination of inflammatory cells into the central nervous system, which is consistent with our results.

The inflammatory cytokines in peripheral blo-

od of EAN rats were detected at the peak of the disease. $1.25(\text{OH})_2\text{D}_3$ decreased the expression of pro-inflammatory cytokines IL-17 and IFN- γ , and increased the expression of anti-inflammatory cytokines IL-10 and TGF- β in peripheral blood of EAN rats. The moderate-dose group (VDm) had a worse effect, while the high-dose group had a better effect. IFN- γ , on the one hand, promotes the pathogenesis of EAN by activating macrophages to produce NO and reactive oxygen intermediates, and on the other hand, down-regulates IL-17 by inhibiting the amplification of Th17 cells in the IL-23 pathway, which plays a bidirectional role in EAN. Speck *et al.*^[23] confirmed that high expression of TGF- β and IL-10 is related to the recovery and remission of EAE, and neutralizing or inhibiting TGF- β and IL-10 can aggravate the severity of EAE. However, Treg adoptive transfer can reduce the levels of TGF- β , IL-10 and IL-4, thereby alleviating EAE. The results of this study suggest that $1.25(\text{OH})_2\text{D}_3$ changed the balance of pro-inflammatory cytokines and anti-inflammatory cytokines in the EAN rat model, alleviated EAN clinical symptoms, and the therapeutic effect was dose-dependent. Further detection of Th17 and Treg cell transcription factors in the spleen of EAN rats at the peak of the disease showed that compared with the control group, the expression levels of IL-17, IFN- γ and RORrt mRNA in EAN rats increased, while FoxP3 mRNA level decreased. $1.25(\text{OH})_2\text{D}_3$ decreased the expression levels of IL-17, IFN- γ and RORrt mRNA in EAN rats, and up-regulated the level of Foxp3 mRNA. Recombinant IL-17 aggravates sciatic inflammatory cell infiltration and demyelination in EAN rats at acute stage. Reinfusion of amplified Treg cells *in vitro* can alleviate neuralgia and peripheral neuroinflammatory demyelination changes after peripheral nerve injury in EAN rats^[24]. In this study, treatment of $1.25(\text{OH})_2\text{D}_3$ and up-regulation of FoxP3 were followed by down-regulation of Th17 and other transcription factors, indicating that the distribution of Th17/Treg cells and inflammatory cytokines in EAN rats changed, and the imbalance of Th17/Treg was corrected. The treatment of $1.25(\text{OH})_2\text{D}_3$ may be related to Th17/Treg re-balance. Ahangar-Parvin *et al.*^[25] and Haqhmorad *et al.*^[26] found that vitamin D could prevent the onset

of EAE and change the proportion of Th1, Th17, Th2 and Treg cells in EAE, which is consistent with our research results.

VDR, as the nuclear receptor of $1.25(\text{OH})_2\text{D}_3$, can play a role in regulating gene transcription by binding to the VDRE sequence of the downstream gene promoter region. Tone *et al.*^[27] found VDRE sequence in the highly preserved non-coding sequence of FoxP3 gene in rats. $1.25(\text{OH})_2\text{D}_3$ stimulates FoxP3 expression in CD4⁺ CD25⁻T cells in human and rats^[26]. FoxP3 has the ability to directly inhibit IL-17 and IFN- γ , FoxP3, RORrt and Runx1 interact to inhibit IL-17 production, and VDR can block the expression of Runx1 and inhibit RORrt transfer viability^[28,29]. These studies show that $1.25(\text{OH})_2\text{D}_3$ may stimulate FoxP3 expression by directly binding to the VDRE sequence of FoxP3 gene intron to promote FoxP3 promoter activity, thereby regulating the expression of RORrt, inhibiting the pro-inflammatory Th17 response in the autoimmune process and alleviating EAN inflammation.

To sum up, $1.25(\text{OH})_2\text{D}_3$ may mediate the protective effect on EAN by influencing the number and function of T cells, inducing the differentiation of Treg cells, reducing the production of pro-inflammatory cytokines and increasing the expression of anti-inflammatory cytokines. Therefore supplementing $1.25(\text{OH})_2\text{D}_3$ may be an adjunct therapy for GBS, but the disease progression of the EAN rat model is self-limited. During the limited treatment period of the EAN model, whether the immunomodulatory effects of $1.25(\text{OH})_2\text{D}_3$ can be reproduced in patients with GBS requires further study. The results of this study expound the mechanism of $1.25(\text{OH})_2\text{D}_3$ treatment for EAN, which provides experimental basis for its future application in the prevention and treatment of GBS.

Conflict of interest

The authors declare no potential conflicts of interest.

Acknowledgements

Science and Technology Development Fund of Bengbu Medical College (BYKF1803); Key Project

of Education Department of Anhui Province (KJ2019A0377); Anhui University Students Innovation and Entrepreneurship Training Program (11812210003).

References

1. Haussler MR, Whitfield GK, Kanekop I, *et al.* Molecular mechanisms of vitamin D action. *Calcified Tissue International* 2013; 92(2): 77–98.
2. Bogdanou D, Penna-Martinez M, Filmann N, *et al.* T-lymphocyte and glycemic status after vitamin D treatment in type 1 diabetes: A randomized controlled trial with sequential crossover. *Diabetes/Metabolism Research and Reviews* 2017; 33(3): e2865.
3. Chun RF, Liu PT, Modlin RL, *et al.* Impact of vitamin D on immune function: Lessons learned from genome wide analysis. *Frontiers in Physiology* 2014; 21(5): 151–165.
4. Finch SL, Rosenberg AM, Hassan V. Vitamin D and juvenile idiopathic arthritis. *Pediatric Rheumatology* 2018; 16: 34–50.
5. Vanherwegen AS, Gysemans C, Mathieu C. Regulation of immune function by vitamin D and its use in disease of immunity. *Endocrinology and Metabolism Clinics of North America* 2017; 46(4): 1061–1094.
6. Spanier JA, Nashold FE, Mayne CG, *et al.* Vitamin D and estrogen synergy in Vdr-expressing CD4⁺ T cells is essential to induce Helios⁺ FoxP3⁺ T cells and prevent autoimmune demyelinating disease. *Journal of Neuroimmunology* 2015; 15(286): 48–58.
7. Meehan TF, Vanhooke J, Prah J, *et al.* Hypercalcemia produced by parathyroid hormone suppresses experimental autoimmune encephalomyelitis in female but not male mice. *Archives of Biochemistry and Biophysics* 2005; 442: 214–221.
8. Ding Y, Han R, Jiang W, *et al.* Programmed death ligand 1 plays a neuroprotective role in experimental autoimmune neuritis by controlling peripheral nervous system inflammation of rats. *The Journal of Immunology* 2016; 197(10): 3831–3840.
9. Gualdoni GA, Mayer KA, Göschl L, *et al.* The AMP analog AICAR modulates the Treg/Th17 axis through enhancement of fatty acid oxidation. *FASEB Journal* 2016; 30(11): 3800–3809.
10. Sun Y, Tian T, Gao J, *et al.* Metformin ameliorates the development of experimental autoimmune encephalomyelitis by regulating T helper 17 and regulatory T cells in mice. *Journal of Neuroimmunology* 2016; 292: 58–67.
11. Wang X, Zheng XY, Ma C, *et al.* Mitigated Tregs and augmented Th17 cells and cytokines are associated with severity of experimental autoimmune neuritis. *Scandinavian Journal of Immunology* 2014; 80(3): 180–190.
12. Joshi S, Pantalena LC, Liu XK, *et al.* 1,25-Dihydroxyvitamin D₃ ameliorates Th17 autoimmunity via transcriptional modulation of interleukin-17A. *Molecular and Cellular Biology* 2011; 31(17): 3653–3669.
13. Shi P, Dong W, Nian D, *et al.* Bifidobacterium alleviates guillain-barré syndrome by regulating the function of T17 cells. *International Journal of Clinical and Experimental Medicine* 2018; 11(5): 4779–4786.
14. Shi P, Qu H, Nian D, *et al.* Treatment of Guillain-Barré syndrome with bidobacterium infantis through regulation of T helper cells subsets. *International Immunopharmacology* 2018; 61: 290–296.
15. Zhou L, Wang J, Li J, *et al.* 1,25-Dihydroxyvitamin D₃ ameliorates collagen-induced arthritis via suppression of Th17 cells through miR-124 mediated inhibition of IL-6 signaling. *Frontiers in Immunology* 2019; 10: 178–190.
16. Marinho A, Carvalho C, Boleixa D, *et al.* Vitamin D supplementation effects on FoxP3 expression in T cells and FoxP3/IL-17A ratio and clinical course in systemic lupus erythematosus patients: A study in a Portuguese cohort. *Immunologic Research* 2017; 65(1): 197–206.
17. Singh K, Gandhi S, Batool R. A case-control study of the association between vitamin D levels and gastric incomplete intestinal metaplasia. *Nutrients* 2018; 10(5): 629–637.
18. Tedeschi SK, Aranow C, Kamen DL, *et al.* Effect of vitamin D on serum markers of bone turnover in SLE in a randomized controlled trials. *Lupus Science & Medicine* 2019; 17(6): e000352.

19. Vlot MC, Boekel L, Kragt J, *et al.* Multiple sclerosis patients show lower bioavailable 25(OH)D and 1,25(OH)₂D, but no difference in ratio of 25(OH)D/24,25(OH)₂D and FGF23 concentrations. *Nutrients* 2019; 11(11): 2774–2789.
20. Hau CS, Shimizu T, Tada Y, *et al.* The vitamin D₃ analog, maxacalcitol, reduces psoriasiform skin inflammation by inducing regulatory T cells and downregulating IL-23 and IL-17 production. *Journal of Dermatological Science* 2018; 92(2): 117–126.
21. Jeffery LE, Henley P, Marium N, *et al.* Decreased sensitivity to 1,25-dihydroxyvitamin D₃ in T cells from the rheumatoid joint. *Journal of Autoimmunity* 2018; 88: 50–60.
22. Mohammadi-Kordkhayli M, Ahangar-Parvin R, Azizi SV, *et al.* Vitamin D modulates the expression of IL-27 and IL-33 in the central nervous system in Experimental Autoimmune Encephalomyelitis (EAE). *Iranian Journal of Immunology* 2015; 12(1): 35–49.
23. Speck S, Lim J, Shelake S, *et al.* TGF-β signaling initiated in dendritic cells instructs suppressive effects on Th17 differentiation at the site of neuroinflammation. *Plos One* 2014; 9(7): e102390.
24. Austin PJ, Kim CF, Perera CJ, *et al.* Regulatory T cells attenuate neuropathic pain following peripheral nerve injury and experimental autoimmune neuritis. *Pain* 2012; 153(9): 1916–1931.
25. Ahangar-Parvin R, Mohammadi-Kordkhayli M, Azizi SV, *et al.* The modulatory effects of vitamin D on the expression of IL-12 and TGF-β in the spinal cord and serum of mice with experimental autoimmune encephalomyelitis. *Iranian Journal of Immunology* 2018; 13(1): 10–22.
26. Haghmorad D, Yazdanpanah E, Tavaf MJ, *et al.* Prevention and treatment of experimental autoimmune encephalomyelitis induced mice with 1,25-dihydroxyvitamin D₃. *Neurological Research* 2019; 41(10): 943–957.
27. Tone Y, Furuuchi K, Kojima Y, *et al.* Smad3 and NFAT cooperate to induce Foxp3 expression through its enhancer. *Nature Immunology* 2008; 9(2): 194–202.
28. Liu HP, Cao AT, Feng T, *et al.* TGF-β converts Th1 cells into Th17 cells through stimulation of Runx1 expression. *European Journal of Immunology* 2015; 45(4): 1010–1018.
29. Kataoka H, Yasuda S, Fukaya S, *et al.* Decreased expression of Runx1 and lowered proportion of Foxp3⁺ CD25⁺ CD4⁺ regulatory T cells in systemic sclerosis. *Modern Rheumatology* 2015; 25(1): 90–95.

REVIEW ARTICLE

Research progress on the role of sialic acid-binding immunoglobulin-like lectin 9 in various diseases

Ling Cao¹, Xiaoliang Yuan^{2*}

¹ Gannan Medical University, Ganzhou 341000, Jiangxi Province, China.

² Department of Respiratory Medicine, The First Affiliated Hospital, Gannan Medical University, Ganzhou 341000, Jiangxi Province, China. E-mail: yxlyyx@126.com

ABSTRACT

Sialic acid-binding immunoglobulin-like lectin 9 (Siglec-9) is a receptor that expresses on the surface of immune cells. It plays an important role in the body's immune response. Increased expression of Siglec-9 has been reported in infectious diseases, autoimmune diseases and cancer. Pathogenic microorganism and tumor cells can inhibit the recognition and killing of immune cells by upregulating their own specific sialic acid and binding with Siglec-9 on the surface of host immune cells, and suppress the release of pro-inflammatory cytokines and promote the release of anti-inflammatory cytokines, eventually leading to immunosuppression, tumor immune escape and the like. However, the immunosuppressive function of Siglec-9 may be advantageous for diseases such as neutrophil asthma and autoimmune diseases. Therefore, further research on the mechanism of action of Siglec-9 is of great significance.

Keywords: Siglec-9; Immune Response; Immunosuppression; Sialic Acid; sSiglec-9

ARTICLE INFO

Received 28 July 2021
Accepted 30 September 2021
Available online 8 October 2021

COPYRIGHT

Copyright © 2021 Ling Cao, *et al.*
EnPress Publisher LLC. This work is licensed under the Creative Commons Attribution-NonCommercial 4.0 International License (CC BY-NC 4.0).
<https://creativecommons.org/licenses/by-nc/4.0/>

1. Introduction

Sialic acid-binding immunoglobulin-like lectins (Siglecs) family is a kind of transmembrane proteins that can recognize sialic acid ligands. It is a major subgroup of type I lectins^[1]. Siglecs found in mammals can be divided into two categories based on evolutionary conservation and sequence similarity. The first group is composed of Sn (sialoadesin, Siglec-1) and CD22 (Siglec-2), MAG (myelin associated glycoprotein, Siglec-4) and Siglec-15; the second group is CD33 related sialic acid-binding immunoglobulin-like lectins (CD33-related Siglecs, CD33rSiglecs), including 10 of human (Siglec-3, -5, -6, -7, -8, -9, -10, -11, -14, -16) and 5 of rodents (Siglec-3, -E, -F, -G, -H). They have 50%–80% sequence similarity^[1,2]. Human Siglec-9 and mouse Siglec-E have high homology, while the structural sequences of Siglec-9 and Siglec-7 in human are highly similar. Most members of the Siglec family are inhibitory receptors, including Siglec-9. At present, many studies have shown that Siglec-9 may play an important role in the pathogenesis of many diseases, including infectious diseases, autoimmune diseases and cancer, but its mechanism of regulating immune response is not yet clear. Further research on the mechanism of Siglec-9 in diseases is of great significance for clinical diagnosis and treatment. This paper summarizes the current research on the mechanism of Siglec-9 in diseases.

2. Biological characteristics of Siglec-9

Siglec-9, also known as CD329, contains 463 amino acids and its

gene is located on the long arm of chromosome 19^[3,4]. Siglec-9 is widely expressed on the surface of immune cells, such as neutrophils, monocytes, macrophages, dendritic cells and natural killer (NK) cells^[1]. All CD33rSiglecs members have similar sequences and are type I transmembrane proteins. Siglec-9 contains an immunoglobulin like N-terminal, a V-region domain and two C2 region domains, in which the V region is the site of sialic acid binding; the cytoplasmic tail includes an immunoreceptor tyrosine-based inhibitor motif (ITIM) and an ITIM like sequence^[5]. Phosphorylation of tyrosine residues on the ITIM motif near the membrane end of Siglec-9 can recruit protein tyrosine phosphatases SHP-1 and SHP-2 (SRC homology 2 domain containing protein tyrosine phosphatase 1/2), and activate tyrosinase phosphorylation, so as to down regulate or inhibit the downstream intracellular activation signal^[6-8]. Therefore, Siglec-9 is an inhibitory receptor on the cell surface.

The ligands of Siglecs are mainly sialic acid containing glycoproteins or glycolipids. Siglecs bind to ligands in roughly the same way, which can be divided into two categories: one is cis interactions, that is, they bind to sialic acid ligands (cis ligands) on the same cell membrane; the second is trans interactions, which combines with sialic acid ligands (trans ligands) on the surface of other cell membranes^[6,9]. A high concentration of sialic acid formed locally on the same cell membrane can achieve cis interactions with Siglec, directly act on or mask the sialic acid binding site of Siglec, so as to weaken trans interactions. Siglec-9 on immune cells preferentially interacts with sialic acids ligands whose terminal are linked in the form of $\alpha(2,3)$ - and $\alpha(2,6)$ -^[10]; the immune response between cells and between cells and pathogenic microorganisms can inhibit the activity of immune cells, facilitating the survival of pathogenic microorganisms and the immune escape of tumor cells^[11-15]. In addition, vascular adhesion protein-1 (VAP-1) is an important molecule regulating leukocyte migration to inflammatory sites. Siglec-9, as a leukocyte ligand, can be used for positron emission tomography (PET) imaging to assist inflammation and cancer diagnosis^[16].

Soluble Siglec-9 (sSiglec-9) is the extracellu-

lar part of Siglec-9, which has antibacterial effect by competitively inhibiting the binding between Siglec-9 and its ligands, and preventing down-regulation of host immune response, and can play an anti-tumor role by inhibiting downstream signal transduction mediated by tumors related mucin1 (MUC1)^[17,18].

3. Mechanism of Siglec-9 in various diseases

3.1 Pulmonary diseases

Siglec-9 ligands are widely distributed in human's lung tissues (submucosal glands, epithelial cells and connective tissue) and are consistent with the distribution of neutrophil inflammation, which may be related to Siglecs-9's involvement in regulating neutrophil function^[19]. And inflammation leads the up regulation of Siglec-9 ligands' expression in lung tissues, which may help to control lung inflammation^[20].

Zeng *et al.* found that Siglec-9 expression on neutrophils increased in alveolar and peripheral blood of patients with the chronic obstructive pulmonary disease (COPD)^[21]. At the same time, cigarette extract (CSE), lipopolysaccharide (LPS), some cytokines and dexamethasone (DEX) can up regulate the expression of Siglec-9. And they further found that DEX may have anti-inflammatory effect on neutrophils by up regulating the expression of Siglec-9. The expression of Siglec-9 also increased in COPD patients, and increased the oxidative burst of neutrophils and the chemotaxis of interleukin (IL)-8 by competitively inhibiting the binding of Siglec-9 to its ligands. Other studies have shown that through the analysis of Siglec-9 genotype and clinical characteristics in patients with COPD, it is found that some variant Siglec-9 weakens the response to inflammation. The inhibition of immune cell activation may be a risk factor for the development of emphysema^[22].

In the mouse model of acute pulmonary inflammation, neutrophil recruitment in the lungs of Siglec-E-deficient mice increased^[23]. In addition, mouse Siglec-E inhibits the recruitment of neutrophils to the lung by promoting the activation of NADPH (nicotinamide adenine dinucleotide phos-

phate) oxidase^[24]. Therefore, it is speculated that human Siglec-9, which is homologous to it, may also regulate the function of neutrophils and inhibit lung inflammation in a similar way. Therefore, Siglec-9 may become a new target for immunosuppressive therapy of neutrophilic pulmonary inflammation (including some COPDs, and severe asthma).

3.2 Tumors

Tumor cells can achieve immune escape by up-regulating inhibitory molecules to inhibit the host immune system, including PD-L1 (programmed death-ligand 1) and Siglec-9 ligands^[25–28]. In addition, the change of sialylation on the surface of tumor cells is of great significance for tumor progression, especially in combination with Siglecs to regulate immunity cell function^[29,30]. Monocytes expressing Siglec-9 have been found to increase in a variety of tumor tissues, including the non-small cell lung cancer^[28].

MUC1 is a kind of transmembrane glycoprotein containing sialoglycan, which is abnormally expressed in a variety of tumor tissues, and can directly bind to Siglec-9 as Siglec-9 ligands. MUC1 expressed by tumor cells is combined with Siglec-9 on the surface of immune cells^[31–33]. On the one hand, it directly inhibits antitumor immunity; on the other hand, it triggers MUC1 mediated immune response signal transduction, inducing recruitment β -catenin to enter into the nucleus, which leads to the growth of tumor cells. In sSiglec-9 transgenic mice, the proliferation of breast tumor cells expressing MUC1 was inhibited, and the expression of MUC1 tended to decrease^[18]. It was found that Siglec-9 inhibits tumor proliferation by inhibiting MUC1 mediated downstream signal transduction, but this antitumor effect does not exist in cell research in vitro^[31]. The difference of this result may depend on many factors. For example, the influence of experimental environment in vivo is more complex than that in vitro.

On the other hand, Siglec-9 or Siglec-E expressed on the surface of macrophages may inhibit the differentiation into M2 macrophages that promote tumors^[1,28]. Heinz L äubi *et al.* found that there were more M2 macrophages and faster tumor

growth in Siglec-E-deficient mice, indicating that Siglec-E can limit tumor growth; moreover, Siglec-9 has polymorphism, and the binding of K131Q Siglec-9 to ligands is reduced, which can improve the early survival rate of patients with non-small cell lung cancers (NSCLC)^[28,34]. Overall, the effect of Siglec-9 on tumors is complex and may be different at different stages of tumor cell growth.

3.3 Autoimmune diseases

Siglec-9 is also up-regulated in rheumatoid arthritis (RA). It inhibits collagen induced arthritis by promoting the differentiation of anti-inflammatory regulatory T cells (Treg) and inhibiting the differentiation of pro-inflammatory helper T cells 17 (Th17) in a certain dependent manner^[35]. In the serum and synovial fluid of RA patients, the level of Siglec-9 was also increased and correlated with the severity of RA disease. On the contrary, the results of Takuya Matsumoto *et al.* may be significantly different due to different animals and conditions used in the experiment^[36], that sSiglec-9 obviously inhibits arthritis incidence rate and severity, and through in vitro experiments, it has been found that the anti-inflammatory role is achieved by inhibiting nuclear factor-kappaB (NF- κ B) pathway to reduce the activity of M1 macrophages. In addition, Siglec-9 can specifically bind to VAP-1, label Siglec-9 peptide with radionuclide ⁶⁸Ga, and detect it by PET imaging VAP-1 in blood vessels, clearly showing synovitis and contributing to the early diagnosis of RA^[37].

However, in systemic lupus erythematosus, the expression of Siglec-9 on monocytes and neutrophils did not change significantly, while the expression of Siglec-14, another member of Siglecs family, increased^[38].

3.4 Sepsis

Although the immune response is the body's protective response in the early stage of sepsis, the subsequent sustained strong immune response will lead to organ dysfunction. Therefore, timely and appropriate intervention of immune response is beneficial to alleviate sepsis.

Macrophage polarization and cytokines play an important role in the development of sepsis^[39].

Siglec-9 can regulate the polarization of macrophages and promote the differentiation into M2 type that inhibits inflammation. On the other hand, the interaction between Siglec-9/Siglec-E and toll-like receptor 4 (TLR4) on immune cells is also involved in the pathogenesis of sepsis; Siglec-9/Siglec-E mediates the endocytosis of TLR4, which may regulate its activity by affecting its signal transduction and degradation, and then change the expression of downstream cytokines^[40–42]. The specific mechanism needs to be further studied. In vitro experiments have shown that Siglec-9 activation can promote the production of anti-inflammatory cytokine IL-10 in macrophages and inhibit pro-inflammatory cytokine IL-6 and tumor necrosis factor by inhibiting LPS induced TLR4 Signal transduction- α (tumor necrosis factor- α , TNF- α)^[43,44]. Therefore, Siglec-9, as an immunosuppressive receptor, may become a new strategy for anti-inflammatory treatment of sepsis.

3.5 Others

Changes in sialylation on the bacterial surface can enhance the virulence of bacteria and contribute to the survival of bacteria in the host^[45]. For example, group B streptococcus (GBS) binds to Siglec-9 on neutrophils, resulting in oxidative burst and damage to the formation of neutrophil extracellular traps (NETs), which inhibits the host immune response and is conducive to the survival of pathogenic microorganisms^[13]. In transgenic mice, sSiglec-9 can inhibit GBS infection by restoring the immune response of neutrophils^[17].

Human immunodeficiency virus (HIV)-1 can interact with Siglec-1, -3, -9 through surface acidulated glycoprotein 120 (gp120), which promotes the sensitivity of macrophages^[46]. In chronic hepatitis B, it was found that the expression of Siglec-9 ligands increased in HBV infected liver tissue; the expression of Siglec-9 positive NK cells decreased and was negatively correlated with the DNA titer of serum hepatitis e antigen and hepatitis B virus (HBV); the expression of Siglec-9 on NK cells of patients with sustained viral response returned to the normal level^[47]. In addition, blocking Siglec-9 can reverse the inhibition of NK cells. Overall, Siglec-9, as an inhibitory receptor on the surface of NK cells, par-

ticipates in the regulation of immunity and is related to the persistence of HBV in the host, but the specific mechanism is not clear.

4. Conclusions

According to many studies, Siglec-9, as an inhibitory receptor on immune cells, is involved in the pathogenesis of many diseases, mainly inhibiting the immune response; on the other hand, Siglec-9 may play different roles in different diseases or different periods of the same disease, having both advantages and disadvantages for the development of the disease. However, the specific mechanism of Siglec-9 is not completely clear and needs to be further studied. sSiglec-9 may weaken the function of Siglec-9 and positively regulate immune function through competitive inhibition, but there are still disputes in the current experimental results in vivo and in vitro.

In addition, Siglec-9 may be used as a potential biological marker to help the diagnosis, staging and treatment of some diseases. Using the immunosuppressive effect of activating Siglec-9 as a treatment strategy can inhibit the sustainable development of inflammation and provide a new choice for autoimmune diseases and allergic diseases. On the other hand, inhibiting or blocking the activity of Siglec-9 can enhance immune response and provide new therapeutic targets for tumors and infectious diseases. In conclusion, in-depth study of the mechanism of Siglec-9 has far-reaching significance for disease diagnosis and treatment.

Conflict of interest

The authors declare no potential conflicts of interest.

Acknowledgements

This research was the Science and Technology Planning Project of Jiangxi Provincial Health and Family Planning Commission (No.: 20141114).

References

1. Varki A, Schnaar RL, Crocker PR. I-type lectins. New York: Cold Spring Harbor Laboratory Press; 2017. p. 453–467.

2. Zhang J, Nicoll G, Jones C, *et al.* Siglec-9, a novel sialic acid binding member of the immunoglobulin superfamily expressed broadly on human blood leukocytes. *Journal of Biological Chemistry* 2000; 275 (29): 22121–22126.
3. Foussias G, Yousef GM, Diamandis EP. Identification and molecular characterization of a novel member of the Siglec family (Siglec9). *Genomics* 2000; 67(2): 171–178.
4. Grimwood J, Gordon LA, Olsen A, *et al.* The DNA sequence and biology of human chromosome 19. *Nature* 2004; 428(6982): 529–535.
5. Crocker PR, Varki A. Siglecs, sialic acids and innate immunity. *Trends in Immunology* 2001; 22(6): 337–342.
6. Crocker PR, Paulson JC, Varki A. Siglecs and their roles in the immune system. *Nature Reviews Immunology* 2007; 7(4): 255–266.
7. Avril T, Floyd H, Lopez F, *et al.* The membrane-proximal immunoreceptor tyrosine-based inhibitory motif is critical for the inhibitory signaling mediated by Siglecs-7 and -9, CD33-related Siglecs expressed on human monocytes and NK cells. *Journal of Immunology* 2004; 173(11): 6841–6849.
8. Macauley MS, Crocker PR, Paulson JC. Siglec-mediated regulation of immune cell function in disease. *Nature Reviews Immunology* 2014; 14(10): 653–666.
9. Adams OJ, Stanczak MA, Von Gunten S, *et al.* Targeting sialic acid-Siglec interactions to reverse immune suppression in cancer. *Glycobiology* 2018; 28(9): 640–647.
10. Angata T, Varki A. Cloning, characterization, and phylogenetic analysis of Siglec-9, a new member of the CD33-related group of Siglecs: Evidence for co-evolution with sialic acid synthesis pathways. *Journal of Biological Chemistry* 2000; 275(29): 22127–22135.
11. Khatua B, Bhattacharya K, Mandal C. Sialoglycoproteins adsorbed by *Pseudomonas aeruginosa* facilitate their survival by impeding neutrophil extracellular trap through Siglec-9. *Journal of Leukocyte Biology* 2012; 91(4): 641–655.
12. Ono E, Uede T. Implication of soluble forms of cell adhesion molecules in infectious disease and tumor: Insights from transgenic animal models. *International Journal of Molecular Sciences* 2018; 19(1): 239.
13. Carlin AF, Uchiyama S, Chang YC, *et al.* Molecular mimicry of host sialylated glycans allows a bacterial pathogen to engage neutrophil Siglec-9 and dampen the innate immune response. *Blood* 2009; 113(14): 3333–3336.
14. Jandus C, Boligan KF, Chijioke O, *et al.* Interactions between Siglec-7/9 receptors and ligands influence NK cell-dependent tumor immunosurveillance. *Journal of Clinical Investigation* 2014; 124(4): 1810–1820.
15. Ikehara Y, Ikehara SK, Paulson JC. Negative regulation of T cell receptor signaling by Siglec-7 (p70/AIRM) and Siglec-9. *Journal of Biological Chemistry* 2004; 279(41): 43117–43125.
16. Aalto K, Autio A, Kiss EA, *et al.* Siglec-9 is a novel leukocyte ligand for vascular adhesion protein-1 and can be used in PET imaging of inflammation and cancer. *Blood* 2011; 118(13): 3725–3733.
17. Saito M, Yamamoto S, Ozaki K, *et al.* A soluble form of Siglec-9 provides a resistance against Group B *Streptococcus* (GBS) infection in transgenic mice. *Microbial Pathogenesis* 2016; 99: 106–110.
18. Tomioka Y, Morimatsu M, Nishijima K, *et al.* A soluble form of Siglec-9 provides an tumor benefit against mammary tumor cells expressing MUC1 in transgenic mice. *Biochemical and Biophysical Research Communications* 2014; 450(1): 532–537.
19. Yu H, Gonzalez-Gil A, Wei Y, *et al.* Siglec-8 and Siglec-9 binding specificities and endogenous airway ligand distributions and properties. *Glycobiology* 2017; 27(7): 657–668.
20. Jia Y, Yu H, Fernandes SM, *et al.* Expression of ligands for Siglec-8 and Siglec-9 in human airways and airway cells. *Journal of Allergy and Clinical Immunology* 2015; 135(3): 799–810.
21. Zeng Z, Li M, Wang M, *et al.* Increased expression of Siglec-9 in chronic obstructive pulmonary disease. *Scientific Reports* 2017; 7(1): 10116.
22. Ishii T, Angata T, Wan E S, *et al.* Influence of SIGLEC9 polymorphisms on COPD phenotypes

- including exacerbation frequency. *Respirology* 2017; 22(4): 684–690.
23. Mcmillan SJ, Sharma RS, Mckenzie EJ, *et al.* Siglec-E is a negative regulator of acute pulmonary neutrophil inflammation and suppresses CD11 β 2-integrin-dependent signaling. *Blood* 2013; 121(11): 2084–2094.
 24. Mcmillan SJ, Sharma RS, Richards HE, *et al.* Siglec-E promotes β 2-integrin-dependent NADPH oxidase activation to suppress neutrophil recruitment to the lung. *Journal of Biological Chemistry* 2014; 289(29): 20370–20376.
 25. Kuol N, Stojanovska L, Nurgali K, *et al.* The mechanisms tumor cells utilize to evade the host's immune system. *Maturitas* 2017; 105: 8–15.
 26. Jandus C, Boligan KF, Chijioke O, *et al.* Interactions between Siglec-7/9 receptors and ligands influence NK cell-dependent tumor immunosurveillance. *The Journal of Clinical Investigation* 2014; 124(4): 1810–1820.
 27. Mu C, Huang J, Chen Y, *et al.* High expression of PD-L1 in lung cancer may contribute to poor prognosis and tumor cells immune escape through suppressing tumor infiltrating dendritic cells maturation. *Medical Oncology* 2011; 28(3): 682–688.
 28. Lubli H, Pearce OMT, Schwarz F, *et al.* Engagement of myelomonocytic Siglecs by tumor-associated ligands modulates the innate immune response to cancer. *Proceedings of the National Academy of Sciences* 2014; 111(39): 14211–14216.
 29. Cohen M, Elkabets M, Perlmutter M, *et al.* Sialylation of 3-methylcholanthrene-induced fibrosarcoma determines antitumor immune responses during immunoediting. *Journal of Immunology* 2010; 185(10): 5869–5878.
 30. Pearce OM, Laubli H. Sialic acids in cancer biology and immunity. *Glycobiology* 2016; 26(2): 111–128.
 31. Tanida S, Akita K, Ishida A, *et al.* Binding of the sialic acid-binding lectin, Siglec-9, to the membrane mucin, MUC1, induces recruitment of beta-catenin and subsequent cell growth. *Journal of Biological Chemistry* 2013; 288(44): 31842–31852.
 32. Macao B, Johansson DG, Hansson GC, *et al.* Auto-proteolysis coupled to protein folding in the SEA domain of the membrane-bound MUC1 mucin. *Nature Structural Molecular Biology* 2006; 13(1): 71–76.
 33. Gendler SJ. MUC1, the renaissance molecule. *Journal of Mammary Gland Biology and Neoplasia* 2001; 6(3): 339–353.
 34. Fraschilla I, Pillai S. Viewing Siglecs through the lens of tumor immunology. *Immunological Reviews* 2017; 276(1): 178–191.
 35. Wang X, Liu D, Ning Y, *et al.* Siglec-9 is upregulated in rheumatoid arthritis and suppresses collagen-induced arthritis through reciprocal regulation of Th17-/Treg-cell differentiation. *Scandinavian Journal of Immunology* 2017; 85(6): 433–440.
 36. Matsumoto T, Takahashi N, Kojima T, *et al.* Soluble Siglec-9 suppresses arthritis in a collagen-induced arthritis mouse model and inhibits M1 activation of RAW264.7 macrophages. *Arthritis Research & Therapy* 2016; 18(1): 133.
 37. Virtanen H, Autio A, Siitonen R, *et al.* 68Ga-DOTA Siglec-9-a new imaging tool to detect synovitis. *Arthritis Research & Therapy* 2015; 17(1): 308.
 38. Thornhill SI, Mak A, Lee B, *et al.* Monocyte Siglec-14 expression is upregulated in patients with systemic lupus erythematosus and correlates with lupus disease activity. *Rheumatology* 2017; 56(6): w498.
 39. Liu Y, Zou X, Chai Y, *et al.* Macrophage polarization in inflammatory diseases. *International Journal of Biological Sciences* 2014; 10(5): 520–529.
 40. Liu Y, Yu M, Chai Y, *et al.* Sialic Acids in the Immune Response during Sepsis. *Frontiers in Immunology* 2017; 8: 1601.
 41. Chen G, Brown NK, Wu W, *et al.* Broad and direct interaction between TLR and Siglec families of pattern recognition receptors and its regulation by Neu1. *Elife* 2014; 3: e4066.
 42. Wu Y, Ren D, Chen G. Siglec-E negatively regulates the activation of TLR4 by Controlling its endocytosis. *Journal of Immunology* 2016; 197(8): 3336–3347.
 43. Ando M, Tu W, Nishijima K, *et al.* Siglec-9 enhances IL-10 production in macrophages via tyrosine-based motifs. *Biochemical and Biophysical Research Communications* 2008; 369(3): 878–883.

44. Chu S, Zhu X, You N, *et al.* The fab fragment of a human anti-Siglec-9 monoclonal antibody suppresses LPS-induced inflammatory responses in human macrophages. *Frontiers in Immunology* 2016; 7: 649.
45. Wessels MR, Rubens CE, Benedi VJ, *et al.* Definition of a bacterial virulence factor: Sialylation of the group B streptococcal capsule. *Proceedings of the National Academy Sciences USA* 1989; 86(22): 8983–8987.
46. Zou Z, Chastain A, Moir S, *et al.* Siglecs facilitate HIV-1 infection of macrophages through adhesion with viral sialic acids. *PLoS One* 2011; 6(9): e24559.
47. Zhao D, Jiang X, Xu Y, *et al.* Decreased Siglec-9 expression on natural killer cell subset associated with persistent HBV replication. *Frontiers in Immunology* 2018; 9: 1124.

REVIEW ARTICLE

Research progress in immunotherapy of advanced non-small cell lung cancer

Xiaojuan Lu¹, Huaqiu Shi^{2*}, Qiuyang Que¹, Song Qiu¹

¹ Gannan Medical University, Ganzhou 341000, Jiangxi Province, China.

² The First Affiliated Hospital of Gannan Medical University, Ganzhou 341000, Jiangxi Province, China. E-mail: shq3677274@163.com

ABSTRACT

Non-small cell lung cancer (NSCLC) poses a serious threat to people's health. Its morbidity and mortality are among the highest among all malignant tumors, and there is an urgent need for more effective new treatment methods. In recent years, NSCLC immunotherapy has made great progress, the first PD-1 inhibitor nivolumab (Nivolumab, O drug) was approved by the US Food and Drug Administration (FDA) in March 2015, applying to the patients who progressed or has received platinum chemotherapy drugs in the past. Immunotherapy of advanced NSCLC has entered a new era. This article reviews the current research progress of NSCLC immunotherapy.

Keywords: Non-small Cell Lung Cancer (NSCLC); Immunotherapy; Chemotherapy; Radiotherapy; Targeted Therapy

ARTICLE INFO

Received 10 July 2021
Accepted 27 September 2021
Available online 10 October 2021

COPYRIGHT

Copyright © 2021 Xiaojuan Lu, *et al.*
EnPress Publisher LLC. This work is licensed under the Creative Commons Attribution-NonCommercial 4.0 International License (CC BY-NC 4.0).
<https://creativecommons.org/licenses/by-nc/4.0/>

1. Introduction

The incidence rate and mortality of Lung cancer are very high. According to the world cancer statistics 2018, the incidence rate of lung cancer ranks first (2.1 million) in all malignant tumors, and the mortality rate is second (1.8 million), which seriously endangers people's health. Non-small cell lung cancer (NSCLC) is the most common clinical type of lung cancer, accounting for about 85% of all lung cancer types^[1]. Most NSCLC patients are in the advanced stage at the time of treatment, and the treatment prognosis is poor. Therefore, it is of great clinical significance to explore new treatment methods for advanced NSCLC to improve the prognosis of patients^[2]. In the past, the main treatment of advanced NSCLC was radiotherapy and chemotherapy, and the 5-year survival rate was less than 15%^[3]. In recent 10 years, studies have confirmed that the driver gene mutation was positive in advanced NSCLC patients can get significant survival benefits through targeted therapy^[4]. Nowadays, tumor immunotherapy has pushed the treatment of NSCLC to a climax again, and some have proved to be beneficial to patients. However, only 20% of patients benefit from immunotherapy, and up to 50% of patients have experienced adverse events^[5]. How to choose immunotherapy to maximize the survival benefit of patients with advanced NSCLC has become an urgent clinical problem to be solved.

2. Immunotherapy of tumor

The human immune system plays an important role in the process

of tumor development. There is an interactive relationship between the two. The human immune system not only can promote tumor growth but also inhibit tumor growth, which is called “immune editing” of cancer^[6]. The immune system clears tumor cells by recognizing tumor-specific antigens and related antigens and generating T cell immune response. It mainly includes the following processes. Firstly, dendritic cells migrate to tumor cells and are activated by new antigens released during carcinogenesis. Secondly, dendritic cells present antigens on major histocompatibility complex (MHC) I and II molecules and capture activated antigens on T cells specific T cells. Finally, activated cytotoxic T lymphocytes (CTL) are transported to the tumor site to produce effective immune surveillance, and finally kill cancer cells and prevent tumorigenesis^[7]. At present, the research of tumor immunotherapy mainly focuses on tumor vaccines and immune checkpoint inhibitors.

2.1 Tumor vaccine

The tumor vaccine is a newly developed vaccine to prevent tumors. Its principle is to activate the patient’s autoimmune system, induce the body’s specific cellular and humoral immune response by using tumor cells or tumor antigen substances, so that enhance the body’s anti-cancer ability, and prevent the growth, diffusion, and recurrence of tumor, to achieve the purpose of eliminating or controlling the tumor. Immune checkpoint inhibitors are mainly effective for patients with immunogenic tumors, such as tumor-infiltrating lymphocytes (TILs), of which antigens are closely related. New antigens are produced by gene mutations in the process of tumorigenesis, represented by tumor mutation burden (TMB). High TMB tumors have been proved to be the most immunogenic and sensitive tumor inhibitors to immune checkpoints. However, in patients with non-immunogenic tumors, TILs have weak or no infiltration, and they are not active. Therefore, a key problem in immune-oncology is: how to transform non-immunogenic tumors into immunogenic tumors? One way to achieve this goal is to use cancer vaccines. Among the developed cancer vaccines, the Provenge vaccine for prostate cancer proved ineffective in phase

III clinical trials, and other cancers, including NSCLC, showed certain clinical benefits^[8]. In a randomized, double-blind, phase IIB trial, NSCLC patients with HLA-A*201 positive and TERT expression who did not progress after first-line platinum chemotherapy were randomly divided into groups and treated with Vx-001 or placebo. The results showed that the study did not reach its primary endpoint (the median OS of placebo and Vx-001 were 11.3 and 14.3 months, respectively; $P = 0.86$)^[9]. A study of the docetaxel autologous tumor-derived autophagy vaccine in patients with advanced NSCLC showed that the GM-CSF drop vaccine could induce the immune response of tumor cells, and it did not observe obvious immunotoxicity, although this study does not continue due to its poor prognosis. However, the research on tumor vaccine for patients with advanced NSCLC has made further development^[10]. Although studies have shown that the tumor vaccine can benefit some patients, the Ctumor vaccine is still in the stage of laboratory research and has not been put into clinical use. We still need to do more prospective trials to study it.

2.2 Application of immune checkpoint inhibitors in NSCLC

2.2.1 Cytotoxic T cell lymphocyte antigen-4 (CTLA-4)

Cytotoxic T cell lymphocyte-associated antigen-4 (CTLA-4), also known as CD152, is a protein receptor that acts as an immune checkpoint and can down-regulate the immune response. Previous studies have shown that the activation of T lymphocytes is considered to require at least two signals: one is transmitted by T cell receptor complex after antigen recognition, and the other is transmitted by costimulatory receptors (such as CD28). CTLA-4 is expressed on activated T cells, about 30% is homologous to CD28, can bind to CD28 ligands (such as CD80 and CD86), and has high affinity, indicating that when CTLA-4 is up-regulated in activated T cells, it may preferentially interact with CD80 and CD86. Ipilimumab is an immunoglobulin monoclonal antibody against CTLA-4. It was approved by FDA in 2011 for the treatment of metastatic malignant melanoma^[11]. Therefore, clinical

studies on the therapeutic efficacy and toxicity of CTLA-4 inhibitors are mostly carried out in melanoma patients. A phase III, randomized, open, multicenter Arctic trial was conducted to evaluate the efficacy and safety of immunotherapy in patients with advanced NSCLC after multi-line treatment. The results showed that in patients with PD-L1 \geq 25%, Durvalumab (drug I) alone improved PFS and OS compared with standard treatment; in patients with PD-L1 \leq 25%, Durvalumab combined with CTLA-4 inhibitor Tremeliumab can only improve PFS and OS numerically, but there is no significant difference. The safety is the same as that of previous treatment^[12]. There is still a long way to go to study the therapeutic efficacy or adverse reactions of CTLA-4 inhibitors in NSCLC.

2.2.2 Programmed death 1(PD-1) and programmed cell death ligand 1(PD-L1)

Blocking PD-1/PD-L1 tumor immunotherapy has been proved to improve the ability to kill tumor cells by blocking the PD-1/PD-L1 signal pathway, restoring the immune activity of T cells in NSCLC, and enhancing immune response^[5]. At present, several PD-1 and PD-L1 inhibitors have been approved by FDA and European Medicines Agency (EMA) approved and recommended as the standard therapeutic drug for NSCLC. For example, EMA and FDA recommend pembrolizumab as a first-line treatment for advanced lung squamous cell carcinoma with negative driver gene and PD-L1 expression \geq 50%. Pembrolizumab is also approved for locally advanced or metastatic NSCLC patients with PD-L1 expression $>$ 1%. In addition, for unresectable locally advanced NSCLC, durvalumab was approved by FDA and EMA as monotherapy for NSCLC patients whose condition did not progress after radiotherapy and chemotherapy regardless of PD-L1 expression level (FDA approval)^[13,14]. At present, the expression of tumor cell PD-L1 is considered to be the best molecular marker for the dominant population in anti-PD-1/PD-L1 treatment. Many clinical studies have found that the positive expression of tumor cell PD-L1 is related to its curative effect and prognosis^[15,16]. However, a large number of studies show that only about 20% of patients can benefit from immunotherapy. Given the

high cost of immunotherapy, how to select the dominant population of immunotherapy and realize the precise treatment of NSCLC is also an important direction for us to explore in the future.

3. Immunotherapy for NSCLC

3.1 Combined immunochemotherapy

The synergistic effect of immunotherapy combined with chemotherapy has been confirmed in clinical trials. A large number of studies have confirmed that chemotherapy combined with immunotherapy can benefit patients more than chemotherapy alone^[17,18]. In 2017, FDA approved pembrolizumab combined with pemetrexed and carboplatin treatment of advanced non-small cell lung cancer^[19]. In 2018, FDA approved pembrolizumab combined with paclitaxel and carboplatin as a first-line treatment for metastatic squamous cell carcinoma, regardless of PD-L1 expression. A meta-analysis included 14 relevant randomized controlled trials (RCTs). A total of 8081 newly diagnosed patients with advanced NSCLC were included in the study. The results showed that in terms of tumor response and long-term survival, immunotherapy combined with first-line chemotherapy showed stronger advantages than chemotherapy alone, but also increased grade 3–5 toxic and side effects. The meta-analysis also showed that although combination therapy was superior to single chemotherapy in tumor response and long-term survival, combination therapy increased grade 3–5 toxicity^[20]. Based on a large number of studies, the combination of immunotherapy can enhance the recognition and clearance of tumor cells by the immune system, to produce a lasting and effective anti-tumor immune response. It is particularly important to formulate an accurate administration plan, obtain the maximum anti-tumor immune response and disease control rate, and minimize adverse reactions. Wu *et al.* proposed “medium dose intermittent chemotherapy (MEDIC)” and the main purpose of the regimen is to increase the anti-tumor immunogenicity and produce a sustained anti-tumor immune response by initiating repeated cytotoxic injury. In addition to the formulation of dose, the use sequence of each regimen also plays an important role in obtaining an

effective anti-tumor response. Some studies have shown that the response rate of immunosuppressants is 23%–25%, while chemotherapy is the first 18%–20%. However, up to now, there is no sufficient evidence to confirm what kind of administration sequence can maximize the survival benefit of patients. How to select the optimal combination scheme, administration sequence, dosage, and how to select the dominant population will be an important direction for our exploration in the future.

3.2 Immunocombined radiotherapy

In recent years, with the understanding of the immune stimulation characteristics of local radiotherapy and its impact on the cell cycle, as well as the understanding of the immune regulation mechanism at the molecular and cellular levels, changes have taken place. The traditional viewpoint on the anticancer effect of ionizing radiation is. Among all newly diagnosed cancer patients, more than 60% will receive radiotherapy with curative purpose or palliative treatment^[21]. More and more evidence shows that tumor cell death induced by local radiation can also act on the distal non-radiation tumor site through injury signal cascade, immunogenic cell death, or both at the same time, to achieve the systemic anti-tumor effect, to activate the immune system. These findings have led to the transformation of the application of radiotherapy in the treatment of various malignant tumors^[22]. Many pieces of evidence show that the combination of radiotherapy and immunotherapy can increase the cellular immune response in patients with advanced solid tumors, including lung cancer, and has a synergistic effect when combined with immune checkpoint blocking therapy^[23]. However, the current research data on immune combined radiotherapy are limited to small sample size, short follow-up period, or lack of randomized controlled trials, or some trials use different immunotherapy, different radiation doses, or grades. Nevertheless, the results of these early clinical trials show that in patients with advanced NSCLC, the clinical effect of combined radiotherapy and immune checkpoint blocking therapy is better than that of treatment alone. The success lies in that the combination of radiotherapy and immunotherapy can make the slow response

tumors more sensitive to immunotherapy.

3.3 Combined immune targeted therapy

The mutation rate of epidermal growth factor receptor (EGFR) in patients with advanced NSCLC is 40.3%–64.5%. Tyrosine kinase inhibitor(TKI) can work on the EGFR gene directly and inhibit tumor development. Studies have shown that the current three generations of EGFR-TKI can significantly prolong the progression-free survival (PFS) of patients. However, drug resistance is inevitable in patients with advanced NSCLC receiving targeted therapy, and about 50% of patients have EGFR-T790M mutation^[25]. Previous studies have confirmed that the EGFR gene can play the role of oncogene through the non-cellular autonomous mechanism and may promote other oncogenes to play the function of immune escape, while EGFR-TKI can improve the antitumor ability of immunotherapy by upregulating PD-L1 expression of tumor cells^[26]. A phase Ib multicenter clinical study was conducted to study the safety of necitumumab combined with pembrolizumab in the treatment of stage IV NSCLC. The results showed that the safety of the combination of the two drugs was tolerable and had no additional toxicity compared with the single drug^[24]. Therefore, the treatment of EGFR-TKI combined with immunosuppressants may become a new treatment strategy for patients with EGFR mutant NSCLC.

3.4 Immune combination against blood vessels

From the traditional platinum-containing dual drug therapy to the molecular targeted therapy in recent 10 years, and then to the rise of the latest immunotherapy, the treatment of advanced NSCLC is no longer limited to radiotherapy and chemotherapy. In 2006, FDA approved the anti-angiogenesis drug bevacizumab as the first-line treatment of advanced SCLC, which provides new decision-making for patients with advanced NSCLC. A large number of experiments have shown that anti-angiogenic drugs combined with chemotherapy, targeting, and immunotherapy can produce synergistic effects^[27]. In a study conducted by Rizvi in 2015, the efficacy and safety of nivolumab alone

and nivolumab combined with bevacizumab were evaluated for patients with advanced NSCLC. The results of nivolumab combined with bevacizumab in the treatment of simple adenocarcinoma and nivolumab alone in the treatment of squamous cell carcinoma and adenocarcinoma showed that both groups did not reach the main endpoint of the study, and the overall survival (OS). The median PFS of patients is 37.1 weeks; the median PFS of patients with squamous cell carcinoma in the single drug group is 16 weeks, and the median PFS of patients with adenocarcinoma is 21.4 weeks. Both drugs are safe^[28]. Although antiangiogenic drugs can bring some clinical benefits, there are still many problems needed our attention. For example, the combined treatment of multi-target antiangiogenic drugs has just started, and biomarkers are not yet available. Therefore, further researches need to explore the best combination therapy and effective biomarkers.

3.5 Double immune therapy

Immune checkpoint inhibitor is the mainstream direction of immunotherapy for lung cancer at present. Since CTLA-4 and PD-L1 act on the activation and effect stages of immune regulation respectively, blocking the key points of these two steps at the same time can play a synergistic role and bring unexpected effects^[29,30]. In 2020, the American Society of Clinical Oncology (ASCO) published the 3-year follow-up data of CheckMate-227 and the results of CheckMate-9LA, the first double immunotherapy study. The data confirmed that PD-1 combined with CTLA-4 double immunotherapy is expected to bring lasting benefits to specific patients. CheckMate-227 brings a new first-line “de chemotherapy” scheme to patients. The three-year follow-up data show that first-line nivolumab combined with low-dose ipilimumab shows more lasting OS benefits than chemotherapy regardless of PD-L1 expression. In terms of safety, the addition of low-dose ipilimumab increases immune-related adverse events, However, the incidence of grades 3–4 is equivalent to that of chemotherapy^[31]. CheckMate 9LA study showed that, regardless of PD-L1 expression and histological changes, in the first-line treatment of NSCLC pa-

tients, nivolumab (360 mg, Q3W) combined with low-dose ipilimumab (1 mg kg⁻¹, Q6W) showed clinical benefits in all efficacy evaluations compared with chemotherapy alone (up to 4 cycles), and 2-cycle chemotherapy was well tolerated for the vast majority of patients^[32]. CheckMate-227 and CheckMate-9LA provide treatment options of “de chemotherapy” and “less chemotherapy” for patients with gene negative advanced NSCLC, which may be one of the trends of future research. We should continue to strengthen the ability to prevent and manage adverse reactions of immunotherapy, accumulate more experience, make better use of immunotherapy, and bring greater clinical benefits to patients.

4. Summary and prospect

In recent years, the treatment of NSCLC has provided new treatment strategies for patients with advanced NSCLC, from the first platinum-containing dual drug to the later targeted therapy, until the emergence of immunotherapy. Although more and more data show that a large number of patients benefit from immunotherapy, immunotherapy is expensive and the effective rate is no more than 45%. How to determine the dominant population and how to make rational use of immunotherapy and combination programs have become an urgent problem for us to breakthrough. Moreover, the subjects included in many clinical studies are patients with relatively young age, no autoimmune diseases, and good PS score, which is different from the real cases we have seen in the actual clinic. Therefore, further researches need for immunotherapy.

Conflict of interest

The authors declare no potential conflicts of interest.

References

1. Lancet T. Globocan 2018: counting the toll of cancer. *Lancet* 2018; 392(10152): 985.
2. Schoenfeld AJ, Hellmann MD. Acquired resistance to immune checkpoint inhibitors. *Cancer Cell* 2020; 37(4): 443–455.
3. Fehrenbacher L, Spira A, Ballinger M, *et al.* Ate-

- zolizumab versus docetaxel for patients with previously treated non-small cell lung cancer (POPLAR): a multicenter, open-label, phase 2 randomized controlled trial. *The Lancet* 2016; 387(10030): 1837–1846.
4. Espana S, Guasch E, Carceren Y, *et al.* Immunotherapy rechallenge in patients with non-small cell lung cancer. *Pulmonology* 2020; 26(4): 252–254.
 5. Duan J, Cui L, Zhao X, *et al.* Use of immunotherapy with programmed cell death 1 vs programmed cell death ligand 1 inhibitors in patients with cancer. *JAMA Oncology* 2020; 6(3): 375–385.
 6. Dunn GP, Old LJ, Schreiber RD, *et al.* The immunobiology of cancer immunosurveillance and immunoediting. *Immunity* 2004; 21(2): 137–148.
 7. Hanahan D, Weinberg RA. Hallmarks of cancer: the next generation. *Cell* 2011; 144(5): 646–674.
 8. Rossi G, Russo A, Tagliamento M, *et al.* Precision medicine for NSCLC in the era of immunotherapy: new biomarkers to select the most suitable treatment or the most suitable patient. *Cancers (Basel)* 2020; 12(5): 1125.
 9. Giaccone G, Bazhenova LA, Nemunaitis J, *et al.* A phase III study of belagenpumatucel-L, an allogeneic tumor cell vaccine, as maintenance therapy for non-small cell lung cancer. *European Journal of Cancer* 2015; 51(16): 2321–2329.
 10. Sanborn RE, ROSS HJ, Aung S, *et al.* A pilot study of an autologous tumor-derived autophagosome vaccine with docetaxel in patients with stage IV non-small cell lung cancer. *Journal of Immunotherapy Cancer* 2017; 5(1): 103.
 11. Lipson EJ, Drake CG. Ipilimumab: an anti-CTLA-4 antibody for metastatic melanoma. *Clinical Cancer Research* 2011; 17(22): 6958–6962.
 12. Planchard D, Reinmuth N, Orlov S, *et al.* ARCTIC: durvalumab with or without tremelimumab as third-line or later treatment of metastatic non-small cell lung cancer. *Annals Oncology* 2020; 31(5): 609–618.
 13. Alsaab HO, Samaresh S, Raimi A, *et al.* PD-1 and PD-L1 checkpoint signaling inhibition for cancer immunotherapy: mechanism, combinations, and clinical outcome. *Frontiers Pharmacology* 2017; 8: 561.
 14. Jia LL, Walsh RJ, Ang Y, *et al.* The evolving immuno-oncology landscape in advanced lung cancer: first-line treatment of non-small cell lung cancer. *Therapeutic Advances Medical Oncology* 2019; 11: 1–22.
 15. Osmani L, Askin F, Gabrielson E, *et al.* Current WHO guidelines and the critical role of immunohistochemical markers in the subclassification of non-small cell lung carcinoma (NSCLC): moving from targeted therapy to immunotherapy. *Seminars in Cancer Biology* 2018; 52(Pt 1): 103–109.
 16. Califano R, Gomes F, Ackermann CJ, *et al.* Immune checkpoint blockade for non-small cell lung cancer: what is the role in the special populations? *European Journal of Cancer* 2020; 125: 1–11.
 17. Rocco D, Malapelle U, Marzia DR, *et al.* Pharmacodynamics of current and emerging PD-1 and PD-L1 inhibitors for the treatment of non-small cell lung cancer. *Expert Opinion Drug Metabolism Toxicology* 2020; 16(2): 87–96.
 18. Leonetti A, Wever B, Mazzaschiet G, *et al.* Molecular basis and rationale for combining immune checkpoint inhibitors with chemotherapy in non-small cell lung cancer. *Drug Resistance Updates* 2019; 46: 100644.
 19. Langer CJ, Gadgeel SM, Borghaei H, *et al.* Carboplatin and pemetrexed with or without pembrolizumab for advanced, non-squamous non-small cell lung cancer: a randomized, phase 2 cohort of the open-label KEYNOTE-021 study. *Lancet Oncology* 2016; 17(11): 1497–1508.
 20. Chen Y, Zhou Y, Lu T, *et al.* Immune-checkpoint inhibitors as the first-line treatment of advanced non-small cell lung cancer: a meta-analysis of randomized controlled trials. *Journal of Cancer* 2019; 10(25): 6261–6268.
 21. Gouveia AG, Zalay OC, Chua KL, *et al.* Response evaluation after stereotactic ablative radiotherapy for localized non-small cell lung cancer: an equipoise of available resource and accuracy. *The British Journal of Radiology* 2020; 93(1106): 100644.
 22. D’Andrea MA, Kesava Reddy G. Systemic immunostimulatory effects of radiation therapy improves the outcomes of patients with advanced NSCLC receiving immunotherapy. *American Jour-*

- nal of Clinical Oncology 2020; 43(3): 218–228.
23. Spaas M, Lievens Y. Is the combination of immunotherapy and radiotherapy in non-small cell lung cancer a feasible and effective approach? *Frontiers in Medicine (Lausanne)* 2019; 6: 244–260.
 24. Besse B, Garrido P, Bennouna J, *et al.* Safety of necitumumab and pembrolizumab combination therapy in patients with stage IV non-small cell lung cancer (NSCLC): a phase 1b expansion cohort study. *Annals of Oncology* 2016; 27(Suppl.6): vi436.
 25. Gahr S, Stoehr R, Geissinger E, *et al.* EGFR mutational status in a large series of Caucasian European NSCLC patients: data from daily practice. *British Journal of Cancer* 2013; 109(7): 1821–1828.
 26. Lisberg A, Cummings A, Goldman JW, *et al.* A phase II study of pembrolizumab in EGFR-mutant, PD-L1+, Tyrosine kinase inhibitor (TKI) naïve patients with advanced NSCLC. *Journal of Thoracic Oncology* 2018; 13(8): 1138–1145.
 27. Qiang H, Chang Q, Xu J, *et al.* New advances in antiangiogenic combination therapeutic strategies for advanced non-small cell lung cancer. *Journal of Cancer Research Clinical Oncology* 2020; 146(3): 631–645.
 28. Shiraishi Y, Kishimoto J, Tanaka K, *et al.* Treatment rationale and design for APPLE (WJOG11218L): a multicenter, open-label, randomized phase 3 study of atezolizumab and platinum/pemetrexed with or without bevacizumab for patients with advanced nonsquamous non-small cell lung cancer. *Clinical Lung Cancer* 2020; 21(5): 472–476.
 29. Dong J, Li B, Zhou Q, *et al.* Advances in evidence based medicine for immunotherapy of non-small cell lung cancer. *Journal of Evidence-Based Medicine* 2018; 11(4): 278–287.
 30. Hellmann MD, Ciuleanu TE, Pluzanski A, *et al.* Nivolumab plus ipilimumab in lung cancer with a high tumor mutational burden. *New England Journal of Medicine* 2018; 378(22): 2093–2104.
 31. O’byrne KJ, Lee KH, Kim SW, *et al.* 1274P First line (1L) nivolumab (NIVO) plus ipilimumab (IPI) in Asian patients (pts) with advanced non-small cell lung cancer (aNSCLC) in CheckMate 227. *Annals of Oncology* 2020; 31(Suppl.4): S824.
 32. John T, Sakai H, Ikeda S, *et al.* 1311P First-line (1L) nivolumab (NIVO) + ipilimumab (IPI) + chemotherapy (chemo) in Asian patients (pts) with advanced non-small cell lung cancer (NSCLC) from CheckMate 9LA. *Annals of Oncology* 2020; 31(Suppl.4): S847–S848.

REVIEW ARTICLE

Research progress of NK cell immunodeficiency in immune escape of acute leukemia

Yuling Zhang¹, Zhong Yu², Hailiang Li^{2*}

¹ Gannan Medical University, Ganzhou 341000, Jiangxi Province, China.

² Department of Hematology, The First Affiliated Hospital, Gannan Medical University, Ganzhou 341000, Jiangxi Province, China. E-mail: gyfyllhl@163.com

ABSTRACT

NK cell immunodeficiency has a variety of manifestations and complex mechanisms in the tumor. NK cell immune deficiency is closely related to immune escape of acute leukemia. This paper demonstrates the immunological escape mechanism of acute leukemia from NK cell immune deficiency manifestation and cause.

Keywords: NK Cell; Activated Killer Cell Receptor; Inhibitory Killer Cell Receptor; MicroRNA-29b; UL16 Binding Protein-3

ARTICLE INFO

Received 13 July 2021
Accepted 26 September 2021
Available online 13 October 2021

COPYRIGHT

Copyright © 2021 Yuling Zhang, *et al.*
EnPress Publisher LLC. This work is licensed under the Creative Commons Attribution-NonCommercial 4.0 International License (CC BY-NC 4.0).
<https://creativecommons.org/licenses/by-nc/4.0/>

1. Introduction

Acute leukemia (AL) is a malignant clonal disease of hematopoietic stem progenitor cells, with rapid onset and progression. The natural course of disease usually lasts only a few weeks or months. Although chemotherapy and immunobiotherapy have seen great advances, 50% to 70% of patients with acute myeloid leukemia (AML) still suffer from relapses, and so do 20% to 30% of children with acute lymphoblastic leukemia (ALL)^[1,2]. Part of the reason for relapse is the immune surveillance dysfunction of the body's innate immune cells. Therefore, in order to develop more effective anti-leukemia drugs, it is necessary to understand how leukemia cells evade innate immunity. NK cell is a kind of large granular lymphocyte, which plays a very important role in the anti-leukemia process. Its immune deficiency can cause leukemia cells to evade the attack of host immune system. In this paper, we review the manifestations and pathogenesis of NK cell immunodeficiency in acute leukemia.

2. Expression of NK cell immunodeficiency

2.1 Abnormal proportion and reduced number of NK cell subsets

NK cells account for about 5%–15% of peripheral blood mononuclear cells (PBMC). Immature NK cells have high expression of CD56 (CD56^{bright} NK cells) and high expression of NKG2A, but no expression of CD16. Mature NK cells have low expression of CD56, but no expression of NKG2A, namely, CD56^{dim} NK cells^[3]. Data showed that the percentage and absolute number of NK cells in peripheral blood of

AL patients decreased^[4-7]. It has been reported that the percentage of NK cells in various organs (spleen, bone marrow, blood and lymph nodes) of mice with leukemia is lower than that of mice without leukemia. The absolute NK cell count of bone marrow and lymph node was lower than that of non-leukemia mice. There is the selective reduction of CD27⁺CD11b⁺ double positive NK cells in various organs of mice with leukemia (the maturation process of mouse NK cells is CD27⁻CD11b⁻→CD27⁺CD11b⁻→CD27⁺CD11b⁺→CD27⁻CD11b⁺)^[8]. Rouce *et al.* reported that CD56^{bright}-CD16⁻NK cells in ALL patients were more than that in healthy people^[9]. However, Mundy Bosse and Rey *et al.* found that the reduction of total CD56^{bright} NK cells and CD56^{bright} CD16⁻NK cells in peripheral blood of patients with AML may be different from that of patients with ALL^[8,10]. In conclusion, NK cells in AL patients are not only abnormal in proportion, but also have trouble maturing, especially in AML patients.

2.2 Weakened NK cell killing ability

Activated NK cells can non-specifically kill tumor cells through the following pathways. (1) Directly kill tumor cells through FASL/FAS, perforin, granulation enzyme pathway. (2) FCγR(CD16) mediated the ADCC effect by binding to the FC segment of anti-tumor antibody^[4]. (3) Secretion of IFN-γ, TNF-α, TNF-β can produce anti-tumor effect. It was found that the B expression of perforin and granase decreased in NK cells of leukemia mice, and the intracellular IFN-γ content decreased after stimulation^[8]. Clinical studies have shown that both IFN-γ and TNF-α of NK cells in patients with leukemia are reduced, and their killing ability is weakened^[9,11].

2.3 Reduced NK cell proliferation^[5]

Immune cells' maintaining certain proliferation ability is the basis of maintaining normal immune function of the body. The percentage of NK cells in spleen mitosis of leukemic mice was lower than that of non-leukemic mice by flow cytometry. 24 h after injection of IL-15 (which can promote NK cell proliferation and differentiation), the NK cell proliferation capacity of all organs (spleen, bone mar-

row, blood, lymph node) was lower than that of non-leukemia mice^[8].

2.4 Abnormal NK cell receptor expression

Ho *et al.* analyzed the bone marrow of 78 newly diagnosed AML patients (46 cases < 60 years old, 32 cases ≥ 60 years old) and found that the receptor spectrum of NK cells was changed; except the activation receptors KIR2DL4, KIR2DS4, CD94/NKG2C, the expression level of other receptors including natural cytotoxic receptors (NKp30, NKp44, NKp46), killing immunoglobulin-like receptors (KIR2DL1, KIR2DL2, KIR3DL1) and activated receptors (DNAM-1, NKG2D) was lower than that of healthy people^[7]. Sanchez-Correa *et al.* found that in AML patients younger than 65 years old, the expression of DNAM-1 in NK cells of bone marrow and the levels of NKp30 and NKp46 also decreased, while the level of NKp46 in elderly AML patients (≥ 65 years old) also decreased^[12]. However, the expression of DNAM-1 and NKp30 was not different from that of healthy people. The reason of different results of these two studies is related to the different age distribution of patients in the two studies, but both of them indicate that the receptor spectrum of NK cells in leukaemia has changed, leading to the weakening of NK cells' recognition and activation ability.

NKG2A is a transmembrane protein with C-type lectin structure in the extracellular region and ITAM in the cytoplasmic region. CD94/NKG2A is a suppressor killer cell receptor, which can block NK cell-mediated cytotoxicity. Multiple studies have shown increased NK cell CD94/NKG2A expression in AML patients^[7,9,11,13]. Sandoval-Borrego *et al.* found that CD158b was overexpressed in NK cells of AML patients^[13]. For example, blocking CD158 recipient epitopes (CD158a, CD158b) can increase the killing activity of NK cells in AML patients^[14].

3. The mechanism of NK cell immunodeficiency

The mechanism of tumor immune escape has not been fully elucidated. The following viewpoints have been proposed: (1) tumor cells lack the components necessary to stimulate immune response; (2)

tumor antigen induces immune tolerance; (3) tumor cells induce apoptosis of immune cells or resist apoptosis; (4) malignant tumors directly or indirectly inhibit immune function^[15]. For AL immune escape, NK cell immune deficiency is one of the reasons. Recent studies have focused on the mechanism of NK cell deficiency leading to AML immune escape, mainly in the following aspects.

3.1 MicroRNA-29b mediates abnormal NK cell development

MicroRNA-29b is one of the three members of MicroRNA-29s family, and a large number of studies have confirmed that MicroRNA-29b is involved in tumor occurrence, migration and invasion^[16-18]. Mundy-Bosse *et al.* showed that the number of CD56^{bright} NK cells in peripheral blood of patients with acute myeloid leukemia (human NK cell de-

velopment process is shown in **Figure 1**) decreased^[18]. In order to find the cause, they used RT-PCR to measure the MicroRNA-29b of NK cells in leukemia mice, and found that CD11b⁺ NK cells (including the NK cells of middle and late stage mice): the expression of MicroRNA-29b in CD27⁺ CD11b⁺ NK cells and CD27⁻CD11b⁺ NK cells was higher than that in non-leukemia mice. NK cells with MicroRNA-29b knockdown were injected into leukemia mice with reduced WBC and improved survival. The same team also found increased MicroRNA-29b expression in CD56^{bright} NK cells from AML patients. Currently, the cause of MicroRNA-29b overexpression in leukemia NK cells is unclear and further research is needed, but many researchers have begun to develop MicroRNA-29b inhibitors to achieve anti-leukemia efficacy.

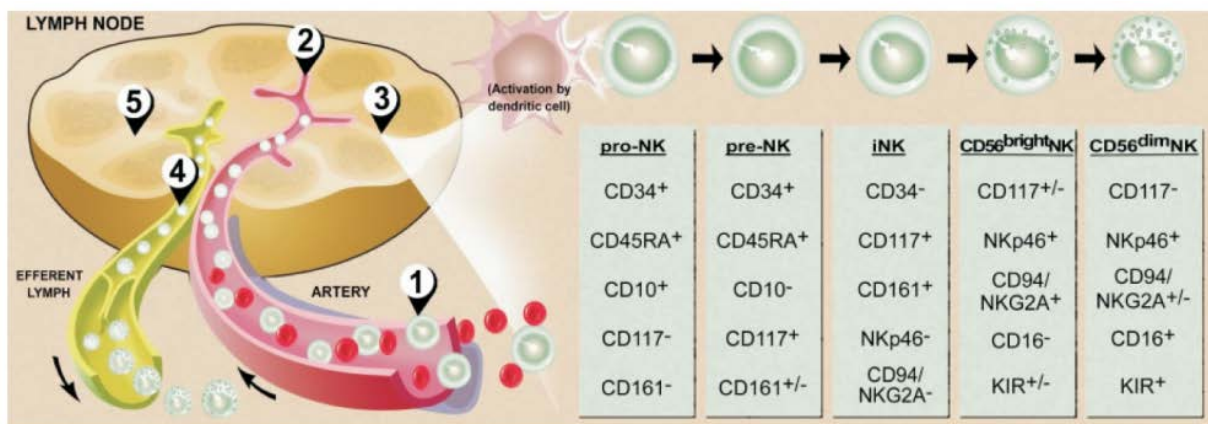


Figure 1. Pattern of human NK cell development process^[3].

3.2 Leukemia cells inhibit NK cells

3.2.1 CD200 binds to CD200L of NK cells

CD200 belongs to the immunoglobulin sub-family, which is expressed on the surface of various immune cells and is increased in solid tumors such as bladder cancer and lung cancer. Damiani *et al.* analyzed 244 AML patients and found that CD200 (also known as OX2) was expressed in leukemia cells of 56% AML patients, and CD200 expression was higher in patients with secondary leukemia^[19]. CD200 on the surface of leukemia cells can bind to CD200L on the surface of NK cells and inhibit the cytotoxicity and cytokine secretion of NK cells. It has been reported that the remission rate of patients with CD200⁺ is lower than that of patients with CD200⁻, which is associated with poor prognosis of

AML patients^[19-21].

3.2.2 Leukemic cells secrete IL-10

IL-10 is a negative regulator, mainly secreted by macrophages and dendritic cells. Stringaris *et al.* found that the killing ability of NK cells in patients with leukemia was weakened^[11]. In order to find the mechanism of NK cell inactivation, they co-cultured NK cells from healthy donors with acute myeloid leukemia cells (NK-AML) for 24 h. The expression level of IL-10 in the supernatant of NK-AML culture medium was significantly increased. Therefore, it is believed that leukemia cells of patients with AML can secrete IL-10, which has a significant immunosuppressive effect on NK cells.

3.2.3 Expression of NKG2D weakens NK cell function

NKG2D is generally expressed in NK cells and T cells. Tang *et al.* found that U937 and THP-1 cell lines not only express MHC I molecular related gene A of NKG2D ligand, but also express NKG2D^[22]. If NKG2D expression of U937 and THP-1 cell lines is blocked, NK cells of patients were activated by NKG2D ligand of U937 and THP-1 cell lines, showing degranulation and increased expression levels of CD107a, IFN- γ and TNF- α , namely, the expression of NKG2D in leukemia cells weakened the immune surveillance function of NK cells.

3.2.4 Secretion of TGF- β induces NK cell in-activation

TGF- β is a polypeptide that regulates tumor proliferation, growth, migration and invasion. Hong *et al.* reported that there were different forms of TGF- β exosomes in AML patients and they were higher than the control group, and the proportion was different at diagnosis, induction chemotherapy and after induction chemotherapy, but they were always present, which could inhibit NKG2D expression of NK cells, and the addition of TGF- β antibody could reverse the inhibition of NK cells^[23]. The authors suggest that TGF- β exosomes may predict the presence of minimal residual disease (MRD). Rouce *et al.* found that TGF- β was the most obvious cytokine in the supernatant of leukemia cells cultured in ALL patients, and TGF- β could be used to reconstruct NK cell functions such as cytokine secretion and degranulation^[9]. Further experiments demonstrated that TGF- β mediated the decline of NK cell immune surveillance function through TGF- β /SMAD signaling pathway, leading to the escape of leukemia cells. TGF- β /SMAD is expected to be the target of novel therapies to restore the anti-leukemic toxicity of NK cells by inhibiting this pathway.

3.2.5 UL16 binding protein-3

UL16 binding protein-3 (ULBP3) is a kind of NKG2D ligands, which is distributed in colorectal adenocarcinoma, gastric adenocarcinoma and lung adenocarcinoma tissue. Soluble ULBP3 exists in serum of colorectal adenocarcinoma and gastric

adenocarcinoma and is considered as a potential tumor marker^[24]. Jiang Q *et al.* reported that serum sULBP3 level in the initial AML group was significantly increased and negatively correlated with the proportion of NK cells^[25]. Vitro experiments showed that exogenous ULBP3 protein affected the number and cytotoxicity of NK cells through the mechanism of apoptosis.

3.2.6 Expression of indoleamine 2, 3-dioxygenase 1

Indoleamine 2, 3-dioxygenase 1 (IDO1) is an enzyme that can degrade tryptophan to canisurine, and is associated with pathological inflammatory response and tumor immune escape. Activation of IDO1 can inhibit T cells, NK cells and promote the proliferation of regulatory T cells. Studies have shown that TIM-3 of NK cells binds to GAL-9 on the leukemia cell membrane of AML patients and releases IFN- γ , which induces increased expression of IDO1 in leukemia cells, and IDO1 reduces the degranulation activity of NK cells, thereby avoiding NK cell killing^[26]. Ma Jinfeng reported that Gal-9 expression was increased in AML patients, and Tim-3 expression level in NK cells of medium-high risk AML patients was higher than that of low-risk AML patients^[27]. These two studies demonstrate that the Tim-3/Galectin-9 pathway mediates immune escape of AML tumor cells by down-regulating the NK cell immune response through IDO1, influencing patient outcomes.

3.2.7 Inducing NK cell to express receptor activator for NF- κ B (RANK)

Tumor necrosis factor family RANKL not only regulates bone metabolism and immune cell function, but also affects the survival of dendritic cells and the ability to stimulate T cells, and promotes tumor cell metastasis. Schmiedel *et al.* reported that 68% of AML patients expressed RANKL in their peripheral blood leukemia cells^[28]. On the one hand, leukemia cells of RANKL⁺ inhibit NK cells directly or by secreting a variety of active substances (TNF, IL-6, IL-8 and IL-10) through RANKL signal; on the other hand, the active substances secreted induce NK cells to express RANK. RANKL on leukemic cells can bind to NK cell RANK. When

RANKL is blocked by Denosumab, the secretion of TNF, IL-6, IL-8 and IL-10 in leukemic cells is significantly reduced and the NK cell inhibition is weakened. In conclusion, a vicious circle is formed between leukemia cells and NK cells, which leads to NK cell inactivation and leukemia cells evade immune surveillance.

3.3 TLR4⁺ MSC inhibits NK cells

Mesenchymal stem cells (MSC) are non-hematopoietic pluripotent cells that can be isolated from bone marrow and adipose tissue and can secrete a variety of cytokines and chemokines to promote tumor growth and metabolism. Lu *et al.* isolated MSC from bone marrow of lung cancer (LC) patients, AML patients and healthy people, and co-cultured MSC from healthy people with Hela cells (named CM^{Hela}-MSC)^[29]. It was found that LC-MSC, AML-MSC and CM^{Hela}-MSC were all highly expressed TLR4mRNA. Further experiments showed that intravenous injection of TLR4⁺ MSC into C57BL/6J mice could induce decrease of peripheral blood NK cells. Co-culture of TLR4⁺ MSC and NK cells reduced the expression level of NKG2D receptor in NK cells, and CytoTox 96 non-radioactive cytotoxicity test showed that NK cell toxicity decreased. When TLR4 function was blocked, NK cell function recovered. This study demonstrates that TLR4 plays a key role in MSC-induced NK cell function inhibition.

3.4 Immunological synapse defects in NK-AML cells

NK cells and tumor cells can form an immunological synapse (IS), also known as supermolecular activation cluster (SMAC). NK cell immune synapse can be divided into two types. One is inhibitory synapse, in which actin recombination is blocked and dissolved particles are not transferred to the synapse. The second is the dissolved synapse, in which the actin skeleton is reorganized and the dissolved particles are transferred to the synapse (requiring NK cell receptor (NCRs) polarization). It has been reported that the decrease of soluble particles in the immune synapse of NK-AML cells, and almost no aggregation of CD3 ζ (a marker of NCRs polarization) in the immune

synapse of NK-AML cells is the cause of the deficiency of the immune synapse. Researchers have found that lenalidomide can increase the dissolved particles in the immune synapse of NK-THP1 and NK-HLA60 cells, while the activation and inhibitory receptors of NK cells are not changed^[30]. However, whether lenalidomide can increase the soluble particles in the immune synapses of NK-AML and NK-ALL cells is unknown and needs further study.

3.5 IFN- γ inhibits NK cells in tumor micro

Type II interferon, or γ -interferon (IFN- γ), is produced mainly by activated Th1 cells and almost all CD8⁺T and NK cells. Previous studies have shown that IFN- γ has antitumor activity, while other studies have shown that IFN- γ has pro-tumor activity, but the reason for this contradictory result remains unclear. Bellucci *et al.* reported IFN- γ or the supernatant of NK cells can induce leukemic cells to up regulate programmed death-1 ligand (PD-1)^[31]. If PD-L1 is blocked by antibodies, the cleavage ability of NK cells is increased. If JAK inhibitors are used, the cleavage ability of NK cells is also increased. Therefore, the researchers believe that IFN in the tumor microenvironment- γ activate JAK1 and JAK2 signaling pathways, and then up regulate PD-L1; PD-L1 binds to programmed death-1 (PD-1) of NK cells, weakening the anti-tumor activity of NK cells.

4. Conclusion

Since one of the causes of AL relapse is immune system dysfunction, understanding the causes of immune system dysfunction is the basis for finding more effective immunobiotherapy. As an important part of the immune system, the deficiency of NK cells is one of the causes of leukemia immune escape. NK cell immune deficiency is manifested in many aspects, including abnormal number of NK cells, maturation disorder, reduced killing ability, reduced proliferation ability, decreased activation receptor expression and increased inhibitory receptor expression. The mechanisms of NK cell immune deficiency include: (1) MicroRNA-29b mediates changes in NK cell dysplasia; (2) leukemia cells inhibit NK cells through various mechan-

isms; (3) TLR4⁺ MSC inhibits NK cells; (4) NK-AML cell immunological synapse defects; (5) IFN- γ in tumor microenvironment inhibit NK cells. With the deepening of research, drugs targeting the above targets have been developed, and some have entered clinical research. NK cell-based immunotherapy is expected to become one of the effective means to treat AL.

References

- Huang X, Huang H. Hematology. 2nd ed. Beijing: People's Medical Publishing House; 2004. p. 9–13.
- Zhang Z, Hao Y, Zhao Y, *et al.* Hematology. 2nd ed. Beijing: People's Medical Publishing House; 2015. p. 853–854.
- Caligiuri MA. Human natural killer cells. *Blood* 2008; 112(3): 461–469.
- Yu X, Gu G, Wang L, *et al.* Peripheral blood lymphocyte subsets of the absolute value of precise and quantitative analysis of immune function in acute leukemia. *China Journal of Modern Medicine* 2014; (17): 63–67.
- Kong L, Ge J, Xia R. The significance of Treg and T lymphocyte subsets in acute myelocytic leukemia. *Acta Universitatis Medicinalis Anhui* 2015; (4): 512–515.
- Sun H, Zhang L, Wang J. Clinical significance of diagnosis and treatment of Treg cells, NK cells and T lymphocyte subsets in patients with acute leukemia. *Journal of Clinical Hematology* 2016; (9): 741–743.
- Ho X, Fook-Chong S, Linn YC. Natural killer cell receptor repertoire is comparable amongst newly diagnosed acute myeloid leukemia of different French-American British subtypes, risk categories and chemosensitivities. *Leuk Lymphoma* 2014; 55(2): 342–348.
- Mundy-Bosse BL, Scoville SD, Chen L, *et al.* MicroRNA-29b mediates altered innate immune development in acute leukemia. *The Journal of Clinical Investigation* 2016; 126(12): 4404–4416.
- Rouce RH, Shaim H, Sekine T, *et al.* The TGF- β /SMAD pathway is an important mechanism for NK cell immune evasion in childhood B-acute lymphoblastic leukemia. *Leukemia* 2016; 30(4): 800–811.
- Rey J, Fauriat C, Kochbati E, *et al.* Kinetics of cytotoxic lymphocytes reconstitution after induction chemotherapy in elderly AML patients reveals progressive recovery of normal phenotypic and functional features in NK cells. *Frontiers in Immunology* 2017; 8(64): 1–12.
- Stringaris K, Sekine T, Khoder A, *et al.* Leukemia-induced phenotypic and functional defects in natural killer cells predict failure to achieve remission in acute myeloid leukemia. *Haematologica* 2014; 99(5): 836–847.
- Sanchez-Correa B, Gayoso I, Bergua JM, *et al.* Decreased expression of DNAM-1 on NK cells from acute myeloid leukemia patients. *Immunology and Cell Biology* 2012; 90(1): 109–115.
- Sandoval-Borrego D, Moreno-Lafont MC, VazquezSanchez EA, *et al.* Overexpression of CD158 and NKG2A inhibitory receptors and underexpression of NKG2D and NKp46 activating receptors on NK cells in acute myeloid leukemia. *Archives of Medical Research* 2016; 47(1): 55–64.
- Wu G, Yang Z, Wang Z, *et al.* Effect of CD158 receptor epitope blocking on killing activity of NK cells in acute myeloid leukemia. *Journal of Guangdong Medical College* 2013; (5): 509–512.
- Gong F. *Medical Immunology*. 4th ed. Beijing: Science Press; 2014.
- Chou J, Lin JH, Brenot A, *et al.* GATA3 suppresses metastasis and modulates the tumour microenvironment by regulating microRNA-29b expression. *Nature Cell Biology* 2013; 15(2): 201–213.
- Yeh YY, Ozer HG, Lehman AM, *et al.* Characterization of CLL exosomes reveals a distinct microRNA signature and enhanced secretion by activation of BCR signaling. *Blood* 2015; 125(21): 3297–3305.
- Kirimura S, Kurata M, Nakagawa Y, *et al.* Role of microRNA-29b in myelodysplastic syndromes during transformation to overt leukaemia. *Pathology* 2016; 48(3): 233–241.
- Damiani D, Tiribelli M, Raspadori D, *et al.* Clinical impact of CD200 expression in patients with acute myeloid leukemia and correlation with other molecular prognostic factors. *Oncotarget* 2015; 6(30):

- 30212–30221.
20. Tiribelli M, Raspadori D, Geromin A, *et al.* High CD200 expression is associated with poor prognosis in cytogenetically normal acute myeloid leukemia, even in FIT₃-ITD-/NPM1⁺ patients. *Leukemia Research* 2017; 58: 31–38.
 21. Zhang X, Shen A, Guo R, *et al.* Expression characteristics of CD200 in acute myeloid leukemia and its clinical significance. *Journal of Experimental Hematology* 2014; (6): 1531–1534.
 22. Tang M, Acheampong DO, Wang Y, *et al.* Tumoral NKG2D alters cell cycle of acute myeloid leukemic cells and reduces NK cell-mediated immune surveillance. *Immunology Research* 2016; 64(3): 754–764.
 23. Hong CS, Muller L, Whiteside TL, *et al.* Plasma exosomes as markers of therapeutic response in patients with acute myeloid leukemia. *Frontiers in Immunology* 2014; 5(160): 1–9.
 24. Mao C, Mou X, Jiang Q, *et al.* Detection and analysis of human ULBP3 in different tumor cells and tumor tissues (in Chinese). *Chinese Journal of Cellular and Molecular Immunology* 2014; (12): 1307–1310.
 25. Jiang Q, Mou X, Mao C, *et al.* The level of serum UL16 binding protein 3 (ULBP3) in patients with acute myeloid leukemia increased and inhibited the killing activity of NK cells (in Chinese). *Chinese Journal of Cellular and Molecular Immunology* 2015; (10): 1396–1398, 1403.
 26. Folgiero V, Cifaldi L, Li PG, *et al.* TIM-3/Gal-9 interaction induces IFN γ -dependent IDO1 expression in acute myeloid leukemia blast cells. *Journal of Hematology & Oncology* 2015; 8(36): 1–5.
 27. Ma J. Characteristics of Tim-3 expression on NK cells and its clinical significance in acute myeloid leukemia patients [Master's thesis]. Suzhou: Soochow University; 2015.
 28. Schmiedel BJ, Nuebling T, Steinbacher J, *et al.* Receptor activator for NF- κ B ligand in acute myeloid leukemia: Expression, function, and modulation of NK cell immunosurveillance. *Journal of Immunology* 2013; 190(2): 821–831.
 29. Lu Y, Liu J, Liu Y, *et al.* TLR4 plays a crucial role in MSC-induced inhibition of NK cell function. *Biochemical and Biophysical Research Communications* 2015; 464(2): 541–547.
 30. Khaznadar Z, Henry G, Setterblad N, *et al.* Acute myeloid leukemia impairs natural killer cells through the formation of a deficient cytotoxic immunological synapse. *European Journal of Immunology* 2014; 44(10): 3068–3080.
 31. Bellucci R, Martin A, Bommarito D, *et al.* Interferon- γ induced activation of JAK1 and JAK2 suppresses tumor cell susceptibility to NK cells through upregulation of PD-L1 expression. *Oncoimmunology* 2015; 4(6): e1008824.

REVIEW ARTICLE

Research progress in immunological mechanisms of *Cryptococcus*

Ying Song¹, Yufang Qiu¹, Weiyu Liu², Xiaoliang Yuan^{2*}

¹ Gannan Medical University, Ganzhou 341000, Jiangxi Province, China.

² Department of Respiratory Medicine, The First Affiliated Hospital, Ganzhou 341000, Jiangxi Province, China. E-mail: yxlyyxs@126.com

ABSTRACT

Whether infection of *Cryptococcus* causes disease in host or not depends on the virulence of the pathogen and the immune defense ability of the host. *Cryptococcus neoformans* (*C. neoformans*) mainly causes opportunistic infections in the immunocompromised or immunodeficient patients. In contrast, *Cryptococcus gattii* (*C. gattii*) mainly attacks the immunocompetent individuals. On the one hand, the host immune cells can eliminate the invasive *Cryptococcus* through a complex immune mechanism; on the other hand, *Cryptococcus* can evade the clearance of host immune cells by adopting various strategies (immune escape). This review mainly focuses on the pathogenic mechanism of *Cryptococcus*, and the host's immune defense mechanism against cryptococcal infection.

Keywords: *Cryptococcus*; Immune Mechanism; Macrophage; Dendritic Cells

ARTICLE INFO

Received 23 August 2021
Accepted 16 October 2021
Available online 22 October 2021

COPYRIGHT

Copyright © 2021 Ying Song, *et al.*
EnPress Publisher LLC. This work is licensed under the Creative Commons Attribution-NonCommercial 4.0 International License (CC BY-NC 4.0).
<https://creativecommons.org/licenses/by-nc/4.0/>

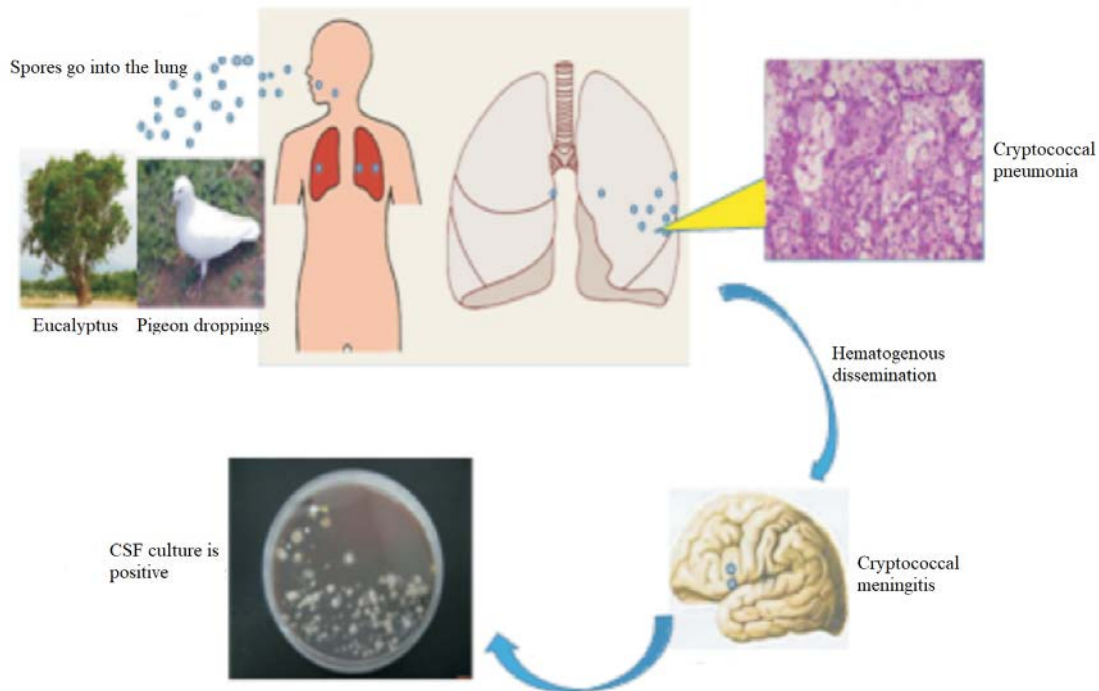
1. Introduction

Cryptococcus belongs to the subfamily of fungal basidiomycetes, including many species. There are mainly two kinds of conditional pathogens causing human opportunistic infection: *Cryptococcus neoformans* (*C. neoformans*) and *Cryptococcus gattii* (*C. gattii*). *Cryptococcus neoformans* is distributed in nature all over the world, mainly in soil and rotten vegetables, especially in pigeon droppings. *C. gattii* mainly exists in Eucalyptus, distributed in tropical and subtropical areas. In 1999, it broke out in temperate Colombia and spread to Washington, Oregon and California^[1]. However, originally reported in the tropics, *C. gattii* infection is now diagnosed worldwide^[2]. *C. neoformans* infection is the leading cause of death among AIDS patients worldwide. Especially in sub-Saharan Africa, the incidence rate is the highest^[3]. In addition to easily cause infections in HIV infection, *C. neoformans* also attacks other individuals with low immune function, such as hematopoietic malignancies, immunosuppressants after organ transplantation and patients with immune deficiency diseases. *C. neoformans* mainly affects individuals with normal immune function, but there are some special reports about *C. neoformans* infection in some immunocompetent patients and *C. gattii* infection in patients with immunodeficiency, such as those with HIV^[4].

Cryptococcus is widely distributed in the air in the form of spores, inhaled into the lungs and deposited in the alveoli through the human respiratory tract. When the host's immune function is normal, most of the invasive *C. neoformans* are cleared by the host, so there are no obvious infection symptoms. However, when the immune function is

damaged or low, a small number of *Cryptococcus* colonized in the host cells multiply, causing cryptococcal pneumonia. It also spreads through the blood-brain barrier and invades the central nervous system, causing cryptococcal meningitis^[5], which is characterized by pneumonia such as cough, pleurisy chest pain, fever and dyspnea, and a series of clinical symptoms of meningoencephalitis. *Cryptococcus* can be cultured in cerebrospinal fluid (Figure 1). The main symptom of *C. neoformans* infection is meningoencephalitis, while *C. gattii*

infection is more common in the lungs^[6]. The study results of animal models also support the difference between the two kinds of pathogens on the main target organs: mice infected with *C. neoformans* die of central nervous system infection, while those infected with *C. gattii* die of lung infection^[7]. It shows that the two species have different effects on their target organs, but its mechanism has not been fully clarified. At present, the research on regulating and enhancing hosts' defense mechanism through immune has attracted extensive attention.



Cryptococcus in the air is inhaled by the host in the form of spores and deposited in the alveoli. When the immune function of the body is low or damaged, cryptococci colonized in the host cells proliferate in large numbers, causing cryptococcal pneumonia, which spreads through the blood-brain barrier, invades the central nervous system, and causes cryptococcal meningitis. Therefore, *cryptococcus* is often cultured in the cerebrospinal fluid of patients with cryptococcal meningitis.

Figure 1. The main pathway of cryptococcal infection.

2. *Cryptococcus* is pathogenic

Cryptococcal capsule is an important virulence factor. Its main components are glucuronoxylan-nan (GXM), galactose xylose mannan (GalXM) and a small amount of mannose protein (MP), among which GXM accounts for more than 90% of polysaccharide components^[8]. *Cryptococcal* virulence factors can interfere with the host protective immune response, including the defense of dendritic cells (DCS) and macrophages (M ϕ) and antigen-presenting cells of the bone marrow lineage of monocyte precursors. In addition to producing specific enzymes and structures conducive to the survival of pathogens, the cell wall structure of *Cryp-*

tococcus also actively regulates host specific signal transduction. This remodeled structure leads to immune escape by shielding more immunogenic surface features^[9]. *Cryptococcus* can evade clearance of host immune cells by adopting various strategies and successfully damage the defense mechanism of the host. GXM can not only adhere to the cell wall to form a capsule structure, but also secrete into the surrounding environment with a large amount (exo-GXM). The virulence and fungal load of mouse infection are related to the release of exo-GXM. During disseminated infection or intracranial infection, exo-GXM can prevent immune cells from infiltrating into the brain and inhibit inflammation^[10].

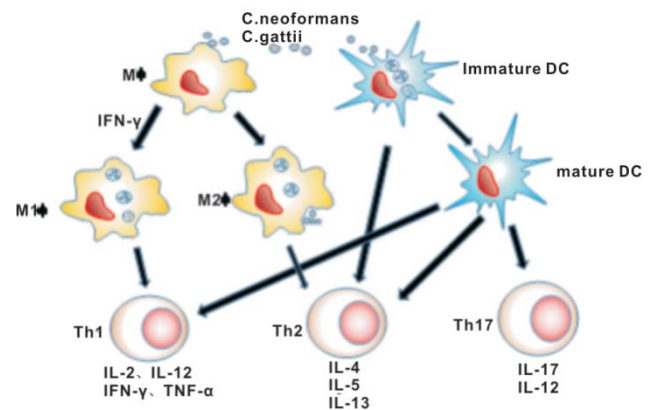
3. Effect of phagocytes on Cryptococcus

After infecting the host, *Cryptococcus* interacts with different phagocytic effector cells^[11]. Macrophages and dendritic cells (DC) play an important role in anti-*Cryptococcus*. *Cryptococcus* exists in the air in the form of spores, is inhaled into the alveoli through the respiratory tract and contacts with phagocytes. Phagocytes act as the first immune defense of the host to phagocytize, kill and invade pathogens and present antigens to activate T cells to mediate adaptive immune response. However, *C. neoformans* can replicate in phagocytes and escape to the extracellular environment through non lytic exocytosis, avoiding the clearance of phagocytes^[12]. The research shows that during the growth, *Cryptococcus* removes maturation markers Rab5 and Rab11 of phagosome, and inhibit the maturation of phagocyte lysosome, and the acidification, calcium channel and enzyme activity of phagosome is blocked, which makes *Cryptococcus* proliferate in cells.

3.1 Macrophage

Macrophages can become the hub of innate and adaptive immunity after phagocytosing *Cryptococcus*. However, *Cryptococcus* can survive and proliferate in the phagocytosis of these infected host cells. *Cryptococcus* can escape host immunity by cleaving macrophages, but the mechanism of cleavage is not clear, which may be due to the rupture of host cell membrane caused by a large number of intracellular *Cryptococcus* replication. This shows that *Cryptococcus* can take macrophages as a protective area in the host. Chrissy M reviewed the interaction between *Cryptococcus* and phagocytes in detail^[14]: macrophages can efficiently phagocytize *Cryptococcus*, but *Cryptococcus* has a variety of virulence factors to resist phagocytosis or enhance its reproductive ability in phagocytosis. However, a recent study^[15] has explored the mechanism of nonspecific uptake of *Cryptococcus* by macrophages. Macrophages ingest *Cryptococcus* through mannose receptor (MR), ingest *C. neoformans* through dectin-1 and dectin-2, and ingest *C. gattii* through dectin-1, which proves that macrophages'

important role of resisting *Cryptococcus*. Macrophages, as antigen-presenting cells (APC), promote T lymphocyte activation, induce Th1-like reaction and eliminate fungi. M1 type (classically activated) macrophages mediate Th1 response (mainly IFN- γ mediation), leading to the up regulation of reactive oxygen mediators, reactive nitrogen substances, proteases and lipid mediators, so that macrophages can effectively kill pathogens. Th1 stimulation can also increase the presentation of major histocompatibility complexes (MHC-I or MHC-II) and mediate adaptive immunity by reducing the activity of phagocyte hydrolases. M2 type (selectively activated) macrophages mediate Th2 response, help to inhibit and regulate inflammatory response, and play a role in the healing process, but have no killing effect on *Cryptococcus*^[16] (Figure 2).



After *Cryptococcus* is recognized and phagocytosed by APC (M ϕ and DC), M1 macrophages mediate Th1 response, and M2 macrophages mediate Th2 response; after immature dendritic cells (DC) phagocytose *Cryptococcus*, the expression of maturation markers CD80, CD86 and MHC II on cell surface increases, which mediate the differentiation of CD4⁺ T into Th1, Th2 and Th17 cells. They produce different inflammatory cytokines and inhibitory cytokines. Immature DC can also mediate Th2 reaction.

Figure 2. Effect of phagocytes on *Cryptococcus*.

3.2 Dendritic cell

As full-time APCs, dendritic cells mainly regulate and activate the adaptive immune system according to the polymorphism of antigen, and produce a specific immune response to infection. After *Cryptococcus* invades the lung, DC preliminarily processes *Cryptococcus* antigen through the endosomal/lysosomal pathway, presents it with MHC-class II molecules, and kills *Cryptococcus* through oxygen dependent and oxygen independent mechanisms^[17]. It was found^[18] that within 2 hours

after intranasal inoculation of *C. neoformans* in mice, *C. neoformans* could be internalized by lung DC, lung macrophages and neutrophils; after 7 days of infection, the expression of maturation markers CD80, CD86 and MHC-II increased. It shows that DC gradually develops into mature DC after phagocytosis of *C. neoformans*, and can present *C. neoformans* antigen to specific T cells to activate T cells. Mature DC can effectively present antigen, start T lymphocytes and mediate Th1 and Th17 immune response, while immature DC can induce immune tolerance and mediate Th2 non protective immune response. Wozniak KL^[19] clarified the process of DC recognizing, processing *Cryptococcus* and mediating immune response to *Cryptococcus*. It shows that DC cells play an important role in both innate and adaptive immune defense against cryptococcosis (**Figure 2**).

DC recognizes *Cryptococcus* presentation antigen and mainly stimulates T cell pathway. Although alveolar macrophages can also activate T cells through cryptococcal antigen presentation, the T cell effect stimulated by DC is more effective. The experimental results showed that^[20]: cryptococcal antigen stimulated bone marrow dendritic cells (BMDC) to induce the release of protective immune factors IL-12/23p40, but did not release these protective factors after stimulating bone marrow macrophages. The possible reason for this difference is that after cryptococcal antigen stimulation, BMDC up regulates MHC-II and CD86, while bone marrow macrophages down regulate MHC-II and CD86. DC has many subtypes according to different sources, and different subtypes have different characteristics in anti-cryptococcal infection. Plasma cell like DCs phagocytize *C. neoformans* and limit its growth through dectin-3 and reactive oxygen species dependent mechanisms^[21]. The protective immune response against cryptococcal antigen is mediated by CD11b⁺ DC and Langerhans cells^[22]. CD11b⁺ DC can also mediate non protective Th2 response^[23]. Recent studies have found that *Cryptococcus* can use the collagen structure of macrophage receptor to promote the accumulation of CD11b⁺ DC and change the Th1/Th2 balance, which is conducive to the reproduction and spread of fungi. Monocyte derived DCs

enhance Th1 response after respiratory tract infected with *C. neoformans*.

3.3 Effect of T cells on *Cryptococcus*

Patients suffered from *C. neoformans* with AIDS are closely related to T cell defects. T cells are necessary for adaptive immune response. In human body, CD4⁺ T cell defect is the main factor inducing cryptococcosis, in which the count of CD4⁺ T cells is less than 100·μ·L⁻¹, indicating an increased risk of HIV related cryptococcosis^[25]. T lymphocytes that participate the response of the host to *C. neoformans* include CD4⁺ T cells, CD8⁺ T cells and natural killer T (NKT) cells. CD4⁺ T cells, CD8⁺ T cells and NK cells can directly bind to *Cryptococcus* and act in a way of inhibiting fungi. Recently, an auxiliary T cell (CD4⁺ Fox P3 Treg) was found to inhibit Th2 response in anti-*Cryptococcus*^[26]. Activated CD4⁺ T cells can activate and proliferate B cells, macrophages and CD8⁺ T cells to produce antibodies. CD8⁺ T cells play an important role in the host immune response to *C. neoformans*^[27]. Both CD4⁺ T cells and CD8⁺ T cells produce pro-inflammatory cytokines against *Cryptococcus*. CD8⁺ T cells contact *C. neoformans* cells directly and release granulysin to kill *C. neoformans*.

CD4⁺ T cells are the key to regulating the type of immune response. Naive CD4⁺ T cells are activated and differentiated into different subsets of Th1, Th2 and Th17 to produce cytokines. Th1 type regulates the host to induce cellular immune response and produce cytokines IL-2, IL-12, IFN-γ and TNF-α, having a protective effect against *Cryptococcus*^[28]. Th17 is necessary for vaccine mediated protection of mice against *C. neoformans*^[29], and mainly secretes cytokines IL-17 and IL-22. Th2 reaction produces cytokines such as IL-4, IL-5 and IL-13, which has a non-protective effect on *Cryptococcus* infection. In HIV infection, cytokines change from Th1 to Th2, and the host immune environment becomes more conducive to cryptococcal infection and diffusion (**Figure 2**).

4. Conclusions

The diseases and mortality caused by *Cryptococcus* infection in the world are very high every

year. Because *Cryptococcus* has unique virulence factors, such as capsular polysaccharide, which plays an important role in resisting the immune response of the body and can escape the clearance of host cells. At present, although there is continuous progress in the study of the pathogenic and immunological mechanism of cryptococcosis, it is still not enough to effectively control the epidemic of cryptococcosis. *C. neoformans* adapts to the intracellular environment and resists the immune response of the host through a variety of strategies. For example, *C. neoformans* colonizes macrophages, symbiotically proliferates and escapes to the extracellular environment, causing disease dissemination. Therefore, future research will need to pay attention to the parasitism capacity of *Cryptococcus* in host cells and related immune mechanisms.

The body's protective immunity against *Cryptococcus* requires T cell response, which produces the key protective inflammatory factor TNF- α , IL-12 and IFN- γ . These responses are triggered by classical DC activation. DC plays an important role in phagocytosis and killing *Cryptococcus*. Studies have shown that TLR4 and TLR2 on the surface of DC can recognize the capsule component GXM of *Cryptococcus*^[30]. Therefore, an in-depth understanding of the interaction between DC and *Cryptococcus* will help to improve the immunotherapeutic effect of *Cryptococcus* infection in the future.

In the model of *Cryptococcus* infection in mouse lung, early inoculation of IL-12 can reduce the load of *Cryptococcus* in lung and inhibit its diffusion to brain, and the therapeutic effect of IL-12 is related to the production of high concentration of IFN in lung- γ ^[31]. Immunocompromised patients were given recombinant IFN- γ 1b can promote the killing of *Cryptococcus* in cerebrospinal fluid and increase the body's drug resistance^[32]. If we want to improve the immune efficacy of cryptococcal infection treatment, we should deeply understand the signal transduction pathway involved in cryptococcal pathogenesis.

Conflict of interest

The authors declare no potential conflicts of interest.

Acknowledgements

Fund Project: Science and Technology Planning Project of Jiangxi Provincial Health and Family Planning Commission (No.: 20141114).

References

1. Byrnes EJ, Marr KA. The outbreak of *Cryptococcus gattii* in Western North America: Epidemiology and clinical issues. *Current Infectious Disease Reports* 2011; 13(3): 256–261.
2. Akins PT, Jian B. The frozen brain state of *Cryptococcus gattii*: A globe-trotting, tropical, neurotropic fungus. *Neurocritical Care* 2019; 30(2): 272–279.
3. Park BJ, Wannemuehler KA, Marston BJ, *et al.* Estimation of the current global burden of cryptococcal meningitis among persons living with HIV/AIDS. *AIDS* 2009; 23(4): 525–530.
4. Springer DJ, Billmyre RB, Filler EE, *et al.* *Cryptococcus gattii* VGIII isolates causing infections in HIV/AIDS patients in Southern California: Identification of the local environmental source as arboreal. *PLOS Pathogens* 2014; 10(8): e1004285.
5. Kwon-Chung KJ, Fraser JA, Doering TL, *et al.* *Cryptococcus neoformans* and *Cryptococcus gattii*, the etiologic agents of cryptococcosis. *Cold Spring Harbor Perspectives in Medicine* 2014; 4(7): a019760.
6. Galanis E, Macdougall L, Kidd S, *et al.* Epidemiology of *Cryptococcus gattii*, British Columbia, Canada, 1999–2007. *Emerging Infectious Diseases* 2010; 16(2): 251–257.
7. Ngamskulrungrroj P, Chang Y, Sionov E, *et al.* The primary target organ of *Cryptococcus gattii* is different from that of *Cryptococcus neoformans* in a murine model. *mBio* 2012; 3(3): e00103–12.
8. Li P, Tan H, Hu C, *et al.* Purification of capsular polysaccharide GXM from *Cryptococcus neoformans* and its role in regulating MR expression in macrophages. *Chinese Journal of Mycology* 2012; (5): 265–268.
9. O'meara TR, Alspaugh JA. The *Cryptococcus neoformans* capsule: A sword and a shield. *Clinical Microbiology Reviews* 2012; 25(3): 387–408.
10. Denham ST, Verma S, Reynolds RC, *et al.* Regulated release of cryptococcal polysaccharide drives

- virulence and suppresses immune infiltration into the central nervous system. *Infectious Immunity* 2018; 86(3): e00662–17.
11. Zhou J, Mao W. Research progress on the interaction between phagocytic effector cells and *Cryptococcus neoformans* (in Chinese). *Chinese Journal of Mycology* 2017; (4): 244–247, 256.
 12. Garelnabi M, Taylor-Smith LM, Bielska E, *et al.* Quantifying donor-to-donor variation in macrophage responses to the human fungal pathogen *Cryptococcus neoformans*. *PLoS One* 2018; 13(3): e194615.
 13. Smith LM, Dixon EF, May RC. The fungal pathogen *Cryptococcus neoformans* manipulates macrophage phagosome maturation. *Cell Microbiology* 2015; 17(5): 702–713.
 14. Leopold Wager CM, Hole CR, Wozniak KL, *et al.* *Cryptococcus* and Phagocytes: Complex interactions that influence disease outcome. *Frontiers in Microbiology* 2016; 7: 105.
 15. Lim J, Coates CJ, Seoane PI, *et al.* Characterizing the mechanisms of nonopsonic uptake of *Cryptococcus* by Macrophages. *Journal of Immunology* 2018; 200(10): 3539–3546.
 16. Davis MJ, Tsang TM, Qiu Y, *et al.* Macrophage M1/M2 polarization dynamically adapts to changes in cytokine microenvironments in *Cryptococcus neoformans* infection. *mBio* 2013; 4(3): e00264–13.
 17. Hole CR, Bui H, Wormley FL, *et al.* Mechanisms of dendritic cell lysosomal killing of *Cryptococcus*. *Scientific Reports* 2012; 2: 739.
 18. Wozniak KL, Vyas JM, Levitz SM. In vivo role of dendritic cells in a murine model of pulmonary *Cryptococcosis*. *Infection and Immunity* 2006; 74(7): 3817–3824.
 19. Wozniak KL. Interactions of *Cryptococcus* with dendritic cells. *Journal of Fungi* 2018; 4(1): 36.
 20. Siegemund S, Alber G. *Cryptococcus neoformans* activates bone marrow-derived conventional dendritic cells rather than plasmacytoid dendritic cells and downregulates macrophages. *Fems Immunology & Medical Microbiology* 2008; 52(3): 417.
 21. Hole CR, Leopold Wager CM, Mendiola AS, *et al.* Antifungal activity of plasmacytoid dendritic cells against *Cryptococcus neoformans* In vitro requires expression of dectin-3 (CLEC4D) and reactive oxygen species. *Infection and Immunity* 2016; 84(9): 2493–2504.
 22. Osterholzer JJ, Chen G, Olszewski M, *et al.* Accumulation of CD11b (+) lung dendritic cells in response to fungal infection results from the CCR2-mediated recruitment and differentiation of Ly-6C (high) monocytes. *Journal of Immunology (Baltimore, Md.: 1950)* 2009; 183(12): 8044–8053.
 23. Wiesner DL, Specht CA, Lee CK, *et al.* Chitin recognition via chitotriosidase promotes pathologic type-2 helper T Cell responses to *Cryptococcal* infection. *PLoS Pathogens* 2015; 11(3): e1004701.
 24. Xu J, Flaczyk A, Neal LM, *et al.* Exploitation of scavenger receptor, macrophage receptor with collagenous structure, by *Cryptococcus neoformans* promotes alternative activation of pulmonary lymph node CD11b (+) conventional dendritic cells and non-protective Th2 bias. *Frontiers in Immunology* 2017; 8: 1231.
 25. Rajasingham R, Smith RM, Park BJ, *et al.* Global burden of disease of HIV-associated cryptococcal meningitis: an updated analysis. *Lancet Infectious Disease* 2017; 17(8): 873–881.
 26. Ma H, Li Y, Wei Y, *et al.* CD⁴⁺ FoxP³⁺ regulatory T cells inhibit the immune effects of Th2 cells in lung fungal infection. *Chinese Journal of Gerontology* 2018; (2): 265–268.
 27. Van De Veerdonk FL, Netea MG. T-cell subsets and antifungal host defenses. *Current Fungal Infection Reports* 2010; 4(4): 238–243.
 28. Rohatgi S, Pirofski LA. Host immunity to *Cryptococcus neoformans*. *Future Microbiology* 2015; 10(4): 565–581.
 29. Szymczak WA, Davis MJ, Lundy SK, *et al.* X-linked immunodeficient mice exhibit enhanced susceptibility to *Cryptococcus neoformans* infection. *mBio* 2013; 4(4): e00265–13.
 30. Yauch LE, Mansour MK, Shoham S, *et al.* Involvement of CD14, toll-like receptors 2 and 4, and MyD88 in the host response to the fungal pathogen *cryptococcus neoformans* in vivo. *Infectious Immunity* 2004; 72: 5373–5382.
 31. Clemons KV, Brummer E, Stevens DA. Cytokine treatment of central nervous system infection: Effi-

cacy of interleukin-12 alone and synergy with conventional antifungal therapy in experimental Cryptococcosis. *Antimicrobial agents and chemotherapy* 1994; 38(3): 460.

32. Pappas PG, Bustamante B, Ticona E, *et al.* Recombinant interferon-gamma 1b as adjunctive therapy for AIDS-related acute Cryptococcal meningitis. *Journal of Infectious Disease* 2004; 189 (12): 2185–2191.

REVIEW ARTICLE

Combination of anti-angiogenic therapy Apatinib and immune therapy potentiate tumor microenvironment

Chunyi Gao, Tianhui Hu*

Cancer Research Center, School of Medicine, Xiamen University, Xiamen 361102, Fujian Province, China. E-mail: thu@xmu.edu.cn

ABSTRACT

Tumor immune therapy, especially anti-programmed cell death ligand-1/programmed cell death-1 (PD-L1/PD-1) treatment, is currently the focus of substantial attention. However, despite its enormous successes, the overall response rate of cancer immunotherapy remains suboptimal. There is an increased interest in combining PD-L1/PD-1 treatment with anti-angiogenic drug Apatinib to enhance antitumor effect. Presently available data seem to suggest that Apatinib may exert immune suppressive effects to make the PD-L1/PD-1 treatment works. Here, we review the extensive tumor microenvironment immune modulatory effects from antiangiogenic agents Apatinib in order to supporting VEGFR2 targettherapies in clinical trials are existing.

Keywords: Apatinib; Tumor Environment; PD-1/PD-L1; Tumor Immune Therapy

ARTICLE INFO

Received 13 September 2021
Accepted 9 November 2021
Available online 16 November 2021

COPYRIGHT

Copyright © 2021 Chunyi Gao, *et al.*
EnPress Publisher LLC. This work is licensed under the Creative Commons Attribution-NonCommercial 4.0 International License (CC BY-NC 4.0).
<https://creativecommons.org/licenses/by-nc/4.0/>

1. Introduction of Apatinib

Apatinib is a small-molecule antiangiogenic targeted drug developed by Jiangsu Hengrui Pharmaceutical Co., Ltd. It was listed in the treatment of gastric cancer in 2014. Furthermore, the drug also shows great potential in the treatment of multiple other solid tumors^[1,2]. The main mechanism of action of Apatinib is the competitive binding of the vascular endothelial growth factor receptor2 (VEGFR-2) intracellular tyrosine ATP binding site. Then selectively inhibiting tyrosine kinase activity and blocking signaling after vascular endothelial growth factor (VEGF) binding, resulting in potent inhibition of tumor angiogenesis. VEGFR-2 is a high-affinity receptor for VEGF and, together with VEGFR-1 and VEGFR-3, forms the Flt subfamily of receptor tyrosine kinases (RTK). VEGFR-1 binds to VEGF with a higher affinity than VEGFR-2, but VEGFR-1 exerts weak tyrosine phosphorylation of VEGF. Thus, VEGFR-2 is the primary RTK that can mediate VEGF signaling in endothelial cells and drive VEGF-mediated angiogenic^[3]. Moreover, VEGFR-2 is the major regulator of endothelial cell proliferation, development, migration, angiogenesis, and budding^[4]. Therefore, Apatinib may have better therapeutic potential than other antiangiogenic agents such as ramoximab, bevacizumab and sunitinib^[5]. In addition, Apatinib can sensitize drug-resistant tumor cells to chemotherapeutic drugs and reverse multidrug resistance (MDR) caused by ATP binding cassette transporter (ABC) protein^[6]. It can also stimulate tumor cell apoptosis, inhibit cell proliferation and enhance the efficacy of conventional chemotherapy drugs to play an anti-cancer role.

In recent years, the clinical application and related mechanism of Apatinib in other tumors have also been widely concerned and explored^[7-9]. However, so far, the clinical application has generally focused on inhibiting abnormal angiogenesis. This review summarizes the unique mechanism of action of Apatinib, based on preclinical and clinical findings, the molecular mechanism behind the pathway of interaction with Apatinib was reexplored. Specifically, Apatinib includes both wellknown anti-angiogenic effects and novel immunomodulatory mechanisms. It can promote the clinical understanding of molecular biology and immunology, and help to expand the scope and prospect of Apatinib treatment.

2. Immunotherapy and VEGF/VEGFR targets

Immune checkpoint inhibitors (ICIS) can break through the bottleneck of tumor immunosuppression, restore the suppressed immune activity in tumor patients, and promote immune cells to recognize and then kill tumor cells. It provide a new idea for immunotherapy^[10,11]. In recent years, programmed cell death 1 (PD-1) antibody, programmed cell death ligand 1 (PD-L1) antibody, and cytotoxic T lymphocyte-associated protein 4

(CTLA-4) antibody and other representative immunotherapies have become an important means of tumor treatment^[12]. Especially for antibodies against PD-1/PD-L1 have achieved significant clinical efficacy in the therapy of malignant tumors such as lung cancer, kidney cancer, and melanoma. The high expression of PD-L1 may be a molecular marker of poor prognosis of cancer, and it is also the basis for clinical treatment with anti- PD-1/PD-L1.

However, the anti-PD-1/PD-L1 treatment also has its limitations, the main problem is the low proportion of beneficiaries, the response rate of single drug use is generally between 10% and 40%, and not all tumor types are effective^[13]. The main reason for the low benefit ratio is that the efficacy of immunotherapy highly depends on the Tumor Microenvironment (TME). The TME is mainly composed of the vasculature, the extracellular matrix, other non-malignant cells around the tumor, as well as the complex signaling molecular networks that maintain internal connections in the microenvironment. These components not only could promote the growth and reproduction of the tumor cells but also induce them to invade and metastasize^[14].

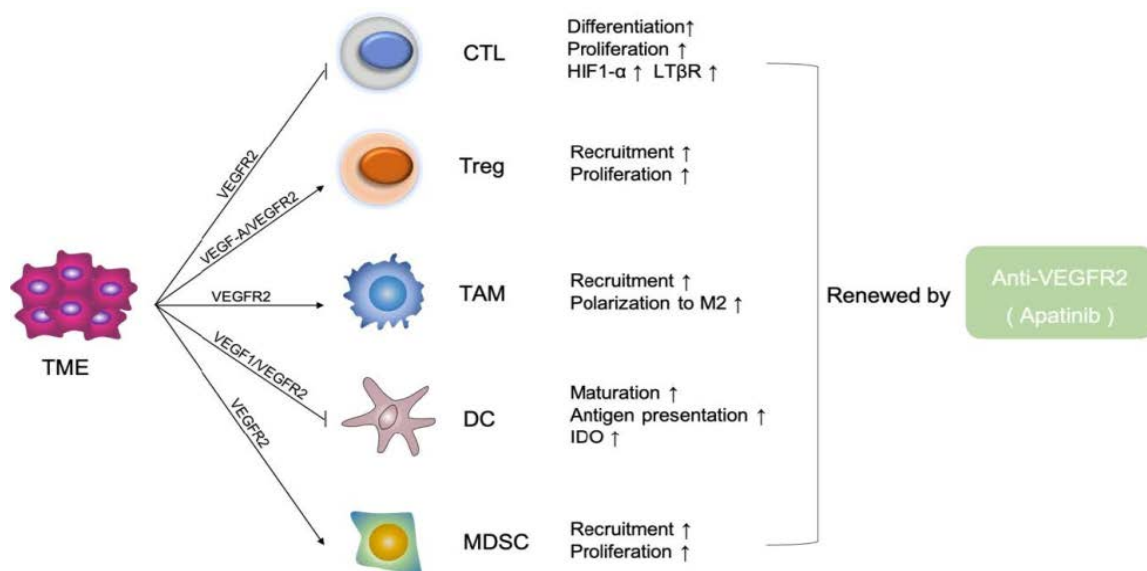


Figure 1. Effect of Apatinib on immune cell populations in the tumor microenvironment.

The anti-tumor immune effect of the body is mainly the adaptive immune response mediated by T lymphocytes (CD8⁺ cytotoxic T cells and CD4⁺ helper T cells)^[15]. However, the existence of TME

and the low immune foci of the tumor itself will lead to the activation disorder of CD8⁺ cytotoxic T cells and CD4⁺ helper T cells in tumor patients. The functions of these two cells are strongly inhibited in

the tumor microenvironment, which is one of the main obstacles to anti-PD-1/PD-L1 immunotherapy^[16]. And it is also one of the main reasons for the low response rate of immunotherapy. Therefore, inhibiting of the negatively regulated recruitment of immune cells in the tumor microenvironment, or inhibiting the secretion of anti-inflammatory factors. That may make the effect of the tumor immunotherapy more significant. In recent years, more studies and clinical trials have found that the combined use of anti-tumor angiogenesis drugs and PD-1/PD-L1 antibodies could effectively improve the efficacy of immunotherapy. Its mechanism is closely related to the remodeling of the tumor microenvironment^[17,18]. Next, we will describe the effects of the antiangiogenic agent Apatinib on the antitumor function of immune cells in preclinical and clinical trials in detail (**Figure 1**).

3 Effect of Apatinib on the immune microenvironment

3.1 Effect of Apatinib on effector T cells

In the terms of T cells, these unusual tumor vascular networks provide an attack barrier for tumor cells. The abnormal vascular network is mostly immature neovascularization, which does not have the tissue structure of normal blood vessels, so it cannot perform a normal function. Neovascular endothelial cells are loosely connected and lack the support of pericytes and basal cells. Therefore, tissue fluid seeps from the abnormal vascular network into the tumor microenvironment to further compress the blood vessels, and the blood cannot transport oxygen and nutrients to the interior of the tumor, resulting in hypoxia and necrosis in the interior of the tumor. Similarly, most killer T cells cannot infiltrate into the tumor, so their killing effect is inhibited. A small number of T cells crossing vascular endothelial cells into the tumor microenvironment still cannot kill tumor cells. The reason is the increased expression of immunosuppressive marker PD-L1 on the surface of tumor cells under long-term hypoxia. Therefore, only after anti-vascular treatment, killer T cells infiltrate into the tumor area, and then anti-PD-1 treatment can exert a good curative effect^[19].

VEGF increased the infiltration of regulatory T cells in the microenvironment and promoted the failure of CD8⁺ T cells. TOX is a transcription factor of T cell development and plays an important role in T cell maturation. In the tumor microenvironment, VEGF up-regulates the expression of TOX in CD8⁺ T cells and activates the failure-related signal pathway of T cells. Anti VEGF treatment can reverse this phenomenon. VEGFR-2 ramucirumab promotes the increase of the proportion of CD8⁺ T cells in peripheral blood of patients with gastric cancer^[20]. More studies have found that VEGFR-2 blocked HIF1- α of CD8⁺ T cells activation of the pathway leads to increased secretion of anti-inflammatory factors^[21]. In the mouse lung cancer model, the use of low-dose Apatinib increased the infiltration of CD8⁺ T cells in tumors^[22]. Comprehensive studies have shown that blocking VEGFR-2 could increase the proportion and activity of CD8⁺ T cells^[23,24]. Moreover, low-dose VEGFR-2 target drug (DC101) is more conducive to promoting the tumor infiltration of CD4⁺ and CD8⁺ T cells^[25]. In spontaneous breast cancer mice, DC101 inhibited tumor growth by increasing the proportion of CD8⁺ T cells^[25,26]. In the exploration of its mechanism, ELIZABETH ALLEN *et al.* proposed that combination therapy of anti-VEGFR-2 and anti-PD-L1 antibodies in mice models of breast, pancreatic and glioblastoma can induce the growth, and proliferation of endothelial micro veins in the tumor microenvironment^[19]. Endothelial micro veins promote lymphocyte infiltration and activity through the activation of the lymphotoxin β receptor (LT β R) on the lymphocyte surface. Using LT β R directly agonist can enhance the activity of cytotoxic T cells (CTL), so that PD-L1 antibody can further improve its antitumor efficacy after combined treatment with anti-VEGFR-2.

3.2 Effect of Apatinib on regulatory T cells

Regulatory T cells, namely CD4⁺ CD25⁺ Treg, account for 5% ~ 10% of the total T cells and are key negative regulatory cells in the tumor immune microenvironment. Classic sub-Types are divided into natural regulatory T cells (nTregs) differentiated from the thymus and inducible regulatory T cells (iTregs) induced by antigens or other cytokines.

Foxp3 is the functional activity index of Treg^[27]. Suzuki H *et al.* found that Foxp3⁺ CD4⁺ T cells specifically express VEGFR-2, and VEGFR-2⁺ CD4⁺ T cells inhibit the proliferation of VEGFR-2⁻ CD4⁺ T cells^[28]. TGF- β further increases the number of VEGFR2⁺ Tregs by promoting VEGF-A secretion^[28]. Targeting VEGFR can effectively reduce the proportion of Treg, weaken its immunosuppressive activity and enhance the antitumor immune response of effector T cells. VEGF-A directly promotes the proliferation of Treg, and blocking VEGF-A/VEGFR-2 pathway can reverse this phenomenon^[29].

TADA Y *et al.* found that PD-L1 + CD8⁺ T cell infiltration in peripheral blood increased after targeted VEGFR-2 treatment in patients with gastric cancer^[20]. The proportion of Treg decreased. Progression-free survival was longer in patients with low expression of VEGFR-2⁺ Treg than in patients with high expression. According to more studies, in the study of mouse colon cancer, PD-1 antibody increased the proportion of Foxp3⁺ Treg in tumor tissue^[30]. This phenomenon can recover by combined use of VEGFR-2 antibody, and the combined use increased IFN- γ in tumor homogenate and TNF- α Level. In hepatoma mice, VEGF-2 antibody (DC101) increased the CTL/Treg ratio in tumor tissues^[31].

3.3 Effect of Apatinib on macrophages

Tumor-associated macrophages (TAM) are the main inflammatory cell population in solid tumors and have an important impact on the composition of TME. Plasticity is an important concept in TAM research, that is, TAM can differentiate into M1/M2 types according to different stimuli of TME. M1 macrophages derived from interferon γ (IFN- γ) and inflammatory cytokines stimulated and secreted by lipopolysaccharide (LPS). Matrix remodeling cytokines activated and released by IL-4 and IL-13 stimulated M2 macrophages. "Remodeling" TAM, that is, transforming M2 into anti-tumor M1, may become a potentially effective strategy for cancer treatment^[32].

In the treatment of lung cancer mice, oral low doses of Apatinib increased the proportion of infiltration of total macrophages and reduced the pro-

portion of cancer type CD163⁺ M2 macrophages^[22]. In liver cancer mice, small-dose VEGFR-2 antibody (DC101) treatment significantly increased the number of F4/80⁺ CD80⁺ and CD86⁺ M1 macrophages infiltrated in the tumor and reduced the number of F4/80⁺ CD206⁺ M2 macrophages after combined anti-PD-1 treatment.

3.4 Effect of Apatinib on DCs

Antigen presentation is a prerequisite for anti-tumor immune response. Immature dendritic cells (DCs) lack effective antigen presentation function, resulting in immune tolerance^[33]. Several studies have reported that VEGF inhibits the maturation of DCs in vitro and vivo by activating NF- κ B. AL-FARO C *et al.* believed that renal cancer cells inhibit the maturation and differentiation of DCs under hypoxia, which can reverse by Sunitinib, a tyrosine kinase inhibitor of VEGFR-2^[34]. There are different opinions on the functional blocking sites of VEGF/VEGFR on DCs. Some studies have said that VEGFR-1 is the main receptor for DCs maturation, and the signal transduction of VEGFR-2 is very important for early DCs differentiation in blood, but only has a slight impact on the final DCs maturation^[35]. Another study shows that VEGF inhibits the ability of mature DCs to present antigens to T cells, and the DCs dysfunction induced by VEGF is mainly mediated by VEGFR-2. Blocking mAb by anti-VEGFR-2 can reverse DCs dysfunction^[36]. During the exploration of its mechanism, MARTI LC *et al.* judged that VEGF up-regulated IDO expression in DCs through VEGF/VEGFR pathway, and IDO further inhibited lymphocyte proliferation^[37].

3.5 Effects of Apatinib on bone marrow-derived inhibitory cells

Myeloid-derived suppressor cells (MDSCs) are generally considered as CD45⁺ CD11b⁺ CD33⁺ CD14⁻ immunosuppressive cell group. MDSCs were found in tumor, spleen, blood, bone marrow, and liver^[38]. In TME, MDSCs attenuate the anti-tumor function of effector T cells and act on NK cells to reduce their cytokines, and inhibit their cytotoxicity^[39]. There is a dual expression of VEGFR-1 and VEGFR-2 on the surface of MDSCs.

VEGFR-2 mediated signal pathway promotes the proliferation of MDSCs^[40]. VEGF/VEGFR-2 signal transduction also directly promotes the differentiation and migration of MDSCs, recruits MDSCs to tumor sites and inhibits T cell function^[26].

4. Clinical application of Apatinib-linked therapy with PD-1/PD-L1

4.1 Non-small-cell lung cancer (NSCLC)

Apatinib showed a significant survival benefit in phase II/IB clinical trials in non-small cell lung cancer, and the effect was better when combined with anti-PD-1. A phase II clinical trial showed that NSCLC patients were treated with 500–750 mg of Apatinib. Among the 38 NSCLC patients evaluated, the objective response rate (ORR) was 13.2%, and the disease control rate (DCR) was 63.2%. The progression-free survival (PFS) was 3.06 months. Overall survival (OS) was 7.69 months. It shows that Apatinib has a certain role in patients with advanced NSCLC and only has slight adverse reactions^[41]. The results of another phase IB clinical trial of NSCLC showed that among the 8 NSCLC patients available for analysis, the ORR and DCR of Apatinib were 55.6% and 88.9%, which were superior to anti-PD-1 monotherapy in the same clinical environment^[22].

4.2 Small-cell lung cancer (SCLC)

Apatinib also showed therapeutic benefits in SCLC patients. Camrelizumab 200 mg combined with Apatinib 375 mg. Of the 47 SCLC patients available for evaluation, ORR reached 34.0%, median PFS was 3.6 months and OS was 8.4 months. Results-oriented patients were classified into platinum-class chemotherapy-sensitive and insensitive groups in SCLC patients. The ORR of platinum chemotherapy-sensitive SCLC patients was 37.50%, the median PFS was 3.6 months, and the OS was 9.6 months. There was no significant difference between SCLC patients and the platinum chemotherapy insensitive group (32.3%, 2.7 months, 8 months). This study showed that camrelizumab combined with Apatinib showed potential antitumor activity in chemotherapy-sensitive and chemotherapy-resistant SCLC patients.

4.3 Hepatocellular carcinoma (HCC)

Jianming Xu *et al.* evaluated the efficacy of Apatinib combined with SHR-1210 (anti-PD-1 antibody) in a study on patients with advanced HCC and GC/EGJC at the same time^[7]. After the end of the trial, 8 of the 16 HCC patients who can be used for evaluation obtained partial remission, and the partial response (PR) was 50.0%. Including GC/EGJC patients, the ORR of 39 assessable patients was 30.8%. This study shows that the maximum tolerated dose of Apatinib as combination therapy is 250 mg, and patients with advanced HCC can obtain practical clinical benefits in combination therapy.

Another study classified patients with HCC. Seventy of these patients did not receive first phase treatment, 120 were ineffective in first phase treatment, and all patients had combined Camrelizumab (anti-PD-1 antibody 200 mg) and Apatinib 250 mg·d⁻¹. For the HCC group not receiving phase I treatment, the ORR was 34.3% and a median PFS of 5.7 months, annual survival was 74.7%. Trials with HCC patients who failed phase I treatment showed that the 120 HCC patients available for evaluation had an ORR of 22.5% and a median PFS of 5.5 months, annual survival of 68.2%. This study demonstrated that Camrelizumab combined with Apatinib has a survival benefit for patients with advanced liver cancer^[42].

4.4 Gastric or esophagogastric junction cancer (GC/EGJC)

In another phase III clinical trial of GC/EGJC patients, the researchers recruited 267 patients^[43]. Compared with the placebo group, the median OS was significantly prolonged in the Apatinib group (6.5 months vs. 4.7 months, $P < 0.05$), and the median PFS was also prolonged (2.6 months vs. 1.8 months, $P < 0.001$).

4.5 Triple-negative breast cancer (TNBC)

Apatinib in the phase II study of TNBC patients, 30 evaluable patients were given Apatinib 250 mg and SHR-1210 200 mg continuously. The results showed that the ORR of patients was 43.3%, DCR was 63.3%, and PFS was 3.7 months. The median PFS of patients with partial remission

was 7.69 months, which was significantly higher than that of patients with TNBC that could not be evaluated clinically (2 months). SHR-1210 combined with Apatinib showed a good therapeutic effect in patients with advanced TNBC^[44].

5. Conclusion

Under physiological conditions, the expression levels of VEGF and VEGFR in normal human mature tissues very low, and only the expression level of VEGF in vascular endothelial cells is high. However, clinical studies have shown that the high expression of VEGF and VEGFR has been detected in most malignant tumors and is associated with the high risk of cancer metastasis^[45]. This is because the growth and development of tumors depend on the oxygen and nutrients provided by tumor blood vessels. In highly metabolized tumors, they grow beyond the supply of blood vessels, leading to hypoxia inside the tumor^[46]. Under hypoxia, hypoxia-inducible factor (HIF-1) regulating angiogenesis is activated, and endothelial cells and tumor cells jointly mediate the upregulation of VEGF expression in TME^[47]. VEGF can indirectly promote the inhibition of T lymphocytes and MDSCs by stimulating endothelial cells to produce prostaglandin E2 (PGE2)^[48]. Moreover, immunosuppression of tumor microenvironment is caused by inducing the proliferation and differentiation of regulatory T cells (Tregs)^[49] and inhibiting the maturation of dendritic cells (DCs) precursor cells^[50].

Apatinib, which is an angiogenesis inhibitor, not only can inhibit Abnormal angiogenesis but also improve the tumor immune microenvironment. According to clinical statistics, at present, there are 33 clinical studies on Apatinib, and among them, there are 29 carried out in China. Comprehensive clinical trial results show that the combination of Apatinib and PD-1/PD-L1 antibody can effectively improve the efficacy of immunotherapy and significantly improve the survival benefit of patients. As a new type of antitumor drug, Apatinib has its superior development prospect and potential. In this paper, we summarized the effects of Apatinib on various immune cells in the tumor microenvironment and summarized the beneficial effects of Apatinib combined with PD-1/PD-L1 antibodies in different

kinds of cancer in the clinical trials.

Conflict of interest

The authors declare no potential conflicts of interest.

References

1. Hoeksema MA, Gijbels MJ, Velden S, *et al.* Targeting macrophage Histone deacetylase 3 stabilizes atherosclerotic lesions. *EMBO Molecular Medicine* 2014; 6(9): 1124–1132.
2. Zhao L, Zhang W, Li C, *et al.* Research progress on antitumor mechanism of Apatinib. *Cancer Research on Prevention and Treatment* 2021; 48(1): 7–11.
3. Li Y, Zhao H, Ren X. Relationship of VEGF/VEGFR with immune and cancer cells: Staggering or forward? *Cancer Biology & Medicine* 2016; 13(2): 206–214.
4. Rangunathrao VAB, Anwar M, Akhter MZ, *et al.* Sphingosine-1-phosphate receptor 1 activity promotes tumor growth by amplifying VEGF-VEGFR2 angiogenic signaling. *Cell Reports* 2019; 29(11): 3472–3487.
5. Maroufin F, Rashidi MR, Vahedian V, *et al.* Therapeutic potentials of Apatinib in cancer treatment: Possible mechanisms and clinical relevance. *Life Sciences* 2020; 241: 117106.
6. Mi Y, Liang Y, Huang H, *et al.* Apatinib (YN968D1) reverses multidrug resistance by inhibiting the efflux function of multiple ATP-binding cassette transporters. *Cancer Research* 2010; 70(20): 7981–7991.
7. Xu J, Zhang Y, Jia R, *et al.* Anti-PD-1 antibody SHR-1210 combined with Apatinib for advanced hepatocellular carcinoma, gastric, or esophagogastric junction cancer: An open-label, dose escalation and expansion study. *Clinical Cancer Research* 2019; 25(2): 515–523.
8. Zheng Y, Yang X, Yan C, *et al.* Effect of Apatinib plus neoadjuvant chemotherapy followed by resection on pathologic response in patients with locally advanced gastric adenocarcinoma: A single-arm, open-label, phase II trial. *European Journal of Cancer* 2020; 130: 12–19.
9. Liu C, Jia Q, Wei H, *et al.* Apatinib in patients with

- advanced chordoma: A single-arm, single-centre, phase 2 study. *Lancet Oncology* 2020; 21(9): 1244–1252.
10. Ribas A, Wolchok JD. Cancer immunotherapy using checkpoint blockade. *Science* 2018; 359(6382): 1350–1355.
 11. Lyon AR, Yousaf N, Battisti NML, *et al.* Immune checkpoint inhibitors and cardiovascular toxicity. *Lancet Oncology* 2018; 19(9): e447–e458.
 12. Wei SC, Aang NAS, Sharma R, *et al.* Combination anti-CTLA-4 plus anti-PD-1 checkpoint blockade utilizes cellular mechanisms partially distinct from monotherapies. *Proceedings of the National Academy of Sciences* 2019; 116(45): 22699–22709.
 13. Wang DY, Salem JE, Cohen JV, *et al.* Fatal toxic effects associated with immune checkpoint inhibitors: A systematic review and meta-analysis. *JAMA Oncology* 2018; 4(12): 1721–1728.
 14. Wei F, Wu Y, Tang L, *et al.* BPIFB1 (LPLUNC1) inhibits migration and invasion of nasopharyngeal carcinoma by interacting with VTN and VIM. *British Journal of Cancer* 2018; 118(2): 233–247.
 15. Vitale I, Manic G, Coussens LM, *et al.* Macrophages and metabolism in the tumor microenvironment. *Cell Metabolism* 2019; 30(1): 36–50.
 16. Shemesh CS, Hsu JC, Hosseini I, *et al.* Personalized cancer vaccines: Clinical landscape, challenges and opportunities. *Molecular Therapy* 2021; 29(2): 555–570.
 17. McDermott DF, Huseni MA, Atkins MB, *et al.* Clinical activity and molecular correlates of response to atezolizumab alone or in combination with bevacizumab versus sunitinib in renal cell carcinoma. *Nature Medicine* 2018; 24(6): 749–757.
 18. Wallin JJ, Bendell JC, Funke R, *et al.* Atezolizumab in combination with bevacizumab enhances anti-gen-specific T-cell migration in metastatic renal cell Carcinoma. *Nature Communications* 2016; 7: 12624.
 19. Allen E, Jabouille A, Rivera LB, *et al.* Combined antiangiogenic and anti-PD-L1 therapy stimulates tumor immunity through HEV formation. *Science Translational Medicine* 2017; 9(385): eaak9679.
 20. Tada Y, Togashi Y, Kotani D, *et al.* Targeting VEGFR2 with Ramucirumab strongly impacts effector/activated regulatory T cells and CD8⁺ T cells in the tumor microenvironment. *Journal for Immunotherapy of Cancer* 2018; 6(1): 106.
 21. Almeida PED, Mak J, Hernandez G, *et al.* Anti-VEGF treatment enhances CD8⁺ T-cell antitumor activity by amplifying hypoxia. *Cancer Immunol Research* 2020; 8(6): 806–818.
 22. Zhao S, Ren S, Jiang T, *et al.* Low-dose Apatinib optimizes tumor microenvironment and potentiates antitumor effect of PD-1/PD-L1 blockade in lung cancer. *Cancer Immunol Research* 2019; 7(4): 630–643.
 23. Xu Y, Zhang X, Wang Y, *et al.* A VEGFR2-MICA bispecific antibody activates tumor-infiltrating lymphocytes and exhibits potent anti-tumor efficacy in mice. *Cancer Immunology, Immunotherapy* 2019; 68(9): 1429–1441.
 24. Li Q, Wang Y, Jia W, *et al.* Low-dose Anti-angio-genic therapy sensitizes breast cancer to PD-1 blockade. *Clinical Cancer Research* 2020; 26(7): 1712–1724.
 25. Huang Y, Yuan J, Righi E, *et al.* Vascular normalizing doses of antiangiogenic treatment reprogram the immunosuppressive tumor microenvironment and enhance immunotherapy. *Proceedings of the National Academy of Sciences of the United States of America* 2012; 109(43): 17561–17566.
 26. Horikawa N, Abiko K, Matsumura N, *et al.* Expression of vascular endothelial growth factor in ovarian cancer inhibits tumor immunity through the accumulation of myeloid-derived suppressor cells. *Clinical Cancer Research* 2017; 23(2): 587–599.
 27. Hori S, Nomura T, Sakaguchi S. Control of regulatory T cell development by the transcription factor Foxp3. *Science* 2003; 299(5609): 1057–1061.
 28. Suzuki H, Onishi H, Wada J, *et al.* VEGFR2 is selectively expressed by FOXP3^{high} CD4⁺ Treg. *European Journal of Immunology* 2010; 40(1): 197–203.
 29. Terme M, Pernot S, Marcheteau E, *et al.* VEGFA-VEGFR pathway blockade inhibits tumor-induced regulatory T-cell proliferation in colorectal cancer. *Cancer Research* 2013; 73(2): 539–549.
 30. Yasuda S, Sho M, Yamato I, *et al.* Simultane-

- ous blockade of programmed death 1 and vascular endothelial growth factor receptor 2 (VEGFR2) induces synergistic anti-tumour effect in vivo. *Clinical & Experimental Immunology* 2013; 172(3): 500–506.
31. Shigeta K, Datta M, Hato T, *et al.* Dual programmed death receptor-1 and vascular endothelial growth factor receptor-2 blockade promotes vascular normalization and enhances antitumor immune responses in hepatocellular carcinoma. *Hepatology* 2020; 71(4): 1247–1261.
 32. Gao C, Jiang Z, Wang G. Mechanism of macrophage polarization in breast cancer associated microenvironment. *Chinese Clinical Oncology* 2019; 24(3): 274–280.
 33. Hato T, Zhu AX, Duda DG. Rationally combining anti-VEGF therapy with checkpoint inhibitors in hepatocellular carcinoma. *Immunotherapy* 2016; 8(3): 299–313.
 34. Alfaro C, Suarez N, Gonzalez A, *et al.* Influence of bevacizumab, sunitinib and sorafenib as single agents or in combination on the inhibitory effects of VEGF on human dendritic cell differentiation from monocytes. *British Journal of Cancer* 2009; 100(7): 1111–1119.
 35. Dikov MM, Ohm JE, Ray N, *et al.* Differential roles of vascular endothelial growth factor receptors 1 and 2 in dendritic cell differentiation. *Journal of Immunology* 2005; 174(1): 215–222.
 36. Mimura K, Kono K, Takahashi A, *et al.* Vascular endothelial growth factor inhibits the function of human mature dendritic cells mediated by VEGF receptor-2. *Cancer Immunol Immunother* 2007; 56(6): 761–770.
 37. Cavalheiro ML, Lorena P, Patricia S, *et al.* Vascular endothelial growth factor-A enhances indoleamine 2, 3-dioxygenase expression by dendritic cells and subsequently impacts lymphocyte proliferation. *Memorias Do Instituto Oswaldo Cruz* 2014; 109(1): 7079.
 38. Ilkovitch D, Lopez DM. The liver is a site for tumor-induced myeloid-derived suppressor cell accumulation and immunosuppression. *Cancer Research* 2009; 69(13): 5514–5521.
 39. Hoechst B, Voigtlaender T, Ormandy L, *et al.* Myeloid derived suppressor cells inhibit natural killer cells in patients with hepatocellular carcinoma via the NKp30 receptor. *Hepatology* 2009; 50(3): 799–807.
 40. Solito S, Falisi E, Diaz-Montero CM, *et al.* A human promyelocytic-like population is responsible for the immune suppression mediated by myeloid-derived suppressor cells. *Blood* 2011; 118(8): 2254–2265.
 41. Wu F, Zhang S, Xiong A, *et al.* A Phase II clinical trial of Apatinib in pretreated advanced non-squamous non-small-cell lung cancer. *Clinical Lung Cancer* 2018; 19(6): e831–e842.
 42. Xu J, Shen J, Gu S, *et al.* Camrelizumab in combination with Apatinib in patients with advanced hepatocellular carcinoma (RESCUE): A nonrandomized, open-label, phase II trial. *Clinical Cancer Research* 2021; 27(4): 1003–1011.
 43. Li J, Qin S, Xu J, *et al.* Randomized, double-blind, placebo-controlled phase III trial of Apatinib in patients with chemotherapy-refractory advanced or metastatic adenocarcinoma of the stomach or gastroesophageal junction. *Journal of Clinical Oncology* 2016; 34(13): 1448–1454.
 44. Liu J, Liu Q, Li Y, *et al.* Efficacy and safety of camrelizumab combined with Apatinib in advanced triple-negative breast cancer: An open-label phase II trial. *Journal for Immuno Therapy of Cancer* 2020; 8(1): e000696.
 45. Takahashi Y, Kitadai Y, Bucana CD, *et al.* Expression of vascular endothelial growth factor and its receptor, KDR, correlates with vascularity, metastasis, and proliferation of human colon cancer. *Cancer Research* 1995; 55(18): 3964–3968.
 46. Park JS, Kim IK, Han S, *et al.* Normalization of tumor vessels by Tie2 activation and Ang2 inhibition enhances drug delivery and produces a favorable tumor microenvironment. *Cancer Cell* 2016; 30(6): 953–967.
 47. Kim Y, Nam HJ, Lee J, *et al.* Methylation-dependent regulation of HIF-1 α stability restricts retinal and tumour angiogenesis. *Nature Communications* 2016; 7: 10347.
 48. Mulligan JK, Rosenzweig SA, Young MRI. Tumor secretion of VEGF induces endothelial cells to sup-

- press T cell functions through the production of PGE₂. *Journal of Immunotherapy* 2010; 33(2): 126–135.
49. Jayaraman P, Parikh F, Lopez-Rivera E, *et al.* Tumor-expressed inducible nitric oxide synthase controls induction of functional myeloid-derived suppressor cells through modulation of vascular endothelial growth factor release. *Journal of Immunology* 2012; 188(11): 5365–5376.
50. Hansen W, Hutzler M, Abel S, *et al.* Neuropilin 1 deficiency on CD4⁺ Foxp3⁺ regulatory T cells impairs mouse melanoma growth. *The Journal of Experimental Medicine* 2012; 209(11): 2001–2016.



Trends in Immunotherapy

Focus and Scope

Trends in Immunotherapy (TI) is an open access, peer-reviewed journal encompassing various disciplines related to all immune-based areas. TI has a target audience consisting of scientific researchers, professional practitioners and medical scholars from academia, medical industry, and education, etc. It provides a forum to share scholarly practice to advance the immunotherapy in the combination of science and medicine.

TI publishes original research articles, review articles, editorials, mini-review articles, case reports, commentaries, correspondence articles, database articles, perspective articles, short reports, etc. Preliminary studies, pre-clinical and clinical investigative reports are welcomed.

The research topics of TI include but are not limited to:

1. Cancer immunotherapy
2. Targeted therapy and tumor microenvironment
3. Immune dysregulation, skin barrier dysfunction
4. Chemoimmunotherapy
5. Antibodies
6. Immunomodulators, inhibitors and intensifiers
7. Therapeutic method for auto-immune disorder
8. Efficacy of drug immunotherapy
9. Allergy disorder and immunotherapy
10. Immunotherapy cell-products
11. Immuno-modulatory effects of natural products
12. Vaccine development and application
13. Cytokines application
14. Wound healing

EnPress Publisher, LLC

EnPress Publisher, LLC, is a scholastic conduit for an assembly of professionals in the domains of science, technology, medicine, engineering, education, social sciences and many more, as a roundtable for their intellectual discourse and presentation, and as an instrument to galvanize research designs, policy implementation and commercial interests, to facilitate the prevailing over their challenges and to encourage to the full advantage of their resources and true potential.

We are the intellectual and academic home for academic, educators, scholars, clinicians, corporate researchers, who all play important roles in a wide range of national and international research organisations, and whose interests, expertise, research approaches and industry objectives from around the world coalesce together to advance significant contributions in their research and professional fields.

As an instrument of information purveyor, we seek to combine academic rigor and originality with the nuanced development of policy and practice. Via our journals, client database, online campaigns and social media presence, we offer a platform for industry professionals to interconnect, as well as opening doors towards cost-effective solutions for them to succeed, and we confidently hope to inspire a new generation of multidisciplinary researchers, think-tank experts, policymakers and business entities to innovate and advance their knowledge across fields.



EnPress Publisher, LLC

Add: 14701 Myford Road, Suite B-1, Tustin, CA 92780, United States

Tel: +1 (949) 299 0192

Email: contact@enpress-publisher.com

Web: <https://enpress-publisher.com>